ELECTRODEPOSITION OF ZINC FOR APPLICATIONS IN ZINC-AIR CELL

BY

ASSAYIDATUL LAILA BT NOR HAIRIN

A thesis submitted in fulfillment of the requirement for the degree of Master of Science (Materials Engineering)

Kulliyyah of Engineering
International Islamic University
Malaysia

MARCH 2012

ABSTRACT

Porous zinc electrodes are prepared from an acidic, chloride electrolytic bath for application in zinc-air microbattery. The aim is to produce a high specific surface area zinc coating in order to obtain high storage capacity and high limiting current density of the microbattery. The correlation between the physical properties of zinc electrodeposits and zinc-air cell discharge performance is also studied. The electrolytic bath consists of zinc chloride as the metal source and ammonium chloride as the supporting electrolyte. The concentration of the supporting electrolyte is varied from 0 to 4 M, while the concentration of zinc chloride is fixed at 2 M. The electrodeposition is performed at a constant current density of 100 $mAcm^{-2}$ for duration of 90 minutes. No electrolyte agitation is attempted. Zinc electrodeposits are characterized according to their X-ray diffraction (XRD) patterns, Scanning Electron Microscopy (SEM) observation, electronic densimeter measurement, and specific surface area and pore volume density determinations from the nitrogen physisorption isotherms at 77 K. X-ray diffractograms and supported by SEM observations are used as main instruments to identify variation in the zinc electrodeposits characteristics. SEM micrographs reveal unique porous network morphology of zinc electrodeposits. As the ammonium chloride concentration increases, flake microstructure appeared and later becomes predominant. High surface area and porous zinc electrodeposits have been prepared by electrodeposition; the BET surface area is in excess of 330 $m^2 g^{-1}$ and the electrode porosity is at least 60 %. Alkaline zinc-air microbattery, 1 cm^2 area x ca. 305 µm thick, is fabricated utilizing the zinc electrodeposits prepared from all electrolytic bath formulations and characterized according to its limiting current density and discharge capacity. The cell is able to deliver a maximum limiting current density of 55 mA cm^{-2} and produce an optimum discharge capacity of 34.5 mAh rated at 20 mA. It is discovered that the variation in limiting current density matches that of BET surface area and the trend for discharge capacity resembles that of pore volume density. These results suggest that zinc-air electrochemical system or metal-air electrochemical system in general can be utilized to gauge porous electrode properties. It is further supported by the fact that since oxygen is not stored within the system and is consumed directly from the ambient air, any variation in the metal-air electrochemical cell performance can be attributed almost exclusively on the metal anode properties or porous electrode properties in this context. Though it might not be a quantitative method, this technique is particularly useful for rapid screening or defect detection purposes. Other advantages include easy test cell assembly, do not require special sample preparation such as degassing, ambient temperature measurement, immediate data interpretation, quick results and low cost.

خلاصة البحث

أقطاب الزنك معدة من حمام كلوريد الحمضية التى يسهل اختراقها كهربائيا لتطبيقها في الهواء microbattery الزنك. الهدف هو إنتاج عالية مساحة محددة طلاء الزنك من أجل الحصول على سعة تخزين عالية وعالية الكثافة الحالية تحد من microbattery. كما درس العلاقة بين الخصائص الفيزيائية للelectrodeposits الزنك والهواء التفريغ أداء الخلية. الحمام كهربائيا يتكون من كلوريد الزنك كمصدر للمعادن وكلوريد الأمونيوم ودعم المنحل بالكهرباء. وتتنوع تركيز الكهارل دعم 4-0م، في حين يتم إصلاح تركيز كلوريد الزنك في 2 M. يتم تنفيذ الكهربي في كثافة تيار ثابت من 100 2 – mAcm لمدة 90دقيقة .هو لم يحاول أي تحريض بالكهرباء. تتميزelectrodeposits الزنك وفقا للحيود الأشعة السينية الخاصة بهم (XRD) الأنماط والمجهر الإلكتروني (SEM) المراقبة ، والقياس الالكترونية مقياس الكثافة، ومحددة المساحة وكثافة حجم المسام قرارات من الأيسوثرم physisorption النيتروجين في 77ك. وتستخدم الأشعة السينية diffractograms وبدعم من الملاحظات SEM كأدوات رئيسية لتحديد التباين في الزنك electrodeposits الخصائص. micrographs SEM تكشف عن شبكة مسامية مورفولوجيا فريدا من electrodeposits الزنك .كما يزيد تركيز كلوريد الأمونيوم، بدا المجهرية تقشر وتصبح في وقت لاحق الغالبة. Electrodeposits have أعد ارتفاع مساحة والزنك يسهل اختراقها من قبل الكهربي؛ المساحة الزائدة الترقيم الدولي الرهان من 330 ز 1 – M2 والمسامية الكهربائي ما لا يقل عن 60 ٪. القلوية الزنك الهواء microbattery ، 1س CM2 منطقة كاليفورنيا .هي ملفقة 305 ميكرون سميكة ، والاستفادة من الزنك electrodeposits المحضرة من كل الصيغ ويتميز حمام كهربائيا وفقا للكثافة الحالية تحد من قدرة والتفريغ. الخلية هي قادرة على تقديم أقصى كثافة التيار يحد من 55 مللي أمبير 2سم ، وتنتج قدرة التفريغ 34.5الأمثل للماه في التصنيف في 20 مللي أمبير. is discovered أن الاختلاف في الحد من كثافة المباريات الحالية

التي من مساحة سطح الرهان والاتجاه للقدرة التفريغ يشبه كثافة حجم المسام. هذه النتائج تشير إلى أن الزنك يمكن استخدامها في الهواء الكهروكيميائية النظام أو معدنية في الهواء نظام الكهروكيميائية بشكل عام لقياس خصائص القطب يسهل اختراقها. ويدعم ذلك حقيقة أن لا يتم تخزين منذ الأوكسجين داخل النظام ويستهلك مباشرة من الهواء المحيط، ويمكن أن يعزى أي تباين في أداء المعدن في الهواء خلية كهروكيميائية بشكل حصري تقريبا على خصائص الأنود المعدن أو خصائص مسامية في القطب هذا السياق. على الرغم من أنه قد لا يكون الأسلوب الكمي ، هذه التقنية مفيدة بشكل خاص لأغراض الفحص السريع أو الكشف عن الخلل. وتشمل المزايا الأخرى سهلة التجميع خلية اختبار ، لا تتطلب إعداد نموذج خاص مثل قياس درجة الحرارة المحيطة التفريغ الفوري وتفسير البيانات، ونتائج سريعة ومنخفضة التكلفة .

APPROVAL PAGE

I certify that I have supervised and read this study and that in my opinion; it conforms to acceptable standards of scholarly presentation and is fully adequate, in scope and quality, as a thesis for the degree of Master of Science (Materials Engineering).

……
Mohd Hanafi Ani
Supervisor

……
Raihan Othman
Co-Supervisor

I certify that I have read this study and that in my opinion it conforms to acceptable standards of scholarly presentation and is fully adequate, in scope and quality, as a thesis for the degree of Master of Science (Materials Engineering).

……
Agus Geter
Internal Examiner

.....
Sukreen Hana
External Examiner

This thesis was submitted to the Department of Materials and Manufacturing Engineering and is accepted as a fulfilment of the requirement for the degree of Master of Science (Materials Engineering).

……
Erry Yulian T. Adesta
Head, Department of Materials
and Manufacturing Engineering

This thesis was submitted to the Kulliyyah of Engineering and is accepted as fulfilment of the requirement for the degree of Master of Science (Materilas Engineering).

……
Amir Akramin Shafie
Dean, Kulliyyah of Engineering

DECLARATION

I hereby declare that this thesis is the result of my own investigations, except where otherwise stated. I also declare that it has not been previously or concurrently submitted as a whole for any other degrees at IIUM or other institutions.

Assayidatul Laila Binti Nor Hairin

Signature…… Date……...

INTERNATIONAL ISLAMIC UNIVERSITY MALAYSIA

DECLARATION OF COPYRIGHT AND AFFIRMATION OF FAIR USE OF UNPUBLISHED RESEARCH

ELECTRODEPOSITION OF ZINC FOR APPLICATIONS IN ZINC-AIR CELL

Affirmed by ASSAYIDATUL LAILA BINTI NOR HAIRIN

…… …….
Signature Date

ACKNOWLEDGEMENTS

First and foremost, I would like to express my utmost gratitude to Allah S.W.T. for His guidance and His blessing that bestowed upon me. Without His love and guidance, surely I would not be able to complete this research and finally complete the dissertation which was physically and mentally challenging.

Warmest appreciation goes to my supervisor, Dr. Mohd Hanafi Ani for his advices and guidance from the beginning till the very end of this project, to ensure it be completed successfully. A lot of knowledge and valuable experiences I have been obtained from him.

Furthermore, I would like to dedicate my sincerest thanks to my co-supervisor, Dr. Raihan Othman, for his through endless supervision, guidance and incredible patience which made this thesis possible. He was there to help me with any kind of difficulty, personal or professional during the course of this research. His encouragements always motivated me to give my best and I hope I have lived up to his expectations. This research would have never been accomplished according and successfully without his anticipation and assistance.

I would also want to acknowledge Ministry of Higher Education (MOHE) and International Islamic University Malaysia (IIUM) for sponsoring my postgraduate study (MSc. in Materials Engineering) for almost two years.

I would also like to convey my heartfelt thanks to lecturers, laboratory assistants, colleagues and staffs of Material Engineering Department for helping me out with their own field of expertise and also for the continuous support throughout this research. A special appreciation to the PhD and masters students; Bro. Hens, Sis Nor Liza, Sis Hanisah, Bro Aziz, Bro. Shahrul, and also Bro. Drajat, which have contributed a lot by helping me to complete this research. Special thanks to laboratory technical assistants, Ahmad Rahimie Awang, Ibrahim Razali and Husni Kamal Mohd Said who have been very helpful in handling the equipments for chemical, morphological and assistance in gathering data during my research

Finally, to my husband and parents, thank you so much for the undivided love and support. It really gives me the strength to get through all the difficulties throughout my student's life. This work has been possible due the support and guidance of many people. I would like to express my greatest gratitude to all these people who have supported me in different ways to make this effort a memorable one for me; I thank you all with a grateful heart.

TABLE OF CONTENTS

LIST OF TABLES

LIST OF FIGURES

LIST OF ABBREVIATIONS

BET	Brunauer, Emmet and Teller
°C	Degree Celcius
cm	centimeter
cm^2	centimeter squared
CO_2	Carbon dioxide
$C_{16}TAB$	Cetyltrimetyl-ammonium bromide
Cu	Copper
e^-	Negative electron
g	gram
HCl	Hydrochloric Acid
H_2O	Water
K	Kelvin
ℓ	Liter
mg	miligram
ml	milliliter
mm	milimeter
mm^2	Milimeter squared
mW	Miliwatt
nm	Nanometer
NaCl	Sodium chloride
NaOH	Sodium hydroxide
O^{2-}	Oxygen ion
OH	Hydroxyl
OH^-	Hydroxyl ion
SEM	Scanning Electron Microscope
TEOS	Tetraethylortosilicate
W	Watt
XRD	X-ray Diffraction
Zn	Zinc
$ZnCl_2$	Zinc Chloride
ZnO	Zinc oxide
ZrO_2	Zirconium Oxide

CHAPTER ONE

INTRODUCTION

1.1 OVERVIEW

Zinc the most widely used active material in primary battery industry. Its presence in the commercial market has been over a century. The world market for batteries was approximately USD 41.1 billion in 2000, out of which USD 13.1 billion or nearly one third dominated by zinc batteries (Broddet al., 2004). Besides its abundance, low cost and environmentally friendly, zinc possesses attractive electrochemical properties. It is the most electropositive metal that can be electrodeposited from an aqueous electrolyte and the most active metal that is relatively stable in caustic alkali electrolyte. Moreover, zinc is compatible with most conventional positive electrode materials, which makes it an effective anode material for a large number of primary and secondary batteries (Linden, 2001; McBreen, 1984). The main commercial zinc batteries are Leclanché cell, alkaline zinc-manganese oxide cell and zinc-air cell. Zinc-air system is currently considered among the prospective power source for electric vehicles. The system possesses the highest volumetric energy density (Wh/kg) as compared to other electrochemical systems including even the lithium batteries (Linden, 2001). This is due to the consumption of oxygen from the ambient air which does not require storage. Consequently the whole holding capacity is utilized by zinc active material producing a high energy density battery.

In general, there are three types of zinc electrode preparation, namely, the compressed dry powder process, the slurry or paste method and the electroformed method. Regardless of type of preparation, the objectives are to produce a high

porosity electrode, a high surface area and also good distribution of alloying element added particularly to raise the hydrogen overvoltage on zinc (Falk and Salkind, 1969). A high porosity electrode is a prerequisite for high discharge rate applications, whereas a low porosity electrode would result in a high energy density electrode suitable for low rate applications (Falk and Salkind, 1969). Cast zinc electrode in the massive or plate form cannot sustain high discharge current. The zinc anode may be prepared in the charged or discharged state. The former comprised of metallic zinc and the latter state is made from a mixture of zinc oxide and additives that can only be used in an alkaline electrolyte.

In the compressed dry powder process, a mixture of zinc metal or zinc oxide, binding agents such as fine Teflon powder or poly(vinyl alcohol) (PVA), and may also contain a corrosion inhibitant agent (traditionally being mercuric oxide), is placed in a mold and compressed around a current collector. The pressure applied is a function of porosity desired and types of mixture employed. The paste or the slurry preparation technique is usually used to fabricate a dry, charged and a high rate zinc electrode. Powdered zinc oxide is mixed with water or KOH solution and, with or without gelling agents such as carboxymethylcellulose (CMC). The resulting paste is the applied onto a suitable metal grid, dried and finally formed against a positive electrode in preferably 5% KOH solution (Falk and Salkind, 1969). Whereas in the electroforming method, the zinc electrode is electrodeposited from a zincate bath, or may also be plated from a slurry of zinc oxide in alkaline solution onto a metal substrate, with subsequent rinsing and drying processes (Falk and Salkind, 1969).

Electrodeposition method enables technologists the ability to pre-design electrocoatings properties. As such, the technique has been widely used in industrial applications for various purposes such as objects decorations, solderability

improvement, wearability improvement, friction reduction, hardness improvement, and corrosion inhibition (Ramanauskas, 1999; Kim et al., 2003; Veeraraghavan et al., 2003).In fact, key industry such as the automotive industry adopts electrodeposition over other methods such as evaporation, sputtering and chemical vapor deposition (CVD) for reasons of economy and convenience (Alfantazi and Dreisinger, 2001).

In particular, electrodeposition is one of the most commonly practiced industrial techniques for the fabrication of zinc coatings (Panagopoulos et al., 2006; Paunovic and Schlesinger, 2000; Zuniga et al., 2004). Zinc electrocoatings are widely used for the corrosion protection of ferrous materials, acting both as a physical barrier from the surrounding corrosive environment and as a self-sacrificial anodic protective layer (Paramonov and Levenkov, 2004; Zhang, 1996).

In this work, zinc electrodeposits are prepared from an acidic chloride bath of various electrolytic formulations, for applications as anodic electrode in zinc-air cell. Though there are numerous work reported on properties of zinc electrodeposits, the present work directly correlates the physical properties of zinc electrodeposits with their electrochemical performance in an electrochemical cell i.e. zinc-air electrochemical system.

1.2 PROBLEM STATEMENT AND ITS SIGNIFICANCE

There are currently three methods to produce thin, charged zinc anode coating for microbattery applications, namely, the sputtering technique, spin coating of a sol gel mixture and electrodeposition method. The zinc coating that is produced by using sputtering technique is sufficiently thin but possessed small surface area. In addition, although zinc coating prepared from spin coating of the sol gel mixture possessed high surface area, the pure and fine zinc particles are susceptible to oxidation. However, by

using electrodeposition method, a thin zinc anode coating zinc of high purity could easily be obtained. In fact, the thickness of the coating can easily be controlled and even the material properties can be pre-designed using electrodeposition. The aim of this work is to produce zinc electrocoating from an acidic chloride bath with favorable properties for use in alkaline zinc-air electrochemical cell.

1.3 RESEARCH OBJECTIVES

The main objectives of this work are as mentioned:

i. To investigate various properties of zinc electrodeposits as a function of chloride electrolyte bath formulations.

ii. To obtain a high surface area and high pore volume density of zinc electrodeposits for use in alkaline zinc-air electrochemical cell.

iii. To optimize the power density output of the alkaline zinc-air electrochemical cell utilizing various qualities of the electrodeposited zinc electrode.

1.4 RESEARCH METHODOLOGY

The research project will be conducted through the following steps:

i. Design and fabrication of an electrolytic cell

   A two electrode configuration is adopted for the electrodeposition process. The electrolytic cell consisted of zinc foil as the working electrode and copper foil as the counter electrode and also deposition substrate. Both electrodes are mounted on a home-made acrylic board clamp.

ii. Electrolytic bath formulation

The electrolytic bath composed of zinc chloride (ZnCl2) as the metal source and ammonium chloride (NH4Cl) as the supporting electrolyte. Zinc electrodeposits are produced from different molar ratios of NH4Cl to ZnCl2.

iii. Characterization of zinc electrodeposits

Zinc electrodeposits properties are studied using X-ray Diffractometer (XRD) for crystallographic identification, Scanning Electron Microscopy (SEM) for microstructure and surface analysis, Gas Chromatography and Autosorb instrumentation for specific surface area, pore volume and pore size distribution measurements, and electronic densimeter for alternative pore volume estimation.

iv. Electrochemical characterizations

Alkaline zinc-air cells are fabricated utilizing various qualities of the zinc electrodeposits. The effect of the zinc electrodeposits qualities on the electrochemical performance of the cellis studied.

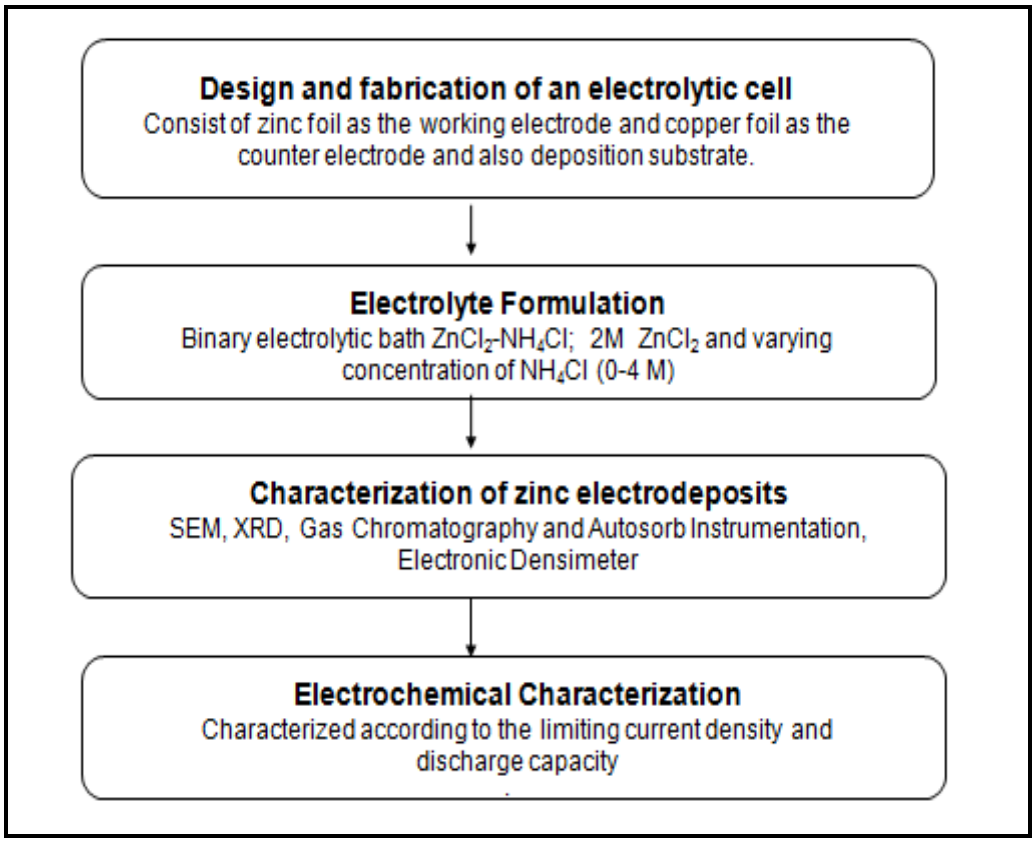

Figure 1.1: Flow chart of research methodology

1.5 SCOPE OF RESEARCH

Electrodeposition technique has been utilized since the thickness of the electrodeposits could easily be controlled and the material properties could be pre-designed. Furthermore, the physical properties of zinc electrodeposits shall be correlated directly with the electrochemical performance of the zinc-air cell. This is due to the fact that in zinc-air cell oxygen as the electropositive reactant is directly consumed from the ambient air and not stored within the cell compartment. Thus any variation in the electrochemical cell performance can be attributed almost exclusively on the zinc anode properties.

1.6 THESIS ORGANIZATION

This thesis consists of five chapters. Chapter One provides an overview of the present work. Chapter Two gives a brief theoretical background of electrodeposition, followed by literature review on electrodeposition of zinc and zinc-air cell. Chapter Three highlights the experimental details of this work which includes electrolytic bath formulation, electrodeposition parameters, physical characterizations of zinc electrodeposits, fabrication of zinc-air cell and electrochemical characterizations, and evaluation of porous electrode properties using metal-air electrochemical system. Chapter Four presents the results, analyses and discussion on the findings of this work. Finally, Chapter Five summarizes the findings of this research including recommendations for further work on this subject.

CHAPTER TWO

LITERATURE REVIEW

2.1 INTRODUCTION

Zinc is a bluish-grey transition metal covered by a protective transparent layer of basic carbonate in air. It exists in oxidation states of 1+ and 2+ but the former oxidation state is rare. At ambient temperature it is brittle, but malleable at 100 to 150°C. It is a reasonable conductor of electricity. Zinc has a hexagonal crystal structure (Figure 2.1).

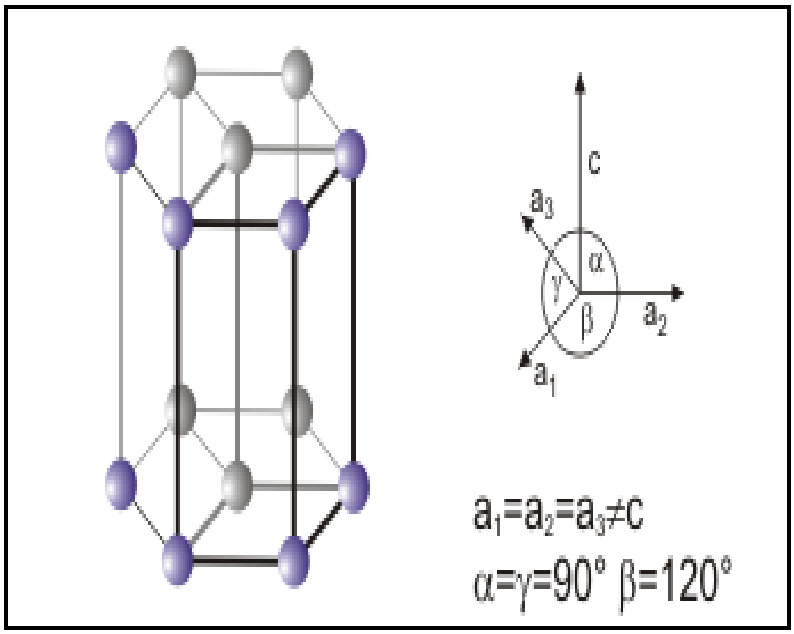

Figure 2.1: Crystal structure of zinc.

Zinc is a favorable anode material in primary batteries because of its high capacity, high discharge efficiency, low cost, low toxicity and high safety features associated with its manufacturing processes and use (Pagotto et al., 1999). Zinc as an anodic electrode has a theoretical capacity of 0.82 Ah g^{-1}. The zinc electrode is the

limiting factor in all alkaline zinc batteries. The method and rate of charge, electrode design and thickness, and the quantity of electrolyte are among the factors that determine the life of the zinc electrode. This work focuses on electrodeposited zinc electrode since the form of electrodeposits, its properties and thickness can easily be controlled. The succeeding sections shall highlight the electrodeposition principles in general, zinc electrodeposition in particular, deposition parameters affecting the properties of zinc electrodeposits and finally concluded with a brief review on zinc-air electrochemical system as the zinc electrodeposits are ultimately utilized as an electronegative electrode in the system.

2.2 PRINCIPLE OF ELECTROPLATING

When an electric potential is applied across a zinc electrode and another conducting electrode such as copper, where the zinc electrode forms the anode (positively charged) and the copper electrode forms the cathode (negatively charged) of the circuit respectively (Figure 2.2), of an electrolytic bath containing the solution of a salt of zinc metal, such as zinc sulphate, two observations will be noticed. Firstly, metallic zinc will be deposited on the copper electrode (cathode) and secondly, the positive electrode (anode) will slowly be dissolved (Raub, 1973). The amount of zinc which deposits on the cathode or dissolves from the anode is determined by the quantity of electricity that has passed and the oxidation state of the metal anode. These relationships were first derived by Faraday in 1833 known as Faraday's Laws, stated as follows (Binder et al, 2002):

"The weight of metal deposited at the cathode or dissolved from the anode is proportional to the quantity of charge (electric current and time) and to the chemical equivalent weight of the metal."

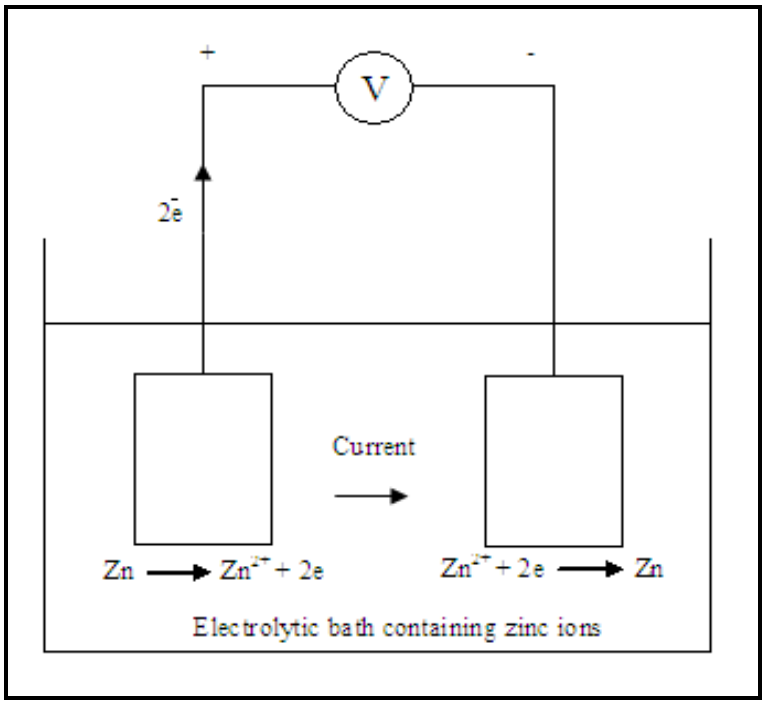

Figure 2.2: Electrolytic cell for zinc plating

Consider for instance a metal anode of formula weight *M* with valence change *n* when oxidized

$$M \rightarrow M^{n+} + ne \tag{2.1}$$

From Eq. 2.1, in order to deposit one mole of *M* from the electrolytic bath, *n* moles of electrons or neN_A Coulombs of charge is required, where N_A is the Avogadro's constant and *e* is the elementary charge constant ($e = 1.60 \times 10^{-19}\ C$). The product of eN_A is known as the Faraday's constant, *F*. Thus to deposit *x*-gram of *M*, the amount of charge required is

$$\frac{x}{M} neN_A = \frac{x}{M} nF(C) \tag{2.2}$$

Conversely, if a current of *I* Amperes flows for *t* seconds through the electrolytic bath, the quantity of *M* substance to be deposited is given by

$$\frac{ItM}{neN_A} = \frac{ItM}{nF}(g) \tag{2.3}$$

These equations underscore the advantage of electrodeposition technique in preparing an electrode for electrochemical cell as compared with the compressed dry powder process and the slurry or paste method; i.e. as well defined controlling parameters which enables a good control over the process and subsequently the properties of electrodeposits.

The efficiency of an electrolytic process or the current efficiency, ϵ_c can be calculated from the ratio of actual chemical change against the theoretical chemical change

$$\epsilon c = \frac{actual chemical change\ (desired)}{theoretical chemical change} \times 100\% \tag{2.4}$$

The theoretical chemical change is obtained from the theoretical value of the mass electrodeposits of Eq. (2.3). The actual chemical change is the mass of metal electroplated. In practice, evolution of hydrogen and oxygen and other decomposition reactions during electroplating consumed charge supplied, and as such the efficiency is less than 100%.

2.3 ZINC ELECTROCOATING AND ELECTROLYTIC BATH FORMULATIONS

Zinc has been the most useful coating materials for iron and steel as it offers good and low cost corrosion protection. Since zinc is anodic to steel and ferrous metal, it serves as sacrificial layer to the underlying material, even when the coating is porous or contains small mechanical defects (Binder and Kordesch, 1985). Electrodeposition is the preferred method to prepare zinc electrocoatings because of ease of fabrication, control and cost. However, electrodeposition is a very sensitive method due to the rapid electrokinetics of zinc species (Cho et al., 2008) and the existence of competing reactions such as oxygen and hydrogen evolutions (Pourbaix et al., 1966). Thus, the electrodeposition variables need to be properly defined and controlled.

Electrodeposition of zinc has been widely investigated using various approaches, which effectively lead to the preparation of coatings that differ in their macro and microstructure, texture, density, uniformity and corrosion resistance (Younman, 2000; Millet et al., 2000; Lin et al., 2000). Table 2.1a-c summarizes several zinc electrolytic bath formulations studied.

In general, electrolytes employed in electroplating can be either simple electrolyte or complex electrolyte, depending on the purposes intended. Simple electrolytes are solution of simple acids, alkaline or salts, having characteristics of high solubility, good conductivity and high metal ion concentration (Varghese, 1993). These baths can be worked at high current densities and can be used to build up heavy deposits but possess relatively poor throwing power i.e. it will not be possible to provide satisfactory coatings for objects of complex designs. Complex electrolytes used in electroplating contain either complex inorganic salts (pyrophosphate, fluoroborates, flurosilicates, sulphamatesetc) or complex organic salts (Rochelle salt,

citrates, tartarates, sulphonates, cyanides etc).Complex electrolytic baths have a good throwing power and among those, cyanides bath are most common complexing agent used (Varghese, 1993).

Table 2.1 (a)
Acid Zinc Plating Bath I

REFERENCE	(Lawrence et al, 1996)	(Lawrence et al, 1996)		(Lawrence et al, 1996)		(Frederick et al,1995)	(Frederick et al,1995)	(Frederick et al,1995)	(Frederick et al,1995)	(Frederick et al,1995)	(Frederick et al,1995)
		Ammoniated solutions	Ammoniated solutions	Potassium solutions	Potassium solutions						
		Rack	Barrel	Rack	Barrel						
Composition											
Zinc sulfate (g/L) $ZnSO_4.7H_2O$	240-360					240	360	410	240	160	480
Zinc chloride (g/L) $ZnCl_2$		74-95	34-64	75-85	50-85						
Ammonium chloride (g/L) NH_4Cl	15-30	90-120	112-225			15	30				
Potassium chloride (g/L) KCl				202-270	180-270						
Aluminum sulfate (g/L) $Al_2(SO_4)_3.18H_2O$ Or (Sodium acetate $NaC_2H_3O_2.3H_2O$)	15					30			30		
Aluminum chloride (g/L) $AlCl_3.6H_2O$								20			
Sodium sulfate (g/L) Na_2SO_4								75		90	90
Sodium chloride (g/L) NaCl										30	30
Boric acid (g/L) H_3BO_3 Or (Ammonium acetate) $NH_4C_2H_3O_2$		19-26	19-26							20	200
Boric acid (g/L) Or (Potassium acetate) $K(CH_3COO)$				22.5-34 (7.2-12.0)	22.5-34 (7.2-12.0)						
Additives											
Glucose Or (Licorice)	120					1			1		

By Analysis											
Zinc	55-83	36-45	16.5-30	36-40	24-40						
Chloride ions		126-170	93-183	135-175	112-175						
pH, Colorimetric	3.5-4.2	4.4-5.6	4.4-5.6	4.4-5.6	4.4-5.6	3.5-4.5	Should be controlled	within 0.3 (rack)	May be raised	until 5 (barrel)	

REFERENCE	(Lawrence et al,1996)	(Lawrence et al,1996)		(Lawrence et al,1996)		(Frederick et al,1995)	(Frederick et al,1995)	(Frederick et al,1995)	(Frederick et al,1995)	(Frederick et al,1995)	(Frederick et al,1995)
		Ammoniated solutions	Ammoniated solutions	Potassium solutions	Potassium solutions						
		Rack	Barrel	Rack	Barrel						
Conditions											
Temperature (°C)	24-30	15-45	15-45	15-45	15-45		25-30				
Current density (A/dm^2)	1.0-3.0										
Anode c.d. (A/dm^2)		0.5-3.0	0.5-3.0	0.5-3.0	0.5-3.0		Not	Critical			
Cathode c.d. (A/dm^2)		0.2-6.0	0.2-6.0	0.5-3.0	0.5-3.0		50-300	With	agitation	may raised	to 1000
Voltage, (V)	6										
Cathode efficiency (%)	95-100										
Ratio anode to cathode area	1:1										
Anode	Intermediate & high purity zinc	High purity zinc	High purity zinc	High purity zinc	High purity zinc						
Agitation	Cathode & solution, optional, recommended for high c.d.										

REFERENCE	(Ye et al, 1994)	(Trejo et al,1998)	(Chiba et al, 1993)	(Jorne et al,1996)	(Wen et al,1992)	(Barkey et al,1994)	(Gomez et al,1996)	(Yan et al,1994)	(Vagramyan et al,1961)	(Vagramyan et al,1961)	(Vagramyan et al,1961)
Composition											
Zinc sulfate (g/L) $ZnSO_4.7H_2O$	0.70 M			1.5 M	0.01 –1 M	0.4 M		620	500	200	
Zinc chloride (g/L) $ZnCl_2$		0.01 – 0.6 M	Not given				0.5 – 4.3 M				10 - 15
Zinc oxide (g/L) ZnO											20 - 22
Ammonium sulfate (g/L) $(NH_4)_2SO_4$										0.2	
Ammonium chloride (g/L) NH_4Cl											
Cetyltrimethyl (g/L) Ammonium bromide										5	
Potassium chloride (g/L) KCl		2.8 M									
Aluminum sulfate (g/L) $Al_2(SO_4)_2.18H_2O$ Or (Sodium acetate $NaC_2H_3O_2.3H_2O$)									30		
Aluminum chloride (g/L) $AlCl_2.6H_2O$											
Sodium sulfate (g/L) $Na_2SO_4.10H_2O$	0.25 M			1.0 M	0.2 M As supporting electrolyte			75	50		
Sodium chloride (g/L) NaCl	0.26 M										
Sodium hydroxide (g/L) NaOH											180 - 200
Boric acid (g/L) H_3BO_3 Or (Ammonium acetate) $NH_4C_2H_3O_2$											
Beta – nsphtol (g/L)											1 - 3
By Analysis											
pH, Colorimetric	2.2 - 5.6	5			4 – 6		3	2		1 – 4	

Table 2.1 (b)
Acid Zinc Plating Bath II

REFERENCE	(Ye et al, 1994)	(Trejo et al,1998)	(Chiba et al,1993)	(Jorne et al, 1996)	(Wen et al,1992)	(Barkey et al,1994)	(Gomez et al,1996)	(Yan et al,1994)	(Vagramyan et al,1961)	Varghese, 1993)	(Varghese ,1993)
Conditions											
Temperature (°C)	28		298 K		25			20 – 25	25	30 (RT)	30 (RT)
Current density (A/dm^2)	2 or 4		50	2 - 6 mA/cm^2			10 – 260 mA/cm^2	500 mA/cm^2	1	3 - 6	4 – 5
Anode c.d. (A/dm^2)											
Cathode c.d. (A/dm^2)											
Voltage, (V)						25					
Cathode efficiency (%)											
Ratio anode to cathode area											
Anode (Counter electrode)	Zn plate 6 x 10 cm	Graphite rod	Pt plate 1.0 x 1.0 cm		2 platinized titanium foils 1x20x80 mm	99.998 % Zn foil 250/100μm	Rotating disk (Zn,Pt) ϕ=0.79-1.27 cm				
Cathode (Working electrode)	Stainless steel plate 6 x 10 cm AISI 316	Glassy carbon 0.07 cm^2	Oxygen-free rolled Cu sheet 1.0 x1.0 cm	Zn ϕ = ¼ , 7/16 in	99.9 % Zn foil 0.5 mm thick A=2x2 cm	99.998 % Zn foil 250/100μm	Zn rod	Mild steel			
Reference electrode		Saturated calomel			SC		SC				
Distance between electrodes	4 cm		2 – 5 cm								
Agitation	Magnetic stirrer										
Electrodeposition cell	1 liter beaker	Conventional 3-electrode cell	Polypropylene cell ϕ = 2.8 cm h = 10.0 cm under hydrostatic pressure.		Polymethacrylate rectangular vessel open to air A=20 x 80 mm L=300 mm						

Table 2.1 (c)
Alkaline Zinc Plating Bath I

REFERENCE	(Lawrence et al, 1996)	(Lawrence et al, 1996)		(Lawrence et al, 1996)	
		Amonisted solutions		Potasium solutions	
		Rack	Barrel	Rack	Barrel
Composition					
Zinc sulfate (g/L) $ZnSO_4.7H_2O$	240-360				
Zinc chloride (g/L)		74-95	34-64	75-85	50-85
Ammonium chloride (g/L) NH_4Cl	15-30	90-120	112-225		
Potassium chloride (g/L)				202-270	180-270
Aluminum sulfate (g/L) $Al_2(SO_4)_3.18H_2O$ Or (Sodium acetate $NaC_2H_3O_2.3H_2O$)	15				
Boric acid (g/L) Or (Ammonium acetate)		19-26	19-26		
Boric acid (g/L) Or (Potassium acetate)				22.5-34 (7.2-12.0)	22.5-34 (7.2-12.0)
Additions, Optional					
Glucose Or (Licorice)	120 (1.0)				
By Analysis					
Zinc	55-83	36-45	16.5-30	36-40	24-40
Chloride ions		126-170	93-183	135-175	112-175
pH, Colorimetric	3.5-4.2	4.4-5.6	4.4-5.6	4.4-5.6	4.4-5.6
Conditions					
Temperature (°C)	24-30	15-45	15-45	15-45	15-45
Current density (A/dm^2)	1.0-3.0				
Anode c.d. (A/dm^2)		0.5-3.0	0.5-3.0	0.5-3.0	0.5-3.0
Cathode c.d. (A/dm^2)		0.2-6.0	0.2-6.0	0.5-3.0	0.5-3.0
Voltage, (V)	6				
Cathode efficiency (%)	95-100				
Ratio anode to cathode area	1:1				
Anode	Intermediate & high purity zinc	High purity zinc	High purity zinc	High purity zinc	High purity zinc
Agitation	Cathode& solution, optional for high c.d.				

However, in recent years, significant research effort has focused on the electrodeposition of zinc coatings from non-toxic acidic electrolytes, where various electrolyte additives have been introduced to improve the deposit properties and morphology (Alfantazi and Dreisinger, 2001; Baik and Fray, 2001; Raeissi et al., 2003; Yim et al., 1995; Youssef et al., 2004).

2.4 CONDITION AFFECTING THE FORM OF ELECTRODEPOSITS

Understanding the effect of various operating parameters on the qualities of electrodeposits would enable us to have a good control of the electrodeposition process and therefore the desired properties of the deposits. It should be noted that although the various deposition parameters mentioned succeedingly affect the properties of the deposit in a certain way, those factors also interact among each other and as a results produced a unique deposit. Wery et al. (2000) observed the influence of several electrochemical parameters on the morphologies of zinc deposit and cathode efficiency from an alkaline electrolytic bath. They discovered that three factors are dominant and also interact: the zinc content, the sodium hydroxide concentration and the sodium carbonate concentration. The zinc content is said to increase the efficiency by a factor of about 3.7 but zinc interacts strongly with caustic soda and carbonate. Secondly, the effects of caustic soda and carbonate are to reduce the efficiency.

2.4.1 Supporting Electrolyte

A supporting electrolyte is a non-reactive ionic species added to the electrolytic bath. Its main purpose is to increase the conductivity of the electrolyte. This, in turn, allows a bigger fraction of the cell voltage change to happen at the reacting surface and thus

makes the current density more uniform over the reacting surface (Glasstone, 1943). Potassium sulphate (K_2SO_4) is commonly used as a supporting electrolyte in aqueous systems since the sulfate ion does not react with the oxide film as chloride ions do. It is also reported to improve brightness of electrodeposits, throwing power, and operating current density (Dwarakadasa, 1988).

2.4.2 Effect of pH

An electrolytic bath pH affects the anode and cathode efficiencies. A low electrolytic bath pH reduces the cathode efficiency but will result in a lesser tendency for base material to be included in the deposit (Ye et al., 1994). Low pH baths of metals which are less noble than hydrogen result in purer, softer deposits and permit the use of high current densities. Ye et al. (1994) reported a loss of ductility in zinc electrodeposits and observed the co-deposition of zinc hydroxides as the pH of the acidic sulphate bath exceeded value of 4. Addition of buffer solution such as boric acid could minimize pH change of the electrolytic bath. Buffer solution has the ability to maintain the hydronium ion and the hydroxide ion concentrations, and consequently stabilizen the pH. It consists commonly of a weak acid and its conjugate base. Eq. (2.5) below shows the equilibrium state between the weak acid (HA) and its conjugate base of a buffer solution

$$(A^-)\,(aq):\ HA(aq) + H_2O(l) \leftrightarrow H_3O^+(aq) + A^-(aq) \qquad (2.5)$$

Any imbalance in the hydroxide ions will be consumed by the hydronium ions and on the other hand the conjugate base will be protonated when imbalance existed in hydronium ions. In principle, the pH is restored by the Le Chatelier's principle and the common ion effect (Glasstone, 1943).

2.4.3 Polarization and Limiting Current Density l

As the electrodeposition process proceeds, the rate at which metal ions get depleted at the immediate vicinity of the cathode is higher than the diffusion process. Concentration gradient of the metal ions develops and consequently may affect the deposition rate under potentiostatic electrodeposition. This phenomenon is known as cathode polarization (Varghese, 1993). At high current density, concentration gradient on anions and cations would contribute towards non-uniform pH across the electrodes and thus affect the deposit (Varghese, 1993). Agitation of the electrolyte would minimize this effect.

The metal ions are deposited at maximum rate when the rate of discharge of ions by the current equals to the maximum rate of diffusion. If the deposition current is increased further there will be no increase in the metal deposition rate, instead other species, in particular hydrogen ions will be discharged (Varghese, 1993).

2.4.4 Deposition Current

Varying the current density or applying pulsating current instead of direct current would influence the forms of deposit. Wery et al. (2000) studied the form of zinc electrodeposits obtained from a direct current and multi-component pulse current (*mcp*). They found out that the electrodeposition from *mcp* current was more beneficial for zinc plating under the experimental conditions of current density at least $10mA/cm^2$, zinc concentration of 0.004 mol/l and copper was used as the substrate.

2.4.5 Addition Agent

Inclusion of organic addition agents such as glue, gelatin and albumin in the plating bath have been reported to give smoother, fine grained and harder deposits (Safranek, 1986; Trejo et al., 2001). Additives studied for zinc electrodeposition include glycin (Loto et al., 1992),dextrin (Loto et al., 1992), glycerol (Galvanic and Carlos, 1997), thiourea (Li et al., 2007; Youssef et al., 2004) and gelatin (Baik and Faray, 2001; Saba and Elsherief, 2000; Sekar and Jayakrishnan, 2006). Gelatin is commonly used in zinc electrodeposition from acidic solutions and it is reported to promote the formation of more finely grained, smoother zinc electrodeposits (Saba and Elsherief, 2000). Gelatin addition is also said to decrease the adsorption of hydrogen ions on active zinc sites as well as to increase current efficiency (Baik and Faray, 2001). It is generally assumed that the addition agents or product derived from them are colloidal in nature and are absorbed into the deposits as they migrated to the cathode (Vermilyea, 1995). Besides, they may also form complex ion within the metal present and when these metal ions are discharged at the cathode, these addition agents are also automatically included in the deposit (Dini, 1995). An addition agent with specific function to improve the brightness of electrodeposits is termed brightening agent. An example of zinc brightening agent is acid zinc brightener which requires acid zinc carrier to permit it to function (Varghese, 1993).

2.5 CHARACTERIZATIONS OF ZINC COATING

Among the main characterization techniques for zinc coatings are physisorption and cyclic voltammetry. This section underlines these two methods for comparison purposes although the present work only utilized physisorption characterization.

2.5.1 Physisorption

Gas adsorption-desorption isotherms is one of the most extensively methods used in the characterization of inorganic porous materials. Material properties that can be elucidated are pore volume density, BET (Brunauer, Emmet and Teller) surface area, pore size distribution and pore shape. In this technique, the adsorption and desorption isotherms of an inert gas, normally N_2 at 77 K, on an outgassed sample are determined by measuring the quantity of gas adsorbed for each value of relative pressure p/p_0. At a particular minimum pressure, the smallest pores will be filled with liquid nitrogen. As the pressure is increased, larger pores will then be filled and near the saturation pressure (p/p_0~1), all pores are filled. The total pore volume is determined by the quantity of gas adsorbed near the saturated pressure. Then the process will be reversed to obtain the desorption curve. Each mesoporous system possesses a distinct characteristic hysteresis loops. The Kelvin equation is usually used for the calculation at mesopore size (Haynes, 1973)

$$\ln(p/p_0) = -f\,\gamma V/r_K RT \qquad (2.6)$$

where

f - the geometrical factors determined by the shape of the meniscus formed by the liquid in the capillary (f=1 for slit-shaped pores, f=2 for cylindrical pores)

γ- the surface tension of the liquid condensate at the absolute temperature T

V - the molar volume of the liquid at the absolute temperature T,

r_K - the Kelvin radius

The pore radius r_P of a cylindrical pore may be calculated from (Haynes, 1973)

$$r_p = r_k + t \qquad (2.7)$$

where t is the thickness of the absorbed layer of vapour in the pores.

The distribution of pore volume and the area as a function of pores diameter in the mesoporous range can be performed by the BJH (Barret, Joyner and Hallenda) method (Saputra, 2003) which considers opened cylindrical pores and may be applied to desorption branch.

Based on BET (Brunauer, Emmet and Teller) theory, the specific surface area of solids can be calculated by

$$1/(w((P_0/P)-1) = (1/w_mC)+((C-1)/(w_mC))(P/P_0) \quad (2.8)$$

where

w - weight of gas adsorbed at a relative pressure P/P_0

w_m - weight of the adsorbate constituting a monolayer of surface coverage

C – BET constant which is related to the energy of adsorption in the first adsorbed layer

The value of BET constant C is an indication of the magnitude of the adsorbent/adsorbate interactions. The total surface area of the sample can be expressed as:

$$St = (w_mN_{Acs})/M \quad (2.9)$$

where

N - Avogadro's number (6.023×10^{23}molecules/mol)

M - molecular weight of the adsorbate.

A_{cs} - cross-section area of inert gas. For the hexagonal close-packed nitrogen monolayer at 77K, the cross-section area A_{cs} for nitrogen is 16.2 $Å^2$

2.5.2 Cyclic Voltammetry

Cyclic voltammetry or liner sweep voltammetry is one of the more versatile methods for electroanalytical technique. The derivation of the various forms of cyclic voltammetry can be traced to the initial studies of Matheson and Nicols (1938) and Randles (1948). In principle, the technique applies a linearly changing scan of voltage to an electrode. The voltage is swept between two values at a fixed rate, as shown in Figure 2.3.

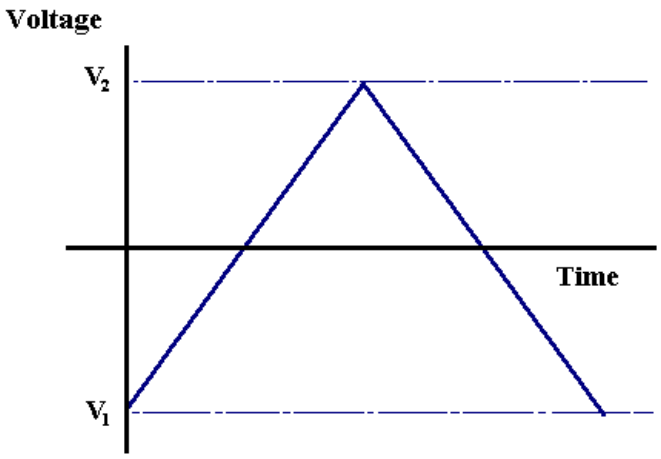

Figure 2.3: Cyclic voltammetry (CV) voltage sweeps

A typical cyclic voltammetry profile is illustrated in Figure 2.4. The plot shows a reversible single electrode transfer reaction.

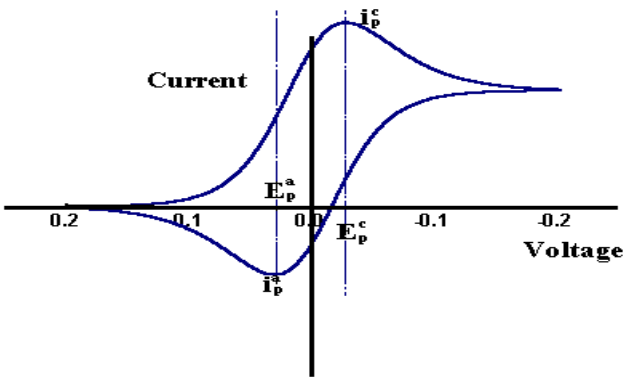

Figure 2.4: A typical cyclic voltammogram

A reversible electrochemical reaction exhibits a certain well defined CV characteristics (Bard et al, 2000) as follows:

i) The voltage separation between the current peaks is given by

$$\Delta E = \frac{2.3RT}{nF} \tag{2.10}$$

where

R – universal gas constant, 8.314472(15) $JK^{-1}mol^{-1}$

T – absolute tempreature

F – Faraday constat, $9.64853399(24)\times10^{4}$ $Cmol^{-1}$

n - the number of electrons transferred

ii) The positions of peak voltage are not affected by the voltage scan rate

iii) The ratio of the peak currents is equal to one

$$\left|\frac{i^{o}_{p}}{i^{c}_{p}}\right| \tag{2.11}$$

where

i^{c}_{p} - peak cathodic current

i^{0}_{p} - peak anodic current

iv) The peak currents are proportional to the square root of the scan rate

$$i^{o}_{p} \text{ and } i^{c}_{p} \propto \sqrt{v} \tag{2.12}$$

2.6 ZINC-AIR ELECTROCHEMICAL SYSTEM

Zinc-air cell is a unique electrochemical system in that it utilizes oxygen from the ambient air as one of the electroactive materials. Hence this provides the system with a practically unlimited and free oxygen supply. The negative electrode (anode) consists of zinc while the positive electrode (cathode) is a porous body made of carbon with air access. Atmospheric oxygen is reduced at this electrode. The active mass is thus not contained in the electrode but is taken from the surrounding air as it is needed. An aqueous solution of potassium hydroxide serves as the electrolyte.

Zinc-air systems have higher capacity-to-volume (and weight) ratio than other types of battery because the air from the atmosphere is not packaged with the battery, so that a cell can use more zinc in the anode than a cell that must also contain, for example, manganese dioxide. This increases capacity for a given weight. As a specific example, a zinc-air battery of 11.6 mm diameter and height 5.4 mm from one manufacturer has a capacity of 620 mAh and weigh 1.9 g; various silver oxide and alkaline cells of the same size supply 150-200 mAh and weigh 2.3-2.4 g (Linden, 2001).

In fact, zinc-air batteries store more energy per unit of weight than almost any other primary type (Linden, 2001). Zinc-air button cells are used almost exclusively for hearing aids. In hospitals, 9-volt zinc-air batteries power cardiac telemetry monitors used for continuous patient monitoring. Other multi-cell zinc-air batteries are used to power bone growth stimulators for mending broken bones. Furthermore, in telecommunication area zinc-air batteries are used for communication receivers such as pagers, e-mail devices and wireless messaging devices. Recently, zinc-air coin type batteries were employed in wireless telecom headsets that use the Bluetooth, low power digital wireless protocol (Linden, 2001). Another prospective application is for

electric vehicle propulsion. Compared to lithium, the availability of zinc metal is 100 times greater. Besides, zinc-air system possesses good environmental compatibility and low materials cost.

2.6.1 Zinc-air cell chemistry and performance

The zinc - air cell has a theoretical specific energy density of 1085 Wh kg^{-1}, which is based on the theoretical cell voltage of 1.65 V and assuming the final reaction product of ZnO (Appleby and Jacquier, 1976/77; McBreen, 1981; Rand, 1979).The chemical equations for the zinc-air cell are (Crompton, 2000):

Anode: $Zn + 4OH^- \rightarrow Zn(OH)_4^{2-} + 2e^-$ ($E_0 = 1.25$ V)

Fluid: $Zn(OH)_4^{2-} \rightarrow ZnO + H_2O + 2OH^-$

Cathode: $O_2 + 2H_2O + 4e^- \rightarrow 4OH^-$ ($E_0 = 0.4$ V)

Overall: $2Zn + O_2 \rightarrow 2ZnO$ ($E_0 = 1.65$ V)

The nominal open circuit voltage (OCV) for a zinc-air cell is 1.4 – 1.5 V. Depending on the external load, the initial discharge at 20 °C ranges from 1.5 to 1.35 V (Bender et al, 1995). As the air cathode is not chemically altered during discharge, the cell voltage remains quite stable with 0.9 V the typical end voltage. Thus, the discharge curves are relatively flat. Below the limiting current, the cell is capable of discharging approximately the same capacity. However as the discharge current approaches the limit, polarization of the cell voltage increases hence the cell delivers

less than the rated capacity. The discharge rate is dependent upon the rate at which air can be admitted. Usually, for high discharge applications air blowers are needed.

2.7 SUMMARY

This chapter highlights a brief theoretical background of electrodeposition, followed by literature review on electrodeposition of zinc and factors affecting the properties of electrodeposits. An emphasis is given to the various electrolytic bath formulations to produce zinc electrodeposits. As the zinc electrodeposits are intended for use as the anode in zinc-air electrochemical system, the cell characteristics and its electrochemical performance are also discussed.

CHAPTER THREE

EXPERIMENTAL SETUP AND PROCEDURES

3.1 INTRODUCTION

The experimental procedures involving electrodeposition of zinc from an acidic chloride bath, physical characterizations of the electrodeposits and, fabrication and electrochemical characterizations of zinc-air cell utilizing the electrodeposits are presented in detail in this chapter.

3.2 ELECTODEPOSITION OF ZINC

The electrolytic cell consisted of zinc foil (99.9 % purity) as the working electrode and copper foil as the counter electrode-cum-substrate. The copper substrate was clamped by a home-made acrylic board holder. The cell holder served to fix the electrode spacing and to define the deposition area. The electrode spacing was fixed at 30 mm and the holder possessed a window of 1 cm x 1 cm square area for zinc deposition. Figure 3.1 illustrates the schematic diagram of the electrolytic cell holder.

The electrolytic bath composed of zinc chloride ($ZnCl_2$) as the metal source and ammonium chloride (NH_4Cl) as the supporting electrolyte. Total electrolyte volume was maintained at 80 ml. The concentration of the supporting electrolyte was varied from 0 M to 4 M, while the concentration of zinc chloride was fixed at 2 M. Table 3.1 provides the details of the electrolytic bath compositions. Figure 3.2 shows the electrolytic cell set up.

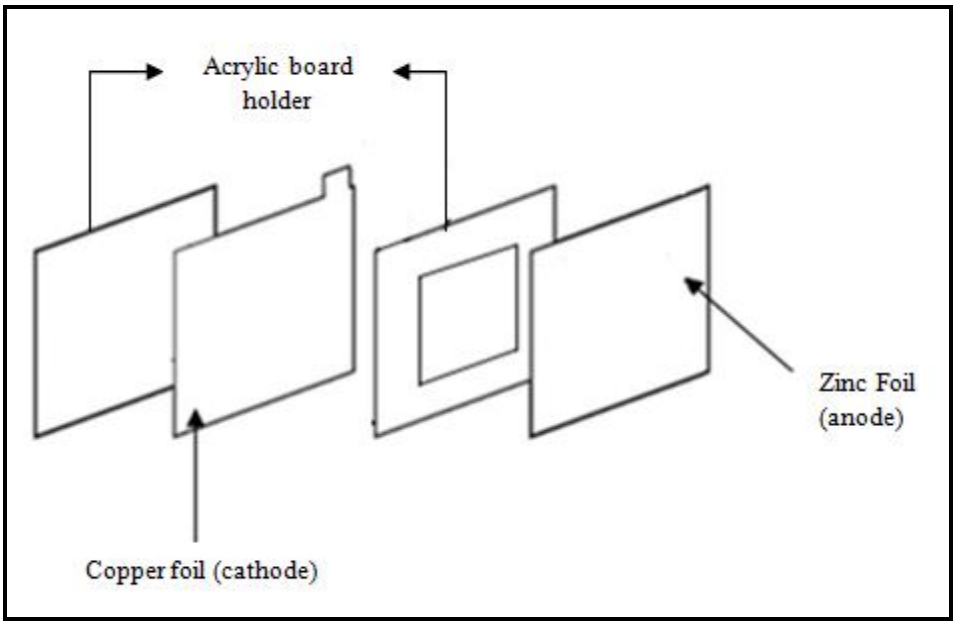

Fig.3.1: The electrolytic cell holder

Table 3.1
Electrolytic bath composition

Plating Batch	Electrolytic bath composition		
	$ZnCl_2$ (g/l) (2 M)	NH_4Cl	
		(g/l)	Molarity (M)
BATH 1	273.0	-	-
BATH 2	273.0	53.5	1
BATH 3	273.0	107.0	2
BATH 4	273.0	160.5	3
BATH 5	273.0	214.0	4

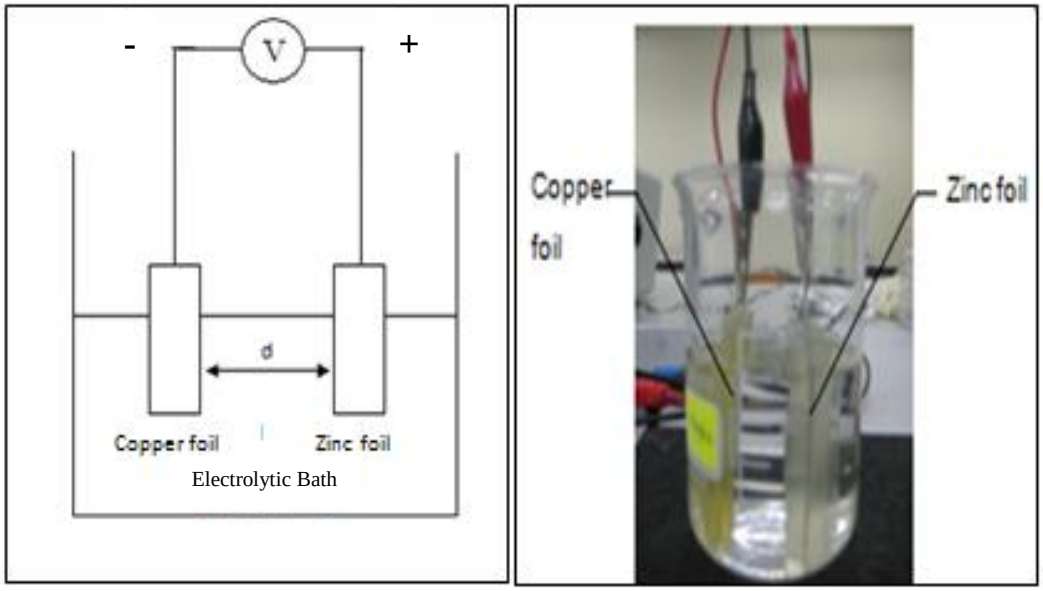

(a) (b)

Figure 3.2: Electrolytic Cell

Zinc coatings were electrodeposited at a constant current of 100 mA for fixed duration of45, 90 and 180 minutes. An Eco Chemie (The Netherland) potentiostat/galvanostat (PGSTAT302N, AUTOLAB) was used. During the electrodeposition no electrolyte agitation was attempted. The pH variation prior and after the deposition was recorded. The cathodic efficiency of the electrodeposition process was then calculated based on the experimental and theoretical zinc electrodeposits gain (i.e. Eq. 3.1), as follow:

$$\epsilon c = \frac{experimental\ electrodeposits\ gain, m_{exp}}{theoretical\ electrodeposits\ gain, m_{th}} \times 100$$

$$= \frac{m_{exp}}{\left(\frac{ItM}{neN_A}\right)} \times 10 = \frac{m_{exp}}{\left(\frac{ItM}{nF}\right)} \times 100\% \qquad (3.1)$$

where,

mole weight of zinc, $\boldsymbol{M}$ = 65.37 g.mol^{-1}

valency of zinc, $\boldsymbol{n}$ = 2

Faraday constant, $\boldsymbol{F}$ = 96500 C.mol^{-1}

electrodeposition current, $\boldsymbol{I}$ = 100 mA

3.3 PHYSICAL CHARACTERIZATION OF ZINC ELECTRODEPOSITS

3.3.1 X-Ray Diffractometer (XRD)

The X-ray diffraction pattern of the zinc electrodeposits were recorded by Shimadzu Diffractometer (XRD 6000) using the CuK_{α} radiation at 30 mA and 40 kV. The scans were performed between 2θ values of 10º to 80º at a scan rate of 2ºC/min. X-ray scattering technique shall reveal information about the crystallographic structure, chemical composition, and physical properties of thin film materials. XRD reference data file for zinc, zinc oxide and copper are listed in Table 3.2 – Table 3.4 respectively. Since copper foil was used as the deposition substrate, its XRD peaks may appear as well. Furthermore, if the surface area of zinc electrodeposits is very high, oxidation to zinc oxide may occur. Thus the XRD data file of zinc oxide and copper are provided for reference.

Table 3.2

Zinc XRD data file (4-083)

dÅ	I/I_1	hkl
2.4730	53	002
2.3080	40	100
2.0910	100	101
1.6870	28	102
1.3420	25	103
1.3320	21	110
1.1729	23	112
1.1236	17	201
0.9064	11	114

Table 3.3

Zinc oxide XRD data file (5-0664)

dÅ	I/I_1	hkl
2.8160	71	100
2.6020	56	002
2.4760	100	101
1.9110	29	102
1.6260	40	110
1.4770	35	103
1.3790	28	112
1.3590	14	201
1.0929	10	203
1.0422	10	211
0.9069	12	213

Table 3.4
Copper XRD data file (4-0836)

dÅ	I/I_1	hkl
2.0880	100	111
1.8080	46	200
1.2780	20	220
1.0900	17	311
1.0436	5	222
0.9038	3	400
0.8293	9	331
0.8083	8	420

3.3.2 Scanning Electron Microscope (SEM)

The surface microstructure and cross sectional analysis of zinc electrodeposits were obtained using a Scanning Electron Microscope (SEM) (JEOL, 5400), at 4 – 5 kV accelerating voltage using secondary electron imaging (SEI). For cross-sectional observation of the zinc electrodeposits, the electroplated zinc on the copper substrate was cold mounted in resin acrylic resin and sectioned using abrasive wet cutting method using a diamond blade. The sample was then polished with diamond polishing as an abrasive to accomplish the fastest material removal and the best possible planeness. There is no other abrasive available which can produce similar results.

3.3.3 Physisorption Instrumentation

BET surface area and pore volume density of porous zinc electrode were analyzed using AUTOSORB-1 (QUANTACHROME). The sorption isotherms of nitrogen at 77 K were determined in a pressure range p/p^0 from 0.001 to slightly below 1.0. The AUTOSORB-1 operates by measuring the quantity of gas adsorbed onto or desorbed from a solid surface at some equilibrium vapour pressure by static volumetric method. The volume-pressure data was then reduced by the AUTOSORB-1 software into BET surface area, adsorption and desorption isotherms, pore size and surface area distribution.

3.3.4 Electronic Densimeter

An electronic densitometer was also utilized for alternative pore volume estimation. Its operation is based on Archimedes' Principle and the determination of (relative) density value is based on the density of water at 4^oC i.e. 1 g/cm^3.

For a composite material, its density is given by

$$\rho = \frac{W_a}{W_a + W_w - W_b}(0.9975) \qquad (3.2)$$

where

ρ = the density of the composite material which is zinc deposit, in g/cm^3

W_a = the weight of the specimen when hung in the air

W_w = the weight of the partly immersed wire holding the specimen

W_b = the weight of the specimen when immersed fully in distilled water, along with the partly immersed wire holding the specimen

0.9975 = the density of distilled water at 23 °C (g/cm^3)

Thus, the pore volume density or void density of zinc electrodeposits could be estimated from the difference between theoretical value for density of zinc and the value obtained from the electronic densimeter.

$$\rho_{void} = \frac{(V_{exp} - V_{th})}{m_{exp}} = \frac{\left(\frac{m_{exp}}{\rho_{exp}} - \frac{m_{th}}{\rho_{th}}\right)}{m_{exp}}$$

$$= \frac{1}{\rho_{exp}} - \frac{1}{\rho_{th}}\frac{m_{th}}{m_{exp}} \qquad (3.3)$$

where

V_{th}= theoretical volume of zinc

M_t = mass of the zinc deposits

P_t = density of zinc (7.14 g/cm^3)

V_{exp} = experimental volume of zinc deposits

m_{exp}=mass of zinc deposits

ρ_{exp}= experimental density of zinc deposits

Alternatively, the void in the electrodeposits can be expressed in term of porosity

$$Porosity = \frac{V_{void}}{V_{th}} \times 100\% = \frac{V_{exp} - V_{th}}{V_{th}} \times 100\% = \left[\frac{\left(\frac{m_{exp}}{\rho_{exp}}\right)}{\left(\frac{m_{th}}{\rho_{th}}\right)} - 1\right] \times 100\%$$

$$= \left[\left(\frac{m_{exp}}{m_{th}}\right)\left(\frac{\rho_{th}}{\rho_{exp}}\right) - 1\right] \times 100\% \qquad (3.4)$$

3.4 FABRICATION OF ZINC-AIR CELL AND ELECTROCHEMICAL CHARACTERIZATIONS

The electrodeposited zinc from all electrolytic bath compositions was then assembled into zinc-air cell to quantify directly its performance as an anode. The air cathode was a commercially available air cathode sheet (E4 electrode acquired from Electric Fuel Ltd.) which consists of laminated fibrous carbon, sandwiched against a nickel mesh current collector. The airside of the electrode is covered with semi permeable hydrophobic Teflon membrane. The membrane allows oxygen diffusion through it but minimizes the dissipation of water vapour from the electrolyte. The cell electrolyte was a 6 M potassium hydroxide (KOH).

An inorganic MCM-41 membrane was employed as the cell separator as well as the electrolyte reservoir. MCM-41 material belongs to a group of mesoporous materials known as M41S. This class of material is characterized by its regular arrays of tunable uniform channels with large surface area (Kresge et al., 1992; Beck et al., 1992; Karge et al., 1998). MCM-41 materials possess the properties of high specific surface area and pore volume of about 1000 m^2/g and 1 cm^3/g respectively, very narrow pore size distribution which centred around 2 nm, tunable pore size, adjustable hydrophobicity and very good thermal stability i.e. up to 900°C (Kresge et al., 1992; Beck et al., 1992; Burggraaf et al., 1996).

MCM-41 membrane was applied onto the electrodeposited zinc anode by dip-coating technique. The parent solution consisted of quarternary ammonium surfactant, cethyltrimethylammonium bromide $C_{16}H_{33}$ $(CH_3)_3NBr$ ($C_{16}TAB$), hydrochloric acid, deionized water, ethanol, and tetraethylortosilicate (TEOS) with molar ratio of 0.05 CTAB, 1.0 TEOS, 0.5 HCl, 25 C_2H_5OH and 75 H_2O. The mixture of parent solution was stirred at about 200 rpm at 30°C for 1 hour. Zinc anode was then dipped into

parent solution and then dried. The procedure can be repeated to prepare membrane that will be thick enough to hinder the damage due to cracking or pinhole. One time dipping process results in MCM-41 film thickness of ca. 1 μm (Ji et al., 2004; Saputra, 2004). The procedures are as summarized in a block diagram of Figure 3.3.

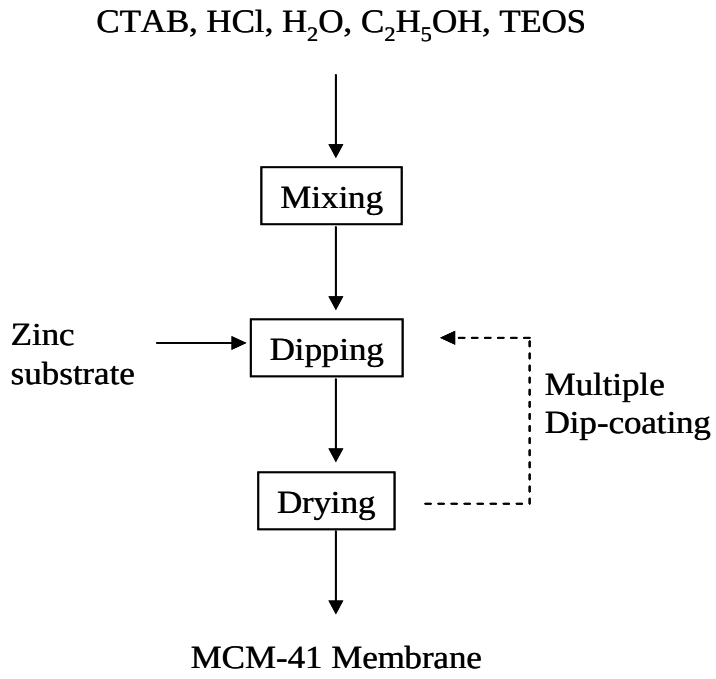

Figure 3.3: Preparation of MCM-41 membrane using dip-coating method.

Figure 3.4 illustrates the zinc-air cell components and the dimensions. A complete cell measured 1 cm^2 area x ca. 305 μm thick. Zinc-air test cell utilizing the electrodeposited zinc anode was characterized according to its limiting current density and discharge performance. The aim was to evaluate directly the influence of various zinc electrodeposits qualities on the zinc-air cell electrochemical performance. The test cell was characterized according to its limiting current density and discharge capacity. Limiting current is the maximum discharge current able to be delivered by an electrochemical cell prior to the abrupt voltage drop. Limiting current value was

obtained from the polarization profile of the cell in which the cell voltage at a particular current drain was recorded as the current was increased, until the cell failed. Fig. (3.5) shows the typical polarization profile of a zinc-air cell and the limiting current value is as indicated on the graph.

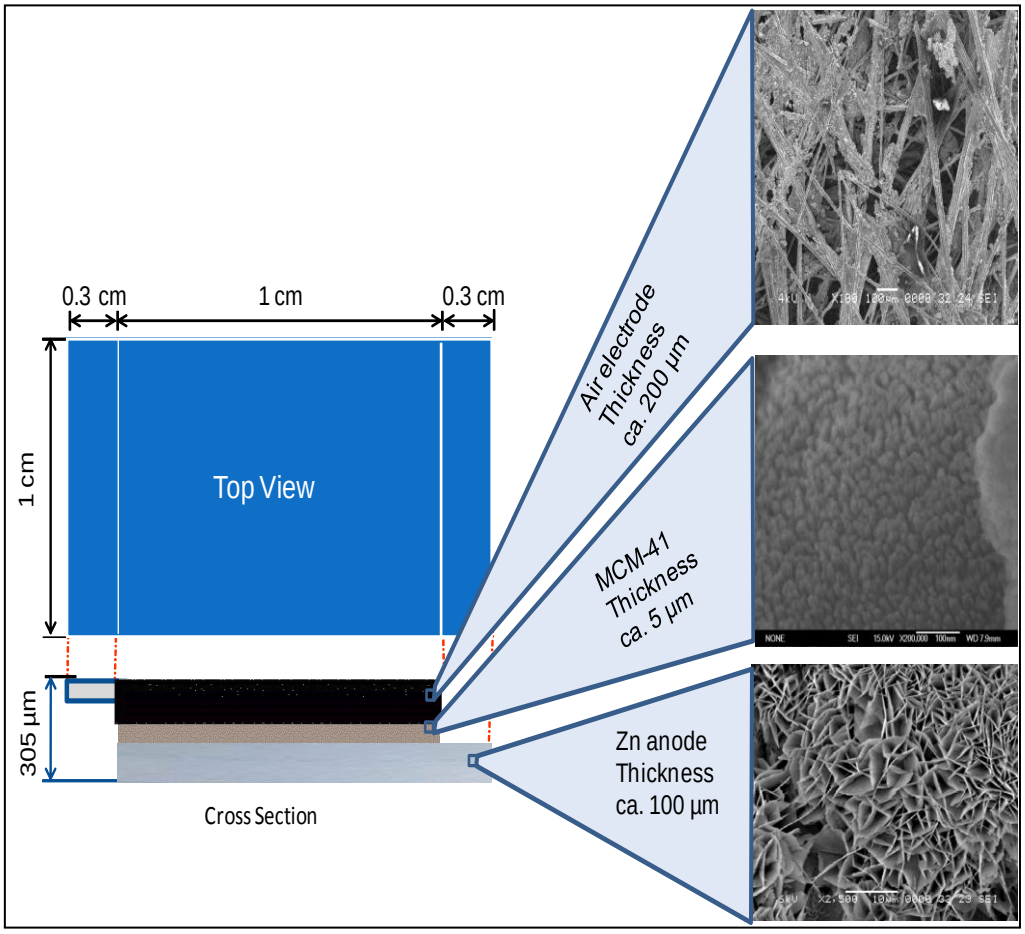

Figure 3.4: Illustration of the zinc-air cell components and its dimensions

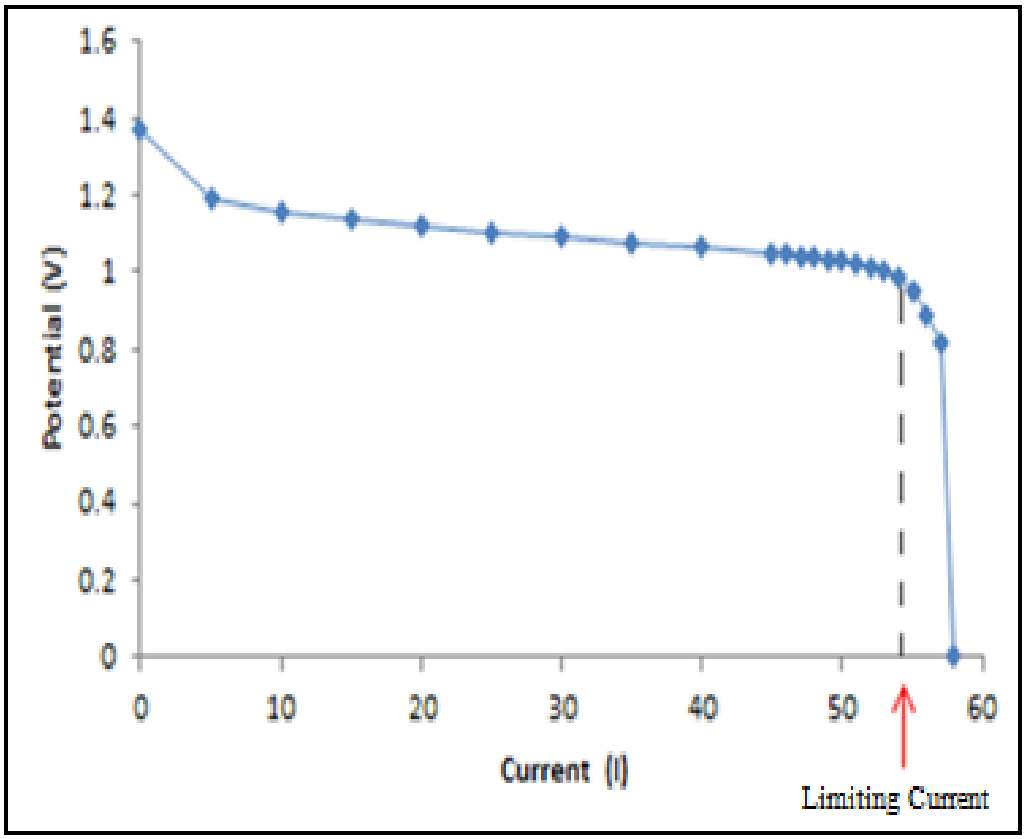

Fig. 3.5: Typical polarization profile of a zinc-air cell

Discharge capacity is the total charge quantity, measured in ampere-hours (*Ah*), which can be withdrawn from an electrochemical cell. It is a measure of zinc active material utilization at a particular load current and calculated from the product of discharge current, I_d and discharge duration, *t*,

$$Capacity = I_d t \ (Ah) \tag{3.5}$$

3.5 SUMMARY

A $ZnCl_2$-NH_4Cl electrolytic bath was employed to prepare zinc electrocoatings. Only the concentration of NH_4Cl supporting was varied while the remaining electrodeposition parameters were fixed. The resulting zinc electrodeposits were characterized and also fabricated into zinc-air cell. The correlation between the physical properties of the electrodeposits and the electrochemical performance of zinc-air cell utilizing the zinc electrodeposits was studied.

CHAPTER 4

RESULTS AND DISCUSSION

4.1 INTRODUCTION

Physical properties of zinc electrodeposits prepared from various $ZnCl_2$-NH_4Cl electrolytic bath formulations are reported in this chapter. The physical characterizations include cathodic efficiency, X-ray diffraction measurement, scanning electron microscopy observation, density measurement and, specific surface area and pore volume density determinations. The zinc electrodeposits were then assembled into zinc-air cells and characterized according to their polarization profile and discharge capacity. The relation between physical properties of zinc electrodeposits and their contribution to zinc-air cell electrochemical performance are then discussed.

4.2 ZINC ELECTRODEPOSITION FROM AN ACIDIC CHLORIDE BATH

In the electrolytic bath formulation, zinc chloride ($ZnCl_2$) serves as the zinc source while ammonium chloride (NH_4Cl) acts as the supporting electrolyte. $ZnCl_2$ concentration was maintained at 2 M while NH_4Cl concentration was varied from 0 to 4 M. Electrolyte volume was fixed at 80 ml and a 150 ml beaker was utilized as the container. No electrolyte agitation was attempted. Zinc was electrodeposited at a constant current of 100 mA for duration of 90 minutes (5400 s). Electrodeposition is a very sensitive technique, as such all parameters need to be clearly specified. Zinc was also electrodeposited for duration of 45 minutes and 180 minutes, from each

electrolytic bath formulation. The purpose was to observe any variation in the qualities of electrodeposits with changing deposition time while maintaining the electrolytic bath formulation. Table 4.1 presents the pH value of each electrolytic bath formulation prior and after deposition. All baths were acidic with pH values of 4 to 5. With increasing NH_4Cl concentration the pH decreases gradually i.e. the solution becomes more acidic. pH values did not change significantly after the deposition. Thus buffer solution is not required for the formulation and set up chosen in this work.

Table 4.1
pH of electrolytic bath prior and after electrodeposition

Electrodeposition Bath (Molarity of NH_4Cl)	**pH Value**	
	Prior deposition	**After deposition**
Bath 1 (0 M)	4.81	4.68
Bath 2 (1 M)	5.08	5.07
Bath 3 (2 M)	4.80	4.83
Bath 4 (3 M)	4.60	4.61
Bath 5 (4 M)	4.50	4.50

Table 4.2 provides the details of the zinc electrodeposits weight gain and the cathodic efficiency of the electrodeposition process.

Table 4.2
Electrodeposits mass gain and electrodeposition efficiency

Electrodeposition Bath (Molarity of NH_4Cl)	**Substrate initial mass (*g*)**	**Substrate final mass(*g*)**	**Mass gain (*g*)**	**Cathodic Efficiency (%)**
Bath 1 (0 M)	0.0808	0.2654	0.1846	100.8
Bath 2 (1 M)	0.0857	0.2694	0.1837	100.3
Bath 3 (2 M)	0.0778	0.261	0.1832	100.0
Bath 4 (3 M)	0.0818	0.2666	0.1848	100.9
Bath 5 (4 M)	0.0803	0.2635	0.1832	100.0

The cathodic efficiency was calculated based on the comparison between the experimental electrodeposits gain on the copper substrate and the theoretical electrodeposits gain i.e. Eq. (4.3). The electrodeposition was performed galvanostatically at 100 mA for a constant duration of 5400 s. Thus the theoretical electrodeposits gain is 0.1832g, calculated as follows.

$$Zn^{2+} + 2e^{-} \longrightarrow Zn \qquad (4.1)$$

Based on the above Eq. (4.1),

2 moles of e^{-} are required to reduce 1 mole of Zn^{2+} ions into 1 mole of Zn electrodeposits.

The electrodeposition current used was 100 mA. Thus the quantity of charge supplied was;

$$Q = I \times t \quad (4.2)$$

$$= (100 \times 10^{-3}\ C/s) \times (5400\ s) = 540\ C$$

2 moles of e^- carry charge quantity of $= 2 \times N_A \times (1.6 \times 10^{-19}\ C)$

$$= 2 \times (6.022 \times 10^{23}) \times (1.6 \times 10^{-19}\ C) = 192708.54\ C$$

Taking the atomic weight of Zn as 65.38 g/mol, the theoretical zinc weight gain is

(540C x 65.38) / 192708 = 0.1832 g

Consequently,

Deposition Efficiency (%) = (weight gain / 0.1832) x 100% (4.3)

Due to the rapid zinc electrokinetics in aqueous electrolyte the efficiency is 100 % or slightly exceeds 100 %. Electrodeposition process occurs through substitution of Zn^{2+} ions from the working zinc electrode as Zn^{2+} ions from the zinc containing electrolyte are plated onto the counter electrode. Thus if the deposition of Zn^{2+} ions from the electrolyte are more rapid than their substitution from the working electrode, the resulting efficiency would be greater than 100%. It is a common phenomenon reported in zinc electroplating (Baik and Fray, 2001).

Figures 4.1 (a) – (e) illustrate the photographs of zinc electrodeposits on the copper substrate. The 10 μm thick copper substrate was clamped by acrylic boards with a 1 cm x 1 cm square window opening for the electrodeposition area. The separation between the zinc foil working electrode and the copper counter substrate was fixed at 30 mm. In general the qualities of zinc deposits were good, i.e. rather smooth deposits, good adhesion and most importantly non-dendritic. Dendritic or tree-

like deposits will cause premature electrochemical cell failure due to internal short-circuiting.

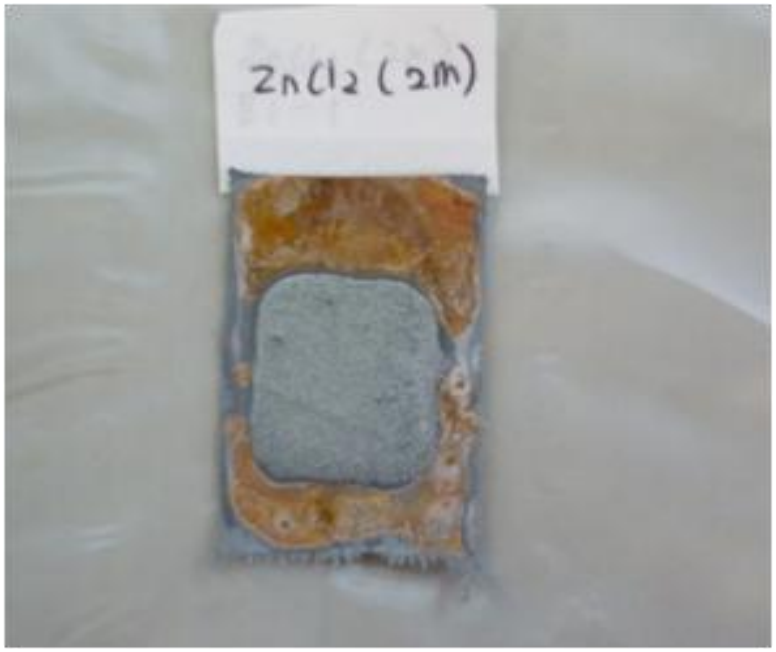

(a)

(b)

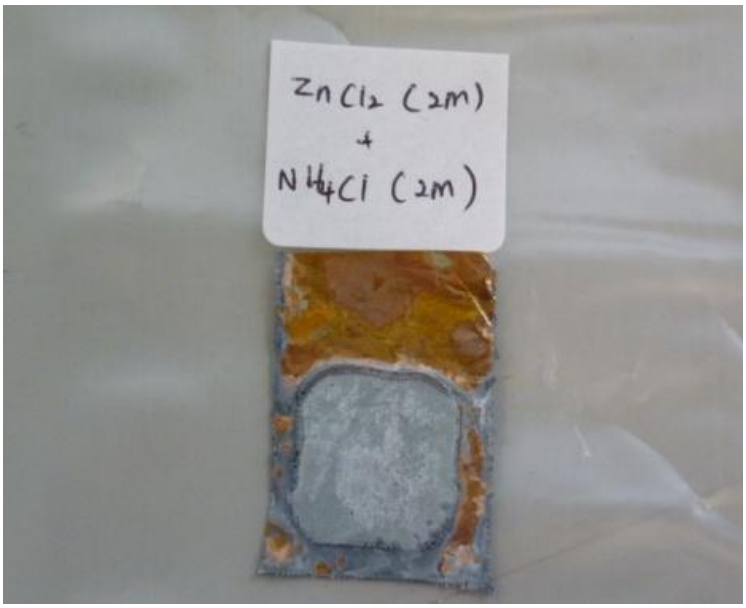

(c)

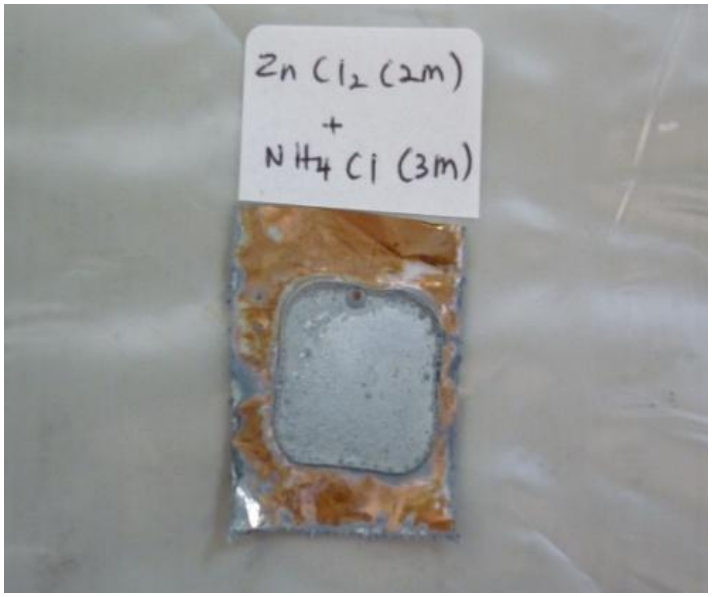

(d)

(e)

Figure 4.1: (a) Zinc electrodeposits from 2M-$ZnCl_2$bath, (b) Zinc electrodeposits from 2M-$ZnCl_2$ / 1M-NH_4Cl bath, (c) Zinc electrodeposits from 2M-$ZnCl_2$ / 2M-NH_4Cl bath, (d) Zinc electrodeposits from 2M-$ZnCl_2$ / 3M-NH_4Cl bath and (e) Zinc electrodeposits from 2M-$ZnCl_2$ / 4M-NH_4Cl bath

4.3 X-RAY DIFFRACTOGRAMS OF ZINC ELECTRODEPOSITS

Figure 4.2 displays X-ray diffraction patterns of the zinc electrodeposits obtained from each electrolytic bath formulation prepared with deposition time of 90 minutes. An interesting crystallographic variation was observed. From basic $ZnCl_2$ bath formulation (i.e. without NH_4Cl), X-ray diffraction from (002) hexagonal plane is the most dominant and followed by (101) plane. There are a total of 6 zinc diffraction peaks observed. As NH_4Cl supporting electrolyte was introduced into the electrolytic bath composition, the most preferred zinc crystallographic orientation becomes the (103) plane, however, (101) diffraction plane still remains the second most dominant peak. The intensity of (002) diffraction is greatly reduced. Moreover, with the

presence of NH_4Cl the (100) diffraction plane totally disappeared and the (004) peak is almost flattened. The peak located at 2°~ 50° is attributed to the copper substrate.

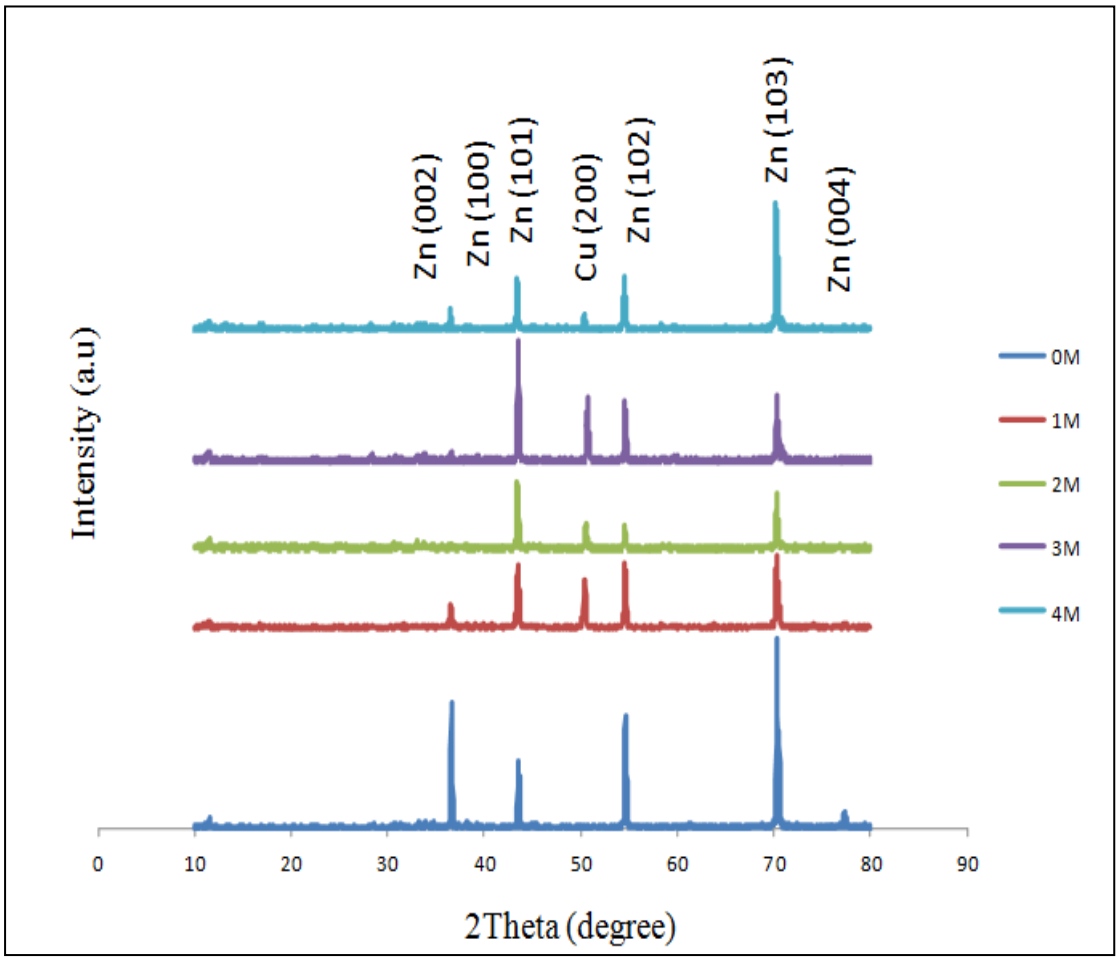

Figure 4.2:X-ray diffraction patterns of zinc electrodeposits obtained from each electrolytic bath formulation prepared with deposition time of 90 minutes

The variation in the XRD patterns could then be used as a tool to detect any changes in the qualities of electrodeposits prepared with different deposition time. Figure 4.3 presents the XRD patterns of zinc electrodeposits prepared with deposition time of 45 minutes. In general, the main features remain the same; for zinc electrodeposits prepared without NH_4Cl supporting electrolyte, the most dominant peak is (002) and with the inclusion of NH_4Cl the most dominant diffraction is from the (103) plane and the intensity of (002) plane is greatly reduced. Besides, the (004)

peak also diminishes as NH_4Cl was included. However some other variation started to occur. The most obvious being forNH_4Cl formulation more than 1 M, the (002) peak becomes almost flattened.

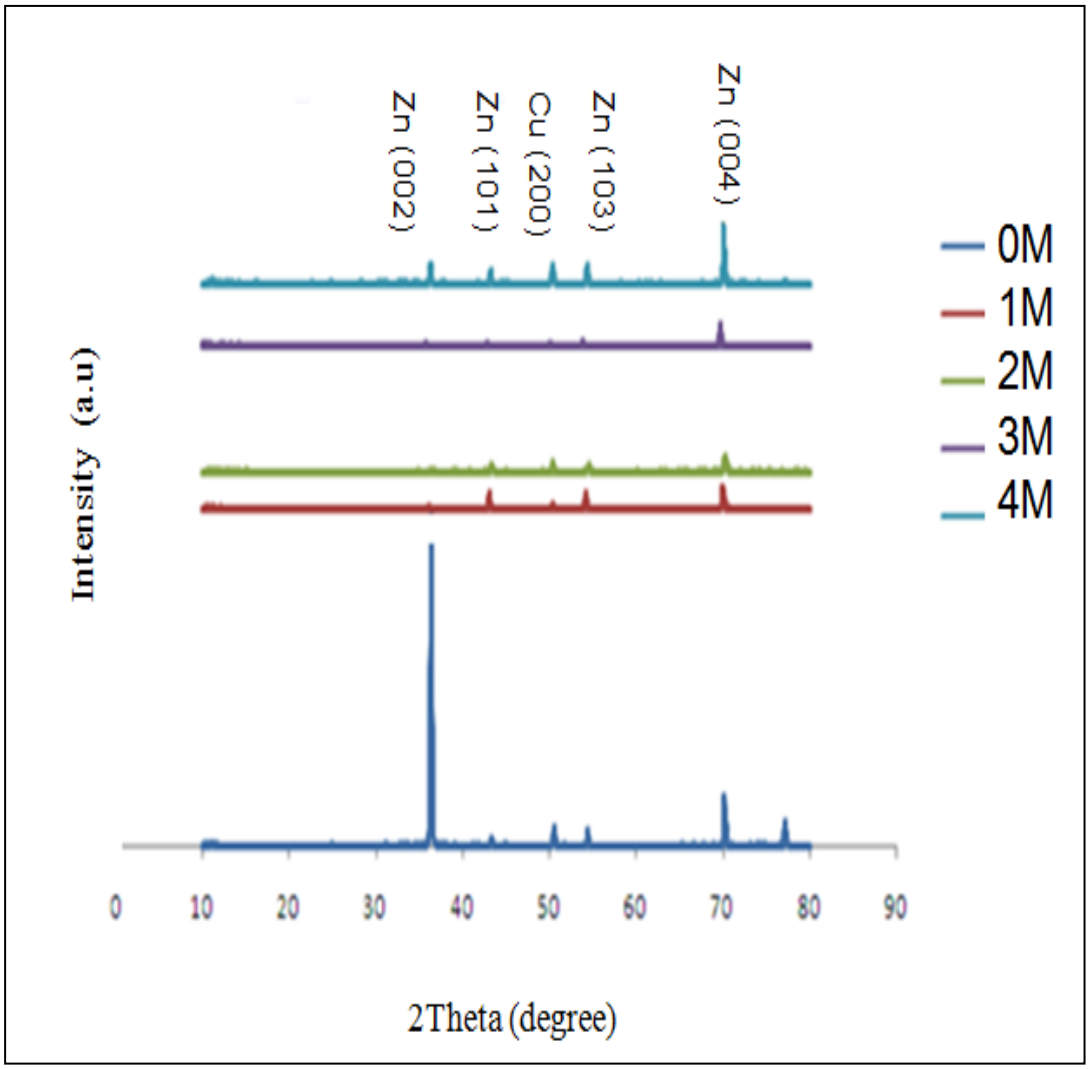

Figure 4.3: The XRD patterns of zinc electrodeposits prepared with deposition time of 45 minutes

When the deposition time was increased to 180 minutes, totally new X-ray crystallographic patterns were observed (illustrated in Figure 4.4), indicating that the zinc electrodeposits obtained would be having different properties. Equally strong diffraction peaks appeared i.e. from the (102) and (103) planes. Inclusion of NH_4Cl

supporting electrolyte resulted in the appearance of many minor peaks and the most obvious is for bath formulation of 4 M-NH_4Cl.

These observations reveal that though all deposition parameters were maintained, different deposition duration resulted in different zinc electrodeposits properties. At least for deposition duration of 45 – 90 minutes, minimum variation in the electrodeposits properties could be expected as inferred from the XRD patterns. The following SEM observations in the following section shall provide further deliberations.

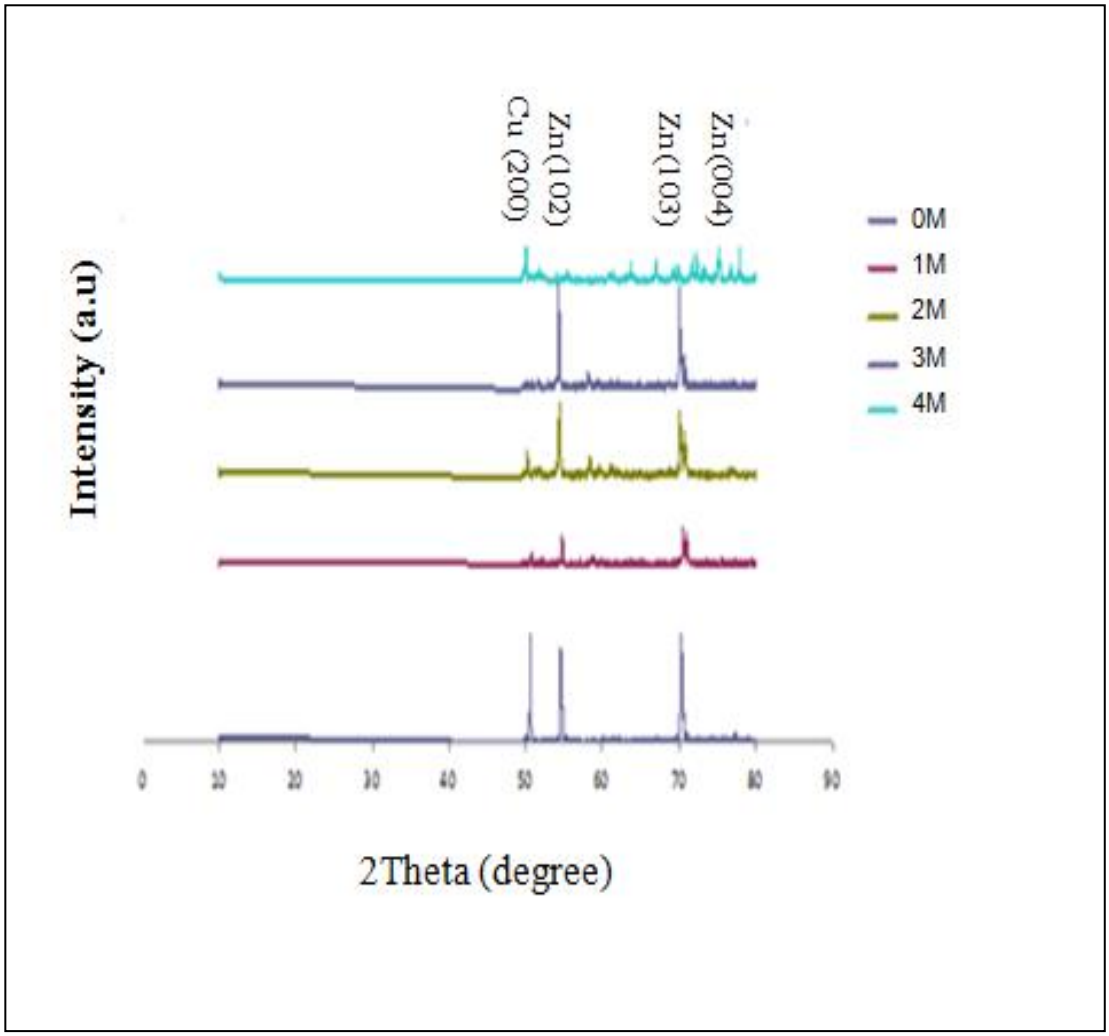

Figure 4.4: The XRD patterns of zinc electrodeposits prepared with deposition time of 180 minutes

4.4 SCANNING ELECTRON MICROSCOPY (SEM) OBSERVATION

SEM top view images reveal unique surface morphology characteristics of zinc electrodeposits produced from each electrolytic bath formulation of 90 minutes deposition time, as depicted in Figures 4.5 (a)-(e). The basic bath formulation without NH_4Cl (Fig. 4.5a) produced porous stacks of laminar planes. As 1 M of NH_4Cl was introduced, zinc electrodeposits grew in a rather dense tiny flakes microstructure (Fig. 4.5b). When NH_4Cl content was doubled to 2 M, a highly porous sponge

microstructure was obtained (Fig. 4.5c). Further increase to 3 M of NH_4Cl content resulted in a porous flakes microstructure (Fig. 4.5d). Finally when NH_4Cl content was 4 M, the flakes microstructure interconnected forming a porous network or foamy deposits (Fig. 4.5e).

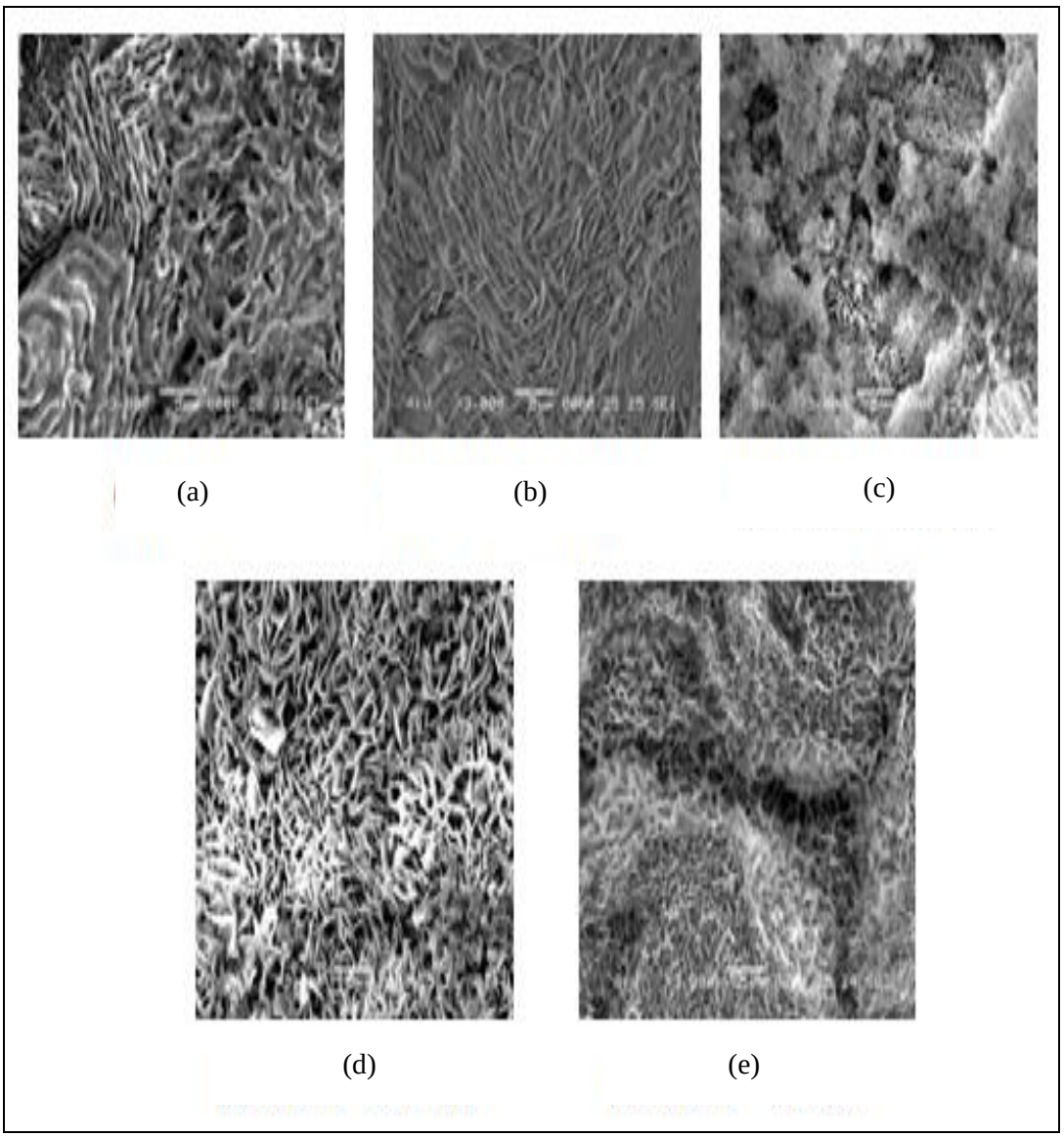

Figures 4.5: SEM images of zinc electrodeposits prepared with deposition time of 90 minutes deposition time (a) 2M $ZnCl_2$, (b) 2M $ZnCl_2$ – 1M NH_4Cl, (c) 2M $ZnCl_2$ – 2M NH_4Cl, (d) 2M $ZnCl_2$ – 3M NH_4Cl and (e) 2M $ZnCl_2$ – 4M NH_4Cl

Figure 4.6 provides the SEM cross sectional view of the electrodeposits. The cross sectional view of sample from 2 M-NH_4Cl bath clearly indicates the porous nature of the zinc electrodeposits as compared to other samples.

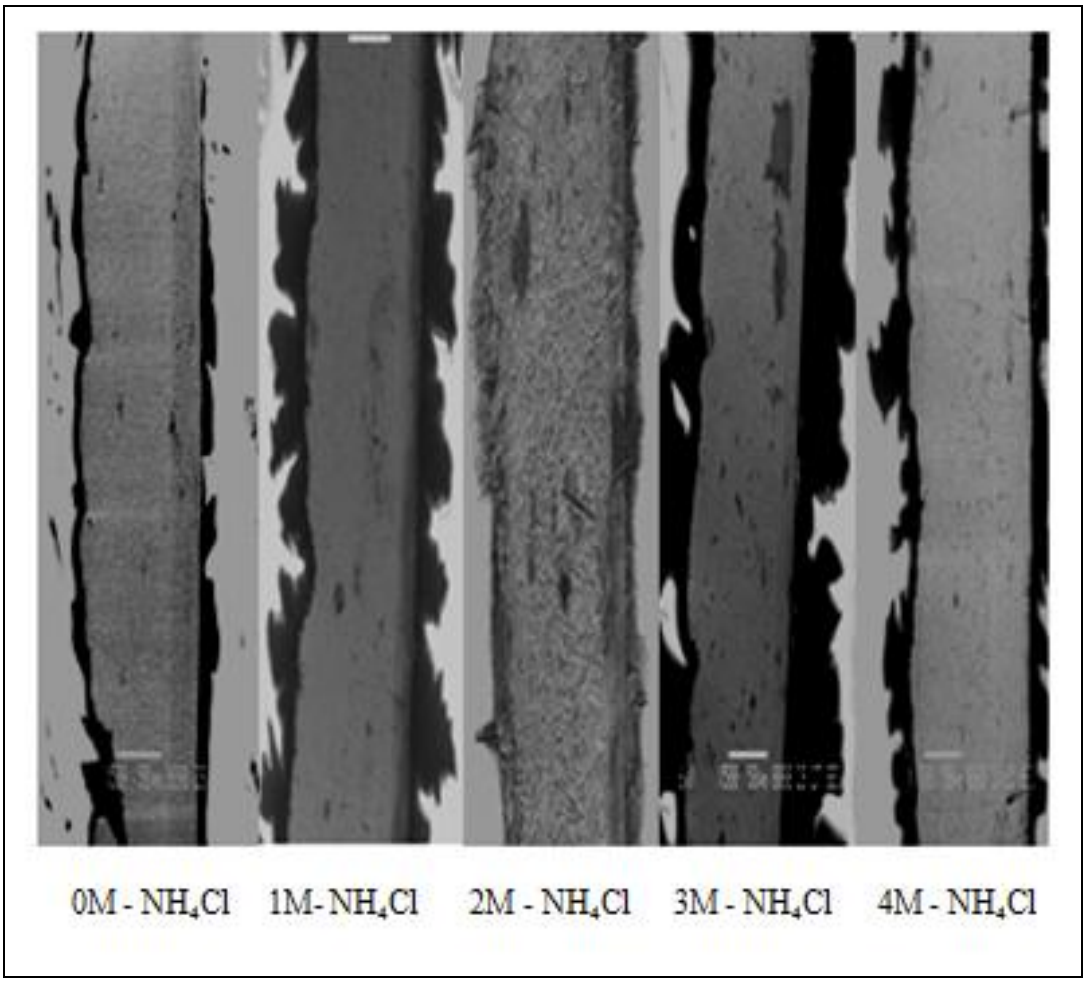

Figure 4.6: SEM cross sectional view of zinc electrodeposits

The microstructure of zinc electrodeposits prepared with deposition time of 45 minutes as depicted in Figure 4.7 shows similar general features to those prepared with deposition time of 90 minutes, of respective electrolytic bath formulations, i.e. the changes from hexagonal plane stacks to flakes microstructure and finally to foamy deposits. Among the variation noticed are as follows. Stacks of hexagonal plane are

more visible and compact for electrodeposits of basic $ZnCl_2$ bath. Flakes microstructure appeared from 2 M of NH_4Cl bath are much coarser than that of Figure 4.5c. Finally both the flakes microstructure and foamy deposits of 3 M-NH_4Cl and 4 M-NH_4Cl bath respectively seemed rather dense as compared to equivalent bath formulation in Figure 4.5.

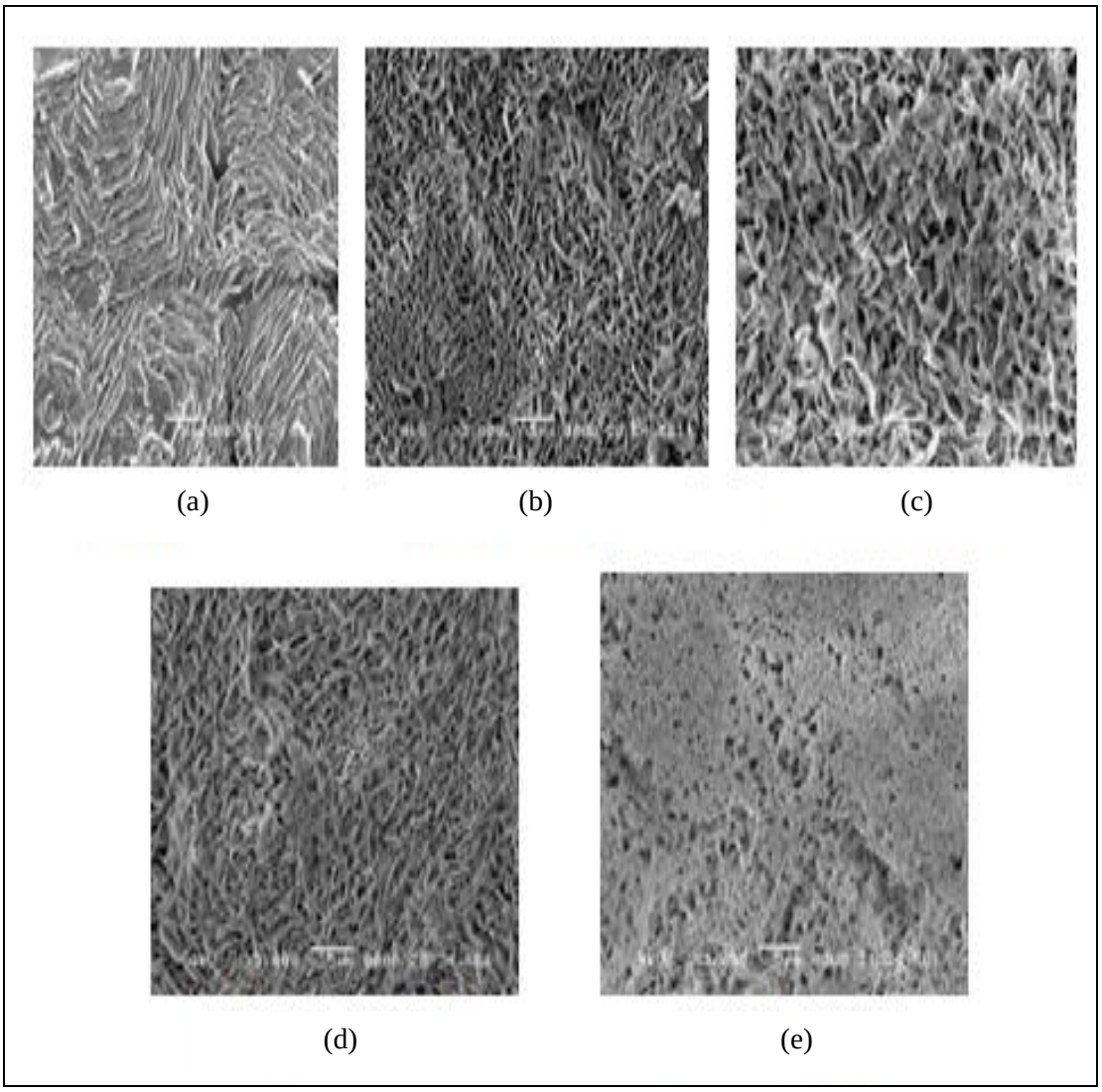

Figures 4.7: SEM images of zinc electrodeposits prepared with deposition time of 45 minutes deposition time (a) 2M $ZnCl_2$, (b) 2M $ZnCl_2$ – 1M NH_4Cl, (c) 2M $ZnCl_2$ – 2M NH_4Cl, (d) 2M $ZnCl_2$ – 3M NH_4Cl and (e) 2M $ZnCl_2$ – 4M NH_4Cl

As the deposition time was further increased to 180 minutes for each electrolytic bath, new features are observed as shown in Figure 4.8. The only similarity noticed is that flake microstructure appeared when NH_4Cl supporting electrolyte was introduced. However, stacks of hexagonal plane are replaced by very fine and dense electrodeposits that even at 3000X magnification the microstructure are not visible. Coarse flakes microstructure predominate the form of the electrodeposits. Only at 4 M-NH_4Cl bath the electrodeposits turned into tiny flakes network.

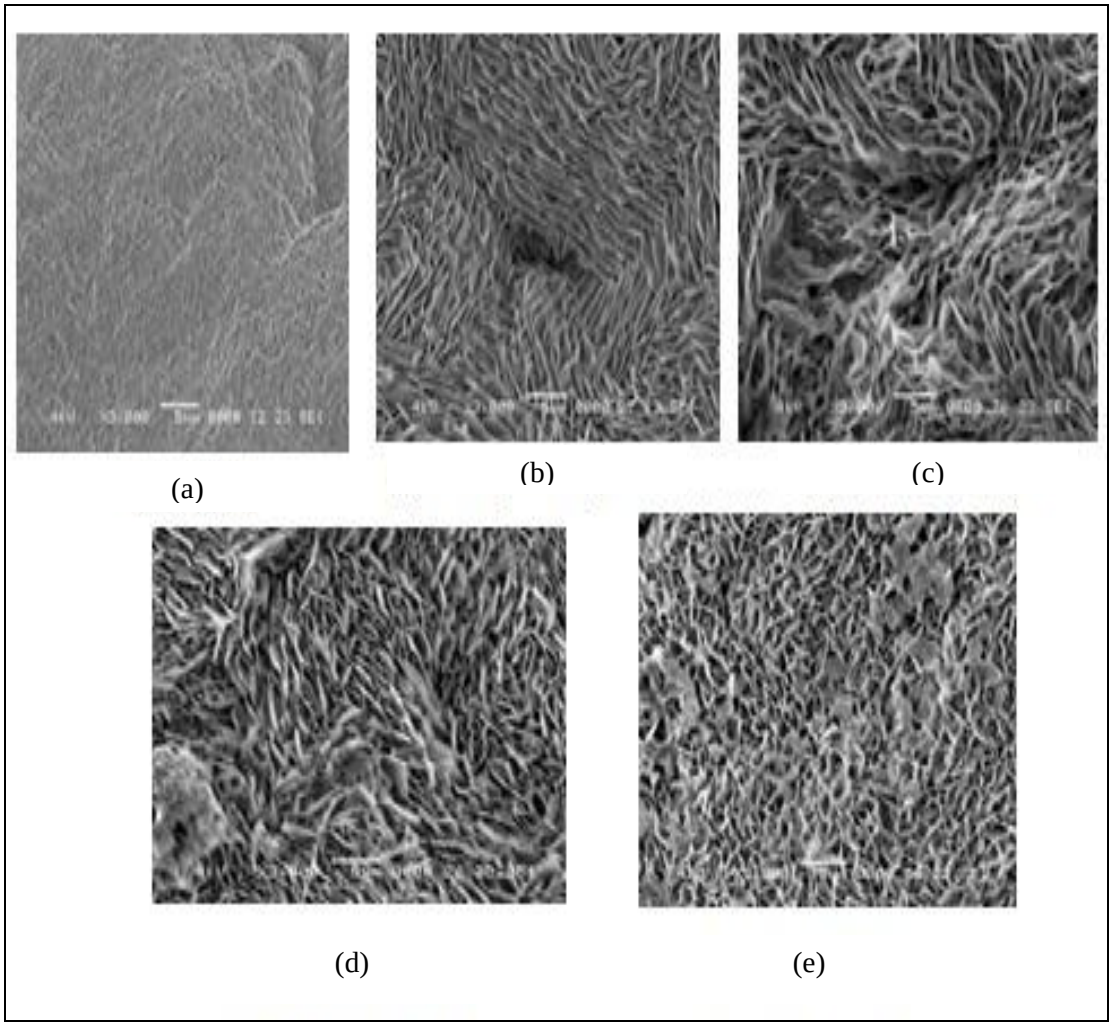

Figures 4.8: SEM images of zinc electrodeposits prepared with deposition time of 180 minutes deposition time (a) 2M $ZnCl_2$, (b) 2M $ZnCl_2$ – 1M NH_4Cl, (c) 2M $ZnCl_2$ – 2M NH_4Cl, (d) 2M $ZnCl_2$ – 3M NH_4Cl and (e) 2M $ZnCl_2$ – 4M NH_4Cl

In summary, SEM observation supported the XRD profiles that zinc electrodeposits prepared from different deposition duration, although of the same electrolytic bath formulation, possessed unique qualities. However, for deposition time of 45 - 90 minutes, zinc electrodeposits obtained from respective electrolytic bath formulations mentioned above, showed similar variation. The remaining characterizations discussed in the following sections were only performed for zinc electrodeposits prepared from 90 minutes duration.

4.5 BET Surface Area and Pore Volume Density

Figure 4.9 shows the variation of BET surface area and pore volume density with NH_4Cl content in the electrolytic bath formulation. Firstly, recall that the deposition area was 1 cm x 1 cm square area. Thus considering 0.25 mm zinc foil used as the working electrode as an example, and using zinc density as 7.14 g cm^{-3}, the apparent specific surface area of the zinc foil is 0.056 m^2/g. By using electrodeposition method, the specific surface area of zinc coatings is now more than 300 m^2g^{-1} which clearly demonstrates the advantage of electrodeposition method. Electrolytic bath with 3 M-NH_4Cl produced zinc electrodeposits with the highest specific surface area i.e. 379 m^2g^{-1}. It seems that the flakes network structure obtained from 3M-NH_4Cl bath (Fig. 4.5d) resulted in a high surface area zinc coating. On the other hand, electrolytic bath formulation with 2 M-NH_4Cl produced the most porous zinc electrodeposits i.e. with pore volume density of 0.227 cm^3 g^{-1} which is equivalent to 62 % porosity. Figure 4.10 compares the porosity data obtained from the nitrogen physisorption instrumentation with the densitometer measurement. It indicates a good agreement and the same trend.

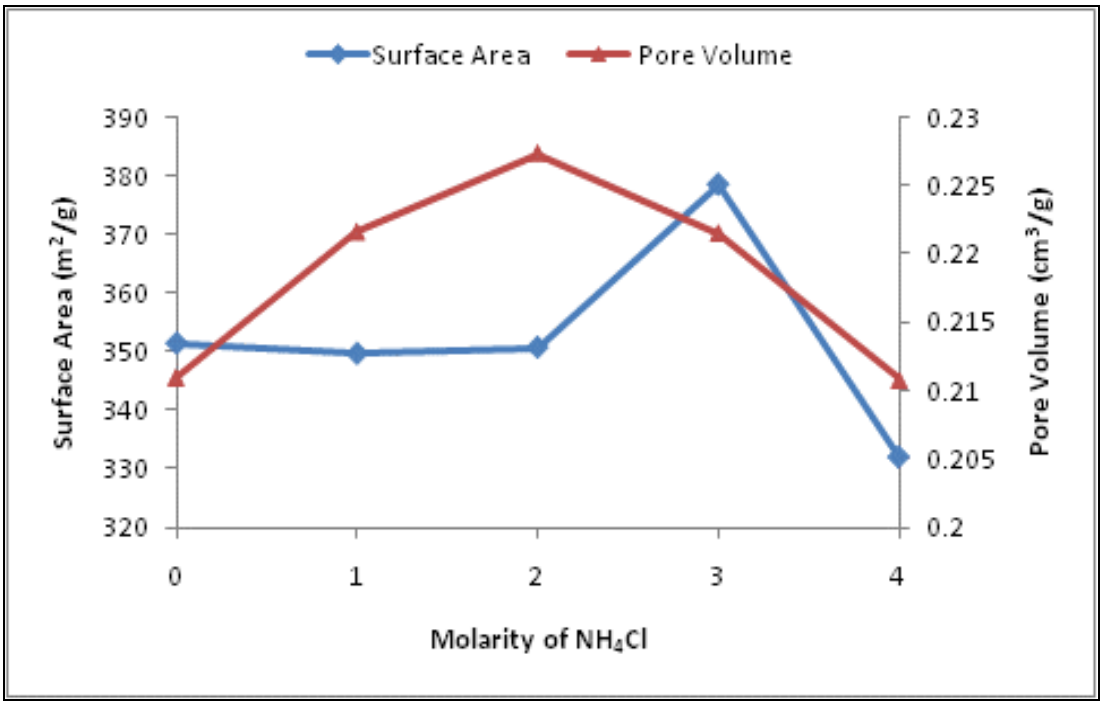

Figure 4.9: Variation of BET surface area and pore volume density with NH_4Cl content in the electrolytic bath formulation

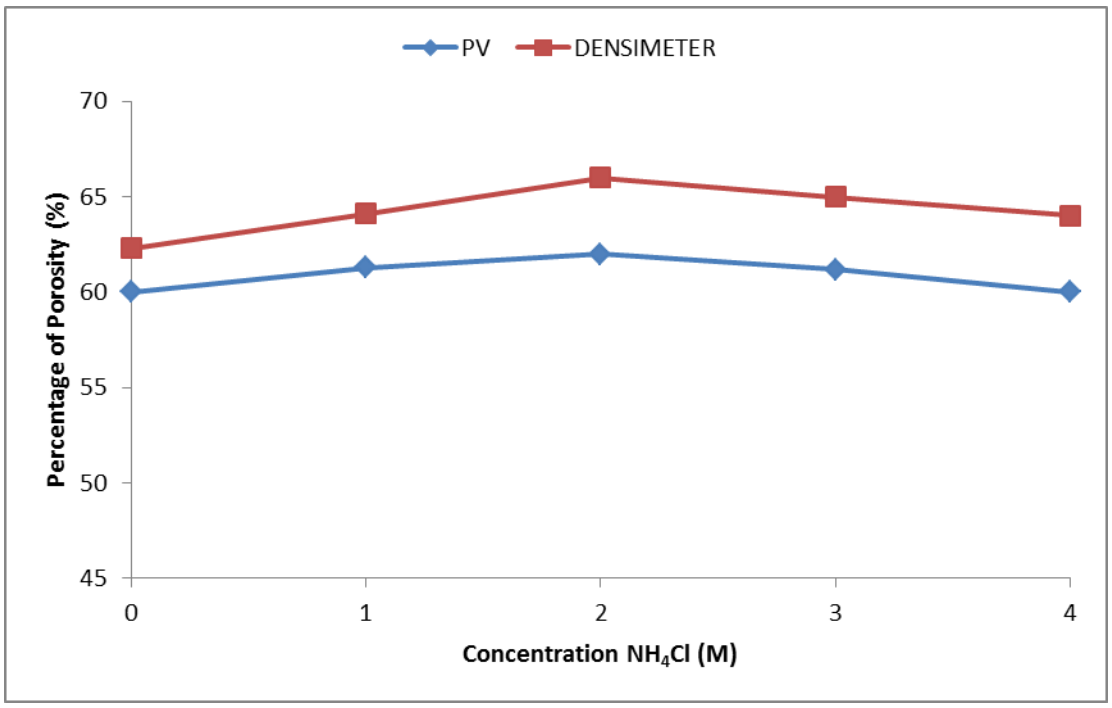

Figure 4.10: Porosity data obtained from the nitrogen physisorption instrumentation with the densitometer measurement

4.6 Zinc-air cell fabrication and electrochemical characterizations

Zinc electrodeposits prepared from all electrolytic bath formulations were assembled into zinc-air cell as the electronegative material or anode. The purpose is to directly correlate the physical properties of zinc electrodeposits with the electrochemical performance of the cell. For zinc-air cell, as the oxygen is not stored within the system, any variation in the electrochemical cell performance can be attributed almost exclusively on the zinc electrodeposits properties.

Figure 4.11 depicts the overlays of polarization profiles of zinc-air cell utilizing electrodeposited zinc anode from all electrolytic bath formulations. From these profiles, the limiting current density parameter of the cell can be extracted. Limiting current is the maximum discharge current that can be supplied by a cell prior to an abrupt voltage drop (refer to Fig. (3.5)). For zinc-air cell the abrupt drop occurs when the operating voltage reaches the value around 0.8 –0.9V.

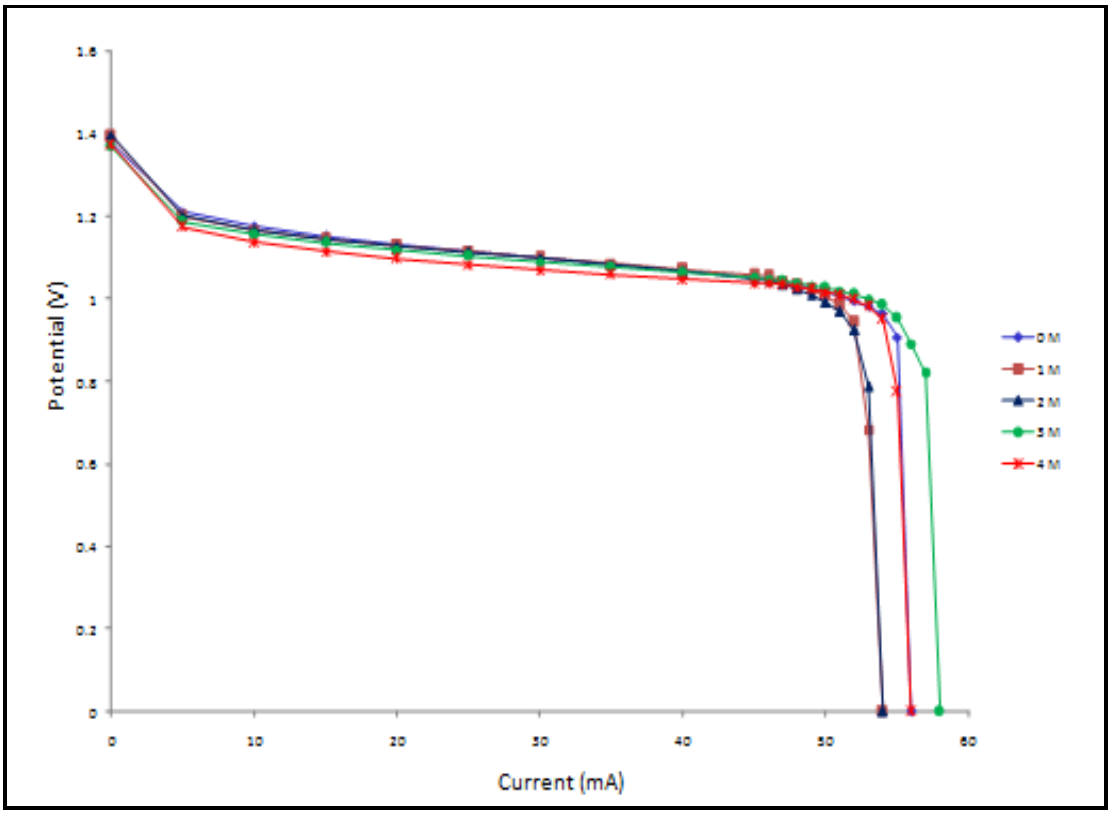

Figure 4.11: The overlays of polarization profiles of zinc-air cell utilizing electrodeposited zinc anode from all electrolytic bath formulations

Figure 4.12 presents the plot of limiting current density against the electrolytic bath formulation of which the zinc anode was prepared. The highest limiting current is obtained from zinc electrodeposits of 3 M-NH_4Cl bath i.e. 55 mA. Though the difference between the highest and lowest limiting current density value seems small, i.e. 3 mA, note that the cell size was 1 cm x 1 cm. If the apparent cell area is increased by ten times for example 33 mm x 33 mm, then the anticipated difference of 40 mA would be quite substantial.

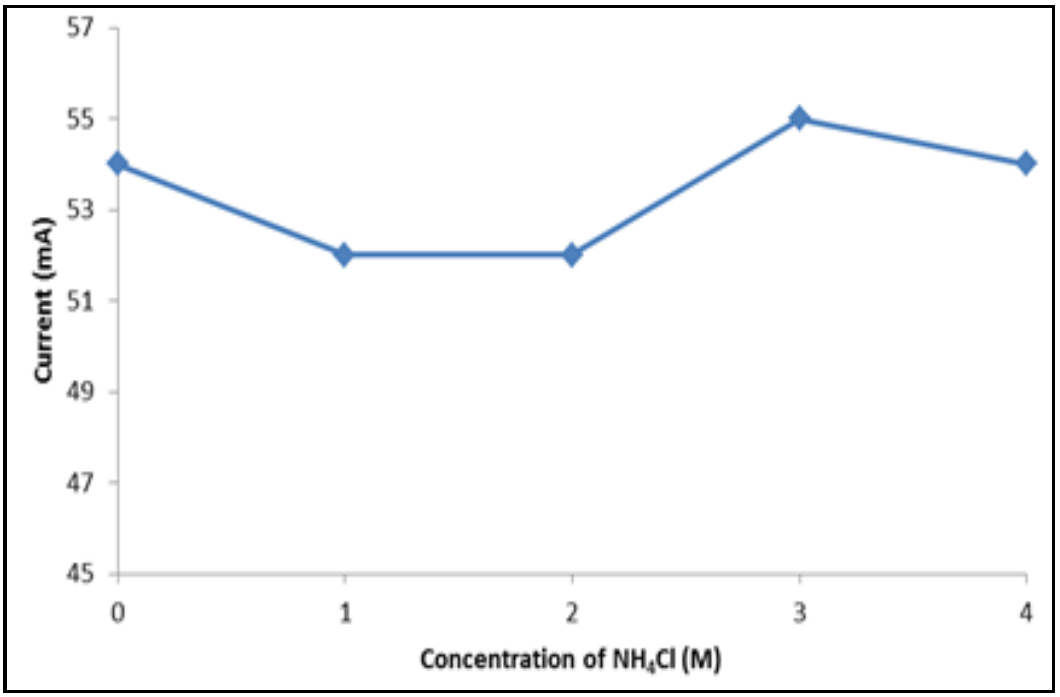

Figure 4.12: Plot of limiting current density against the electrolytic bath formulation

Cell capacity or discharge capacity is a measure of quantity of charge supplied per unit time by an electrochemical cell. It is customary measured in mAh (milliampere-hour) or Ah for large cells. A cell with capacity of 100 mAh means that if 100 mA of discharge current is utilized, then the cell discharge can last for an hour. However, it is only a rough estimate since cell capacity is a function of rated current.

Figure 4.13 displays the discharge profiles of zinc-air cell utilizing electrodeposited zinc anode prepared from 2M-NH_4Cl bath. The aim was to identify the discharge current to be used in rating the cell so as to get an optimum capacity. Firstly, note the distinct profile of zinc-air cell; the discharge curve is relatively flat with an abrupt voltage drop marks the end of discharge (Othman et al., 2002). This is mainly attributed to the fact that as the electropositive oxygen reactant is not stored within the electrochemical system, the changes in the internal resistance of the cell is small thus producing a rather flat discharge profile (Binder et al., 2002).

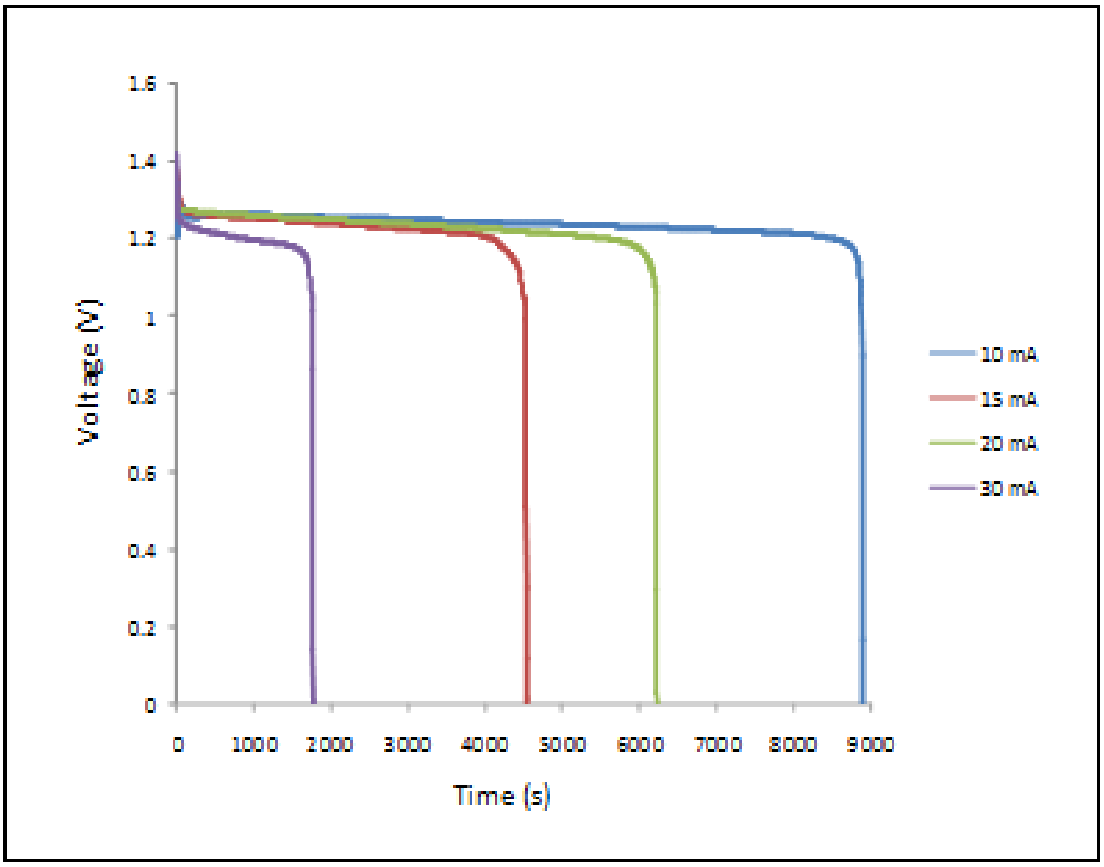

Figure 4.13: Discharge profiles of zinc-air cell utilizing electrodeposited zinc anode prepared from 2M-NH_4Cl bath

Figure 4.14 translates the discharge profiles of Figure 4.13 into discharge capacity values calculated from the product of discharge duration and rated current (Eq. 3.5). An optimum discharge capacity of 34.5 mAh is obtained when the cell is rated at 20 mA. Therefore for the subsequent characterization, rating current of 20 mA was used.

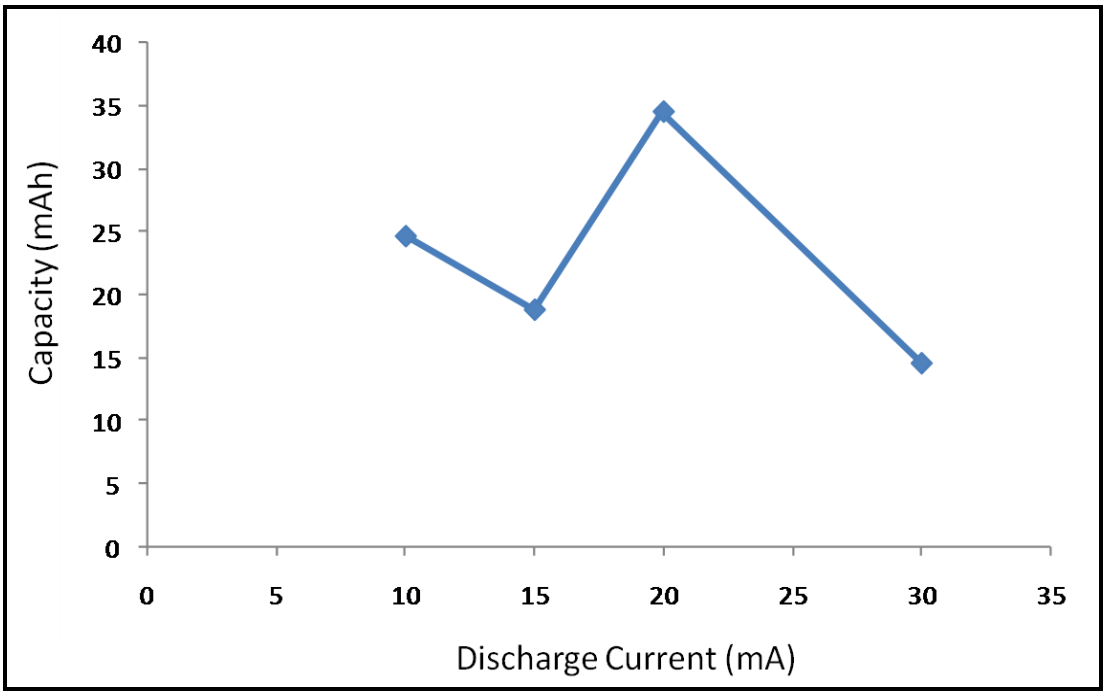

Figure 4.14: Discharge capacity values calculated from the product of discharge duration and rated current

Figure 4.15 shows the discharge profiles of zinc-air cell utilizing electrodeposited zinc anode prepared from all electrolytic bath formulations. The cells were rated at 20 mA of discharge load. The graph clearly reveals that the cell utilizing zinc electrodeposits of 2 M-NH_4Cl electrolytic bath produces the longest discharge duration i.e. 2 hours 15 mins. The highest cell limiting current density is found for zinc electrodeposits of 3 M-NH_4Cl bath whereas the highest cell capacity is obtained for zinc electrodeposits of 2M- NH_4Cl bath.

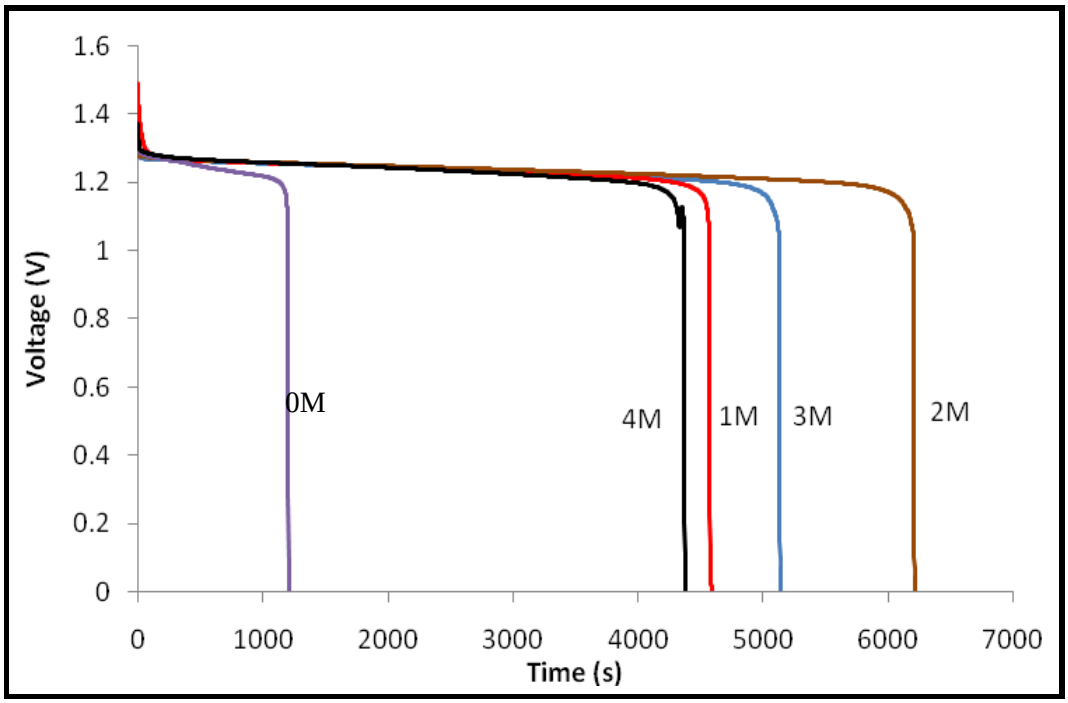

Figure 4.15: Discharge profiles of zinc-air cell utilizing electrodeposited zinc anode prepared from all electrolytic bath formulations

Interestingly the variation in limiting current density matches that of BET surface area and the trend for discharge capacity resembles that of pore volume density, as displayed in Figure 4.16 and Figure 4.17 respectively. These observations open up the possibility of using zinc-air electrochemical system to gauge porous zinc electrode properties. Zinc-air cell parameters of limiting current density and discharge capacity can be correlated with the electrode properties of specific surface area and pore volume density, respectively. Nitrogen physisorption characterization at 77 K as well as densitometer measurement supported these conjectures. Moreover, metal-air system in general could now be utilized to evaluate porous electrode properties. The following section further discusses on this prospect.

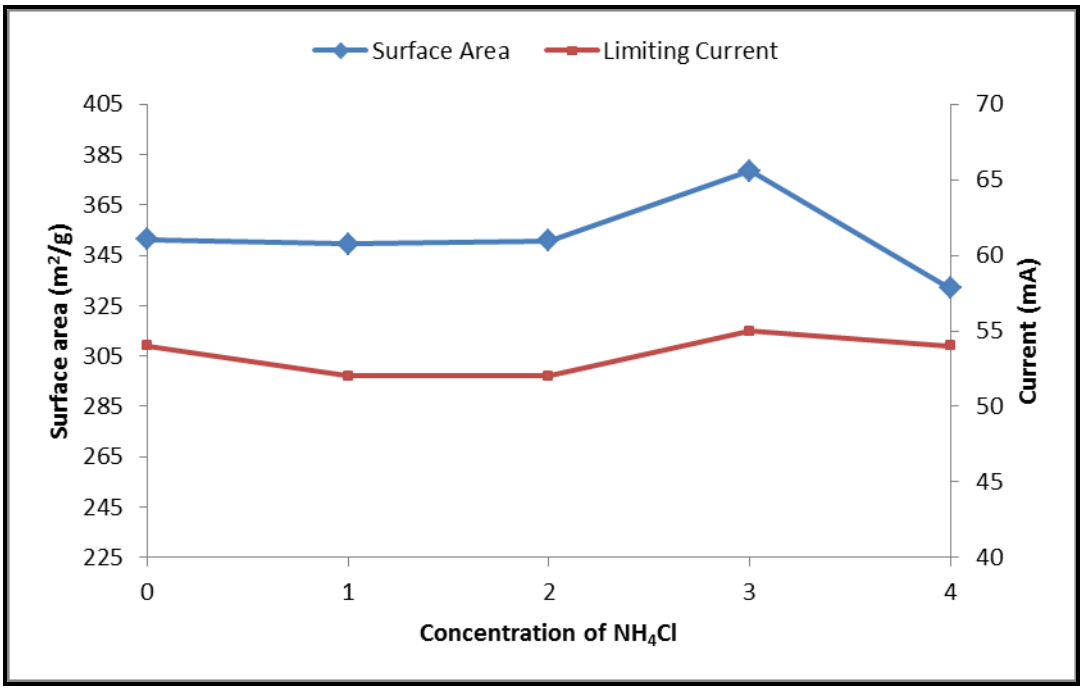

Figure 4.16: Variation in limiting current density of zinc-air cell and BET surface area of electrodeposited zinc anode with electrolytic bath formulation

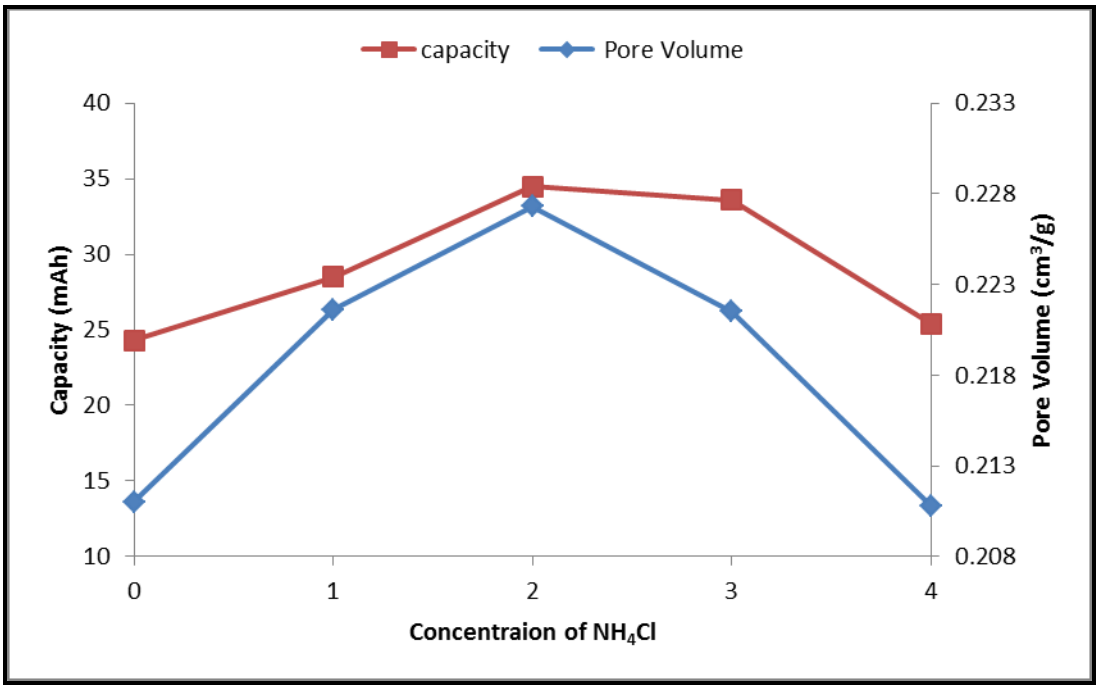

Figure 4.17: Variation in discharge capacity of zinc-air cell and pore volume density of electrodeposited zinc anode with electrolytic bath formulation

4.7 EVALUATION OF POROUS ELECTRODE PROPERTIES USING METAL-AIR ELECTROCHEMICAL SYSTEM

This chapter presented four different types of piezoelectric energy harvester designed based on the key design parameters that affect the performance of piezoelectric energy harvester. Cantilever structure has been identified as the most suitable structure for maximum energy conversion. The piezoelectric thin film material selection, doping effect, resonance frequency applied, and modes of operation applied, and volume of the proof mass are the vital design parameters Selection of piezoelectric material was also essential to get the optimize output power. Aluminium doped zinc oxide on stainless steel substrates is the preliminary design to observe the performance of aluminium doped zinc oxide as the piezoelectric layer. 4 inch <100> undoped and high resistivity silicon was chosen as the substrate. The next chapter discusses in detail the finite element simulation of proposed design of MEMS piezoelectric energy harvester.

Metal-air electrochemical system could be utilized as an alternative evaluation method for metal-based porous electrodes, and at a very low cost compared to nitrogen physisorption technique. As highlighted earlier, since the oxygen is not stored within the system and consumed directly from the ambient air surrounding, any variation in the electrochemical cell performance can be attributed almost exclusively on the metal anode properties i.e. the porous electrode properties in this context. Though it might not be a quantitative method, this method is particularly useful for rapid screening or defect detection purposes.

Other advantages include easy test cell assembly, does not require special sample preparation such as degassing, ambient temperature measurement, immediate data interpretation, quick results and low cost. Metals that have been extensively studied in metal-air system include aluminum (Doche et. al, 1997; MacDonald and English, 1990; Mukherjee and Basumallick, 1993; Niksa and Wheeler, 1988) and iron (Anderson and Ojefors, 1974; Cnobloch et. al, 1974; Kannan and Shukla, 1991).

4.8 SUMMARY

High surface area and porosity zinc electrodeposits have been successfully prepared by electrodeposition from $ZnCl_2$-NH_4Cl binary electrolyte. Electrolytic bath of 2 M NH_4Cl produced zinc electrodeposits with the highest BET surface area while electrolytic bath of 3 M NH_4Cl produced zinc electrodeposits with the highest pore volume density or porosity. Zinc-air microbattery, utilizing the electrodeposited zinc anode, was able to deliver high limiting current density. It was also discovered that the variation in pore volume density or porosity of the zinc electrodeposits resembled the trend for discharge capacity of the cell. On the other hand, the changes in BET surface area of zinc electrodeposits matched that of limiting current density of zinc-air cell.

CHAPTER FIVE

CONCLUSION AND RECOMMENDATION

5.1 CONCLUSION

Zinc electrodeposits have been prepared from a $ZnCl_2$-NH_4Cl acidic bath. The metal source, zinc chloride ($ZnCl_2$), was fixed to a concentration of 2 M, whereas the concentration of the supporting electrolyte, ammonium chloride (NH_4Cl), was varied from 0 - 4 M. Each electrolytic bath formulation produced unique electrodeposits characteristics.Though all electrodeposition parameters were fixed, zinc electrodeposits prepared from different deposition time of 45, 90 and 180 minutes, respectively, possessed different morphology and most likely different characteristics, as determined from the X-ray diffraction measurement and supported by Scanning Electron Microscopy observation. This is the key attribute of electrodeposition technique. Often times, apart from various deposition parameters, namely chemical compositions, quantity of electrolyte, agitation, temperature, substrate material, electrodes spacing, deposition current, deposition time, pH, temperature etc., even a specific electrolytic bath design will give unique electrodeposits properties. Besides, each deposition parameter may interact with one other producing a distinctive effect. As such, an electrodeposition process must be thoroughly described to ensure reproducibility.

XRD patterns and supported by SEM observations were used as main tools to identify variation in zinc electrodeposits characteristics. At least for deposition duration 45 – 90 minutes, minimum variation in electrodeposits properties could be expected. SEM micrographs reveal unique porous network morphology of zinc

electrodeposits. As ammonium chloride supporting electrolyte was introduced, the microstructure changes from hexagonal plane stacks to flakes form. When ammonium chloride concentration increases, flake microstructure becomes predominant and finally turned into foamy deposits. However when the deposition time was doubled to 180 minutes, a totally new crystallographic orientation and electrodeposits microstructure were obtained. Thus, the subsequent results obtained in this work were only valid for zinc electrodeposits prepared for duration of 45 – 90 minutes, for the parameters and set up as described earlier.

High surface area and porous of zinc electrodeposits have been prepared by electrodeposition; the BET surface area was in excess of 330 m^2 g^{-1} and the electrode porosity was at least 60 %, as determined from the nitrogen physisorption characterization. Electrolytic bath of 3 M -NH_4Clproduced zinc electrodeposits with the highest BET surface area i.e. 379 m^2g^{-1}while electrolytic bath of 2 M -NH_4Cl resulted in the zinc electrodeposits with highest pore volume density i.e. 0.2273 cm^3 g^{-1} which is equivalent to 62 % porosity. Zinc-air microbattery, 1 cm^2 area x ca. 305 µm thick, utilizing the electrodeposited zinc anode was able to deliver a maximum limiting current density of 55 mA cm^{-2} and produced an optimum discharge capacity of 34.5 mAh rated at 20 mA. Interesting correlations were observed between the properties of electrodeposited zinc anode and the electrochemical characteristics of zinc-air cell. The changes in BET surface area of zinc electrodeposits prepared from various electrolytic bath formulations matched that of limiting current density of zinc-air cell. Furthermore, the variation in pore volume density or porosity of the zinc electrodeposits resembled the trend for discharge capacity of the cell. These observations supported the conjecture that zinc-air system or metal-air system in

general could be used as low cost and rapid tools to screen porous electrode properties.

5.2 RECOMMENDATIONS FOR FUTURE RESEARCH

The most interesting finding was the correlation between the physical properties of zinc electrodeposits i.e. specific surface area and pore volume density, with the electrochemical performance of zinc-air cell utilizing the electrodeposited anode, namely, limiting current density and discharge capacity, respectively. These correlation could serve as a novel method to characterize porous electrode properties; utilizing metal-air electrochemical system. From the present work, it seemed that the proposed approach is not a quantitative method and is particularly useful for rapid screening or defect detection purposes. However, it is believed that for a certain experimental regime, a quantitative correlation could be established.

Although all electrodeposition parameters were fixed, zinc electrodeposits prepared from different deposition time of 45, 90 and 180 minutes, respectively, revealed different crystallography orientations, as determined from the X-ray diffraction measurement and supported by Scanning Electron Microscopy observation. It is interesting if one could focus particularly on the preferred crystal structure as a function of the electrolytic bath formulations.

Electrodeposition is a highly sensitive technique. A particular experimental set up will produce unique characteristics. As such, for electrodeposition parameters and set up used in this work alone, there are scores of possibilities to be studied. Among others, various $ZnCl_2$-NH_4Cl binary electrolytic bath formulations and other electrolyte combinations such as $ZnSO_4$ – K_2SO_4 bath, bath temperature, current density, electrolyte additives, electrode spacing, substrate material etc. For

characterization of the electrodeposits another useful instrument to be considered is cyclic voltammetry technique.

BIBLIOGRAPHY

Alfantazi, A. M. & Dreisinger, D. B. (2001). The role of zinc and sulfuric acid concentrations on zinc electrowinning from industrial sulfate based electrolyte. *J. Appl. Electrochem.,* 31, 641–646.

Andersson, B. & Ojefors, L. (1975). Optimization of iron-air and nickel oxide-iron traction batteries: Power Sources 5, *10th International Symposium on 'Research and Development in Non-Mechanical Electrical Power Sources 1974'*. London: Academic Press, Inc., 329-343.

Appleby, A. J. & Jacquier, M. (1977). The C.G.E. circulating zinc/air battery: A practical vehicle power source. *J. Power Sources* 1, 17-34.

Baik, D. S. & Fray, D. J. (2001). Electrodeposition of zinc from high acid zinc chloride solutions, *J. Appl. Electrochem.,* 31, 1141–1147.

Barbic, P. A., Binder, L., Voss, S., Hofer, F. & Grogger, W. (1999).Thin-film zinc/manganese dioxide electrodes based on microporous polymer foils. J. Power Sources, 79, 271.

Bard, A. J. & Larry, R.F. (2000). *Electrochemical Methods: Fundamentals and Applications* (2nd edn.). Wiley.

Beck, J. S., Vartuli, J. C., Roth, W. J., Leonowicz, M. E., Kresge, C. T., et al. (1992). A new family of mesoporous molecular sieves prepared with liquid crystal templates. *J. Am. Chem. Soc*., 114, 10834.

Binder, S. F., Cretzmeyer, J. W. & Reise, T .F. (2002). D. Linden (ed.), *Handbook of Batteries* (3rdedn), New York: McGraw-Hill, Inc., 13.1.

Binder, L. & Kordesch, K. (1986). Electrodeposition of zinc using a multi-component pulse current. *ElectrochimiaActa***.**31, 255-262.

Brodd, Bullock, K. R., Leising, R. A., Middaugh, R. L., Miller, J.R. & Akeuchi, E. (2004). Batteries 1977 to 2002. *J. Electrochem. Soc*., 151, K1-K11.

Burggraaf & Cot, L. (1996). *Fundamentals of Inorganic Membrane Science and Technololgy*. Elsevier, Amsterdam., 6.

Cnobloch, H., Groppel, D., Kuhl, D., Nippe, W. & Siemsen, G. (1975). Performance of iron-air secondary cell under practical operation conditions: Power Sources 5, *10th International Symposium on Research and Development in Non-Mechanical Electrical Power Sources 1974,* London: Academic Press Inc., 261-282.

Cho, Y. D. & Fey, G. T. (2008). Surface treatment of zinc anodes to improve discharge capacity and suppress hydrogen gas evolution. *J. Power Source*, 184 ,610.

Chu, Breen, J. M.& Adzic, G. (1981). *J. Electrochem. Soc.*, 128, 2282.

Crompton. (2000). Metal air batteries: *Batteries Reference Book (3rd edn)*, Newnnes., 12/1 and 26/1.

Despic, Pavlovd, R. & Pavlovd, M. G. (1982). Deposition of zinc of foreign substrates. *ElectrochemActa,* 27, 1539.

Dini. (1995). Electrodeposition: *The Material Science of Coatings and Substrates*. New Jersey: Noyes Publications.

Doche, M. L., Novel-Cattin, F., Durand, R. & Rameau, J.J. (1997). Characterization of different grades of aluminium anodes for aluminium/air batteries. *J. Power Sources,* 65, 197-205.

Dwarakadasa, Dambal, R. P. & Balachandra, I. (1988). Electrodeposition and Electroforming proceedings of the International Conference on *Electrodeposition and Electroforming*, Tata: McGraw-Hill, Inc.

Falk, S. U.& Salkind, A. J. (1969). *Alkaline Storage Batteries*, John Wiley and Sons Inc. Chap.3.

Galvani & Carlos, L.A. (1997). Effect of the additive glycerol on zinc electrodeposition on steel, *Met. Finish.*,2, 70–72.

Glasstone. (1943). The Fundamentals of Electrochemistry and Electrodeposition, *American Electroplaters Society* .

Gupta, K. & Jena, A. K. (1999). A Novel Technique for Surface Area and Particle Size Determination of Components of Fuel Cells and Batteries Filtration News, 17, 40.

Haynes. (1973). Pore size analysis according to Kelvin equation. *Materiaux Et Construction*, 6, 33.

Ji, L., Katiyar, A., Pinto, N. G., Jaroniec, M. &Smirniotis, P.G. (2004). Al-MCM-41 sorbents for bovine serum albumin: relation between Al content and performance, *MicroporousMesoporous Mater*, 75, 221–229.

Jin, X.& Lu, J. (2001). Simplied methods for determining the ionic resistance in a porous electrode using linear voltammetry, *Power Sources*, 93, 8.

Kannan, A. M. & Shukla, A. K. (1991). Rechargeable iron/air cells employing bifunctional oxygen electrodes of oxide pyrochlores, *J. Power Sources,* 35, 113-121.

Karge & Weitkamp., J. (1998). *Molecular Sieves* 1, Netherland: Springer, 157.

Kim, Popov, B. N. & Chen, K. S. (2003). A Novel Electrodeposition Process for Plating Zn-Ni-Cd Alloys. *J. Electrochem. Soc*., 150, 1505.

Kresge, C. T., Leonowicz, M. E., Roth, W. J., Vartuli, J. C. & Beck, J. S. (1992). Ordered mesoporous molecular sieves synthesized by a liquid-crystal template mechanism. *Nature,* 359, 710.

Kriegsmann, J. J. & Cheh, H. Y. (1999). The importance of the equilibrium zincate ion concentration in modeling a cylindrical alkaline cell. *J. Power Sources* , 77 , 127.

Lasia, A. (1997). Porous electrodes in the presence of concentration gradient. *J. Electroanal. Chem.,* 428, 155-164.

Li, Jiang, L. L., Zhang, W. Q., Qian, Y. H., Luo, S. Z.& Shen, J. N. (2007). Electrodeposition of nanocrystalline zinc from acidic sulfate solutions containing thiourea and benzalacetone as additives. *J. Solid State Electrochem.,* 11, 549–553.

Lin, C. S., Lee, H. B. & Hsieh, S. H. (2000). Microstructure and formability of ZnNi alloy electrodeposited sheet steel. *Metal. Trans*., A 31, 475.

Lin. Y. P. & Selman, J. R. (1991). Periodic-Current-Modulation Effects in Alkaline and Acidic Electrodeposition of Zinc. *J. Electrochem. Soc*., 138, 3525.

Lindbergh, G. (1997). Experimental determination of the effective electrolyte conductivity in porous lead electrodes in the lead-acid battery. *Electrochim.Acta,* 42, 1239.

Linden. (2001). *Handbook of Batteries* (3rd edn), McGraw Hill, Inc.

Loto, Olefjord, I. & Mattsson, H. (192). Surface effects of organic additives on the electrodeposition of zinc on mild steel in acid–chloride solution. *Corros. Prevent. Control.*, 8, 82–88.

MacDonald, D. D. & English, C. (1990). Development of anodes for aluminium/air batteries-solution phase inhibition of corrosion. *J. Appl. Electrochem*., 20, 405-417.

Marozzi, C.A. &Chialvo, A.C. (2000).Development of electrode morphologies of interest in electrocatalysis: Part 2: Hydrogen evolution reaction on macroporous nickel electrodes. *Electrochim.Acta* , 45, 2111.

Matheson, L. A. & Nichols, N. (1938). *J. Electrochem. Soc.,* 73, 193.

McBreen, J. (1984). Rechargeable zinc batteries. *J. Electroanal. Chem*., 168, 415-432 .

McBreen, J. (1981). Secondary batteries-Introduction: A. Bockris, J.O'M., Conway, B.E., Yeager, E. and White, R., *Comprehensive Treatise of Electrochemistry.* New York: Plenum Press, 3, 303-335.

Millet, Gravria, M., Mazille, H., Marchandise, D. & Cuntz, J. M. (2000). Electrolytic deposition and corrosion resistance of Zn–Ni coatings obtained from sulphate-chloride bath. *Surf.Coat. Technol.,* 123, 164.

Mukherjee, A. & Basumallick, I. N. (1993). Matallized graphite as an improved cathode material for aluminium-air batteries. *J. Power Sources*, 45, 243-346

Newman, J. & Tiedemann,W. (1975). Porous-electrode theory with battery applications. *AIChE J*., 21, 25.

Niksa, M. J. & Wheeler, D. J., (1988). Aluminium-oxygen batteries for space applications. *J. Power Sources,* 22 , 261-267.

Othman, R., Yahaya, A. H. & Arof, A. K. (2002). Zinc-air cell employing porous zinc electrode fabricated from zinc-graphite-natural biodegradable polymer paste. *J. Appl. Electrochem.,* 32 ,1347-1353.

Panagopoulos, C. N., Georgarakis, K. G. & Petroutzakou, S. (2006). Sliding wear behaviour of zinc–cobalt alloy electrodeposits. *J. Mater. Process. Technol.,* 160 , 234–244.

Pagotto Jr., S. O., Alvarenga Freira, C. M. & Ballester, M. (1999). Influence of voltammetric parameters on Zn–Ni alloy deposition under potentiodynamic conditions. *Surf.Coat.Techol.*,122, 10.

Paramonov, V.A. & Levenkov, V.V. (2004). Production of automobile sheet with coatings, *Metallurgist*,48, 473–477

Paunovic, M. & Schlesinger, M. (1998). *Fundamentals of Electrochemical Deposition*, New York: A Wiley–Interscience Publication.

Pourbaix. (1996). Atlas of Electrochemical Equilibria: *Aqueous Solutions*, Pergamon, London.

Ramanauskas, R. (1999). Electrochemical studies of zinc–cobalt alloy coatings deposited from alkaline baths containing glycine as complexing agent. *Appl. Surf. Sci.,* 153, 53.

Rand, D. A. J. (1979). Battery Systems for Electric Vehicles: State of the Art Review. *J. Power Sources*, 4, 101.

Randles, J. E. B. (1948). A cathode ray polarograph. Part II.—The current-voltage curves. *Trans. Faraday Soc.*,44, 327.

Raub. (1973). Comprehensive Treatise of Electrochemistry*: Electrochemical Processing.* New York and London:Plenum Press, Vol.2.

Safranek. (1986.). The Properties of Electrodeposited Metals and Alloys. AESF: Florida.

Saputra, H. (2003). Masters Thesis, Osaka University, Japan.

Saputra, H., Othman, R., Sutjipto, A. G. E. & Muhida, R. (2011). *J. Mem.Sci.*,367 , 152.

Senders. (1999). Presented in Chem Show, New York, 35.

Sekar & Jayakrishnan, S. (2006). Characteristics of zinc electrodeposits from acetate solutions . *J. Appl. Electrochem.,* 36, 591.

Szekeres, Toth, J. & Dekany, I. (2002). Various Experimental Methods Langmuir. *American Chemical Society,* 18, 2678.

Trejo, Ortego, B. R. & Meas, V. S. (1998). Simulation of the Effect of Additives on Electrochemical Nucleation. *J. Electrochem Soc.*,145, 4090.

Trejo, Ruiz, H., Ortega Borges, R. & and Meas, Y. (2001). *J. Appl. Electrochem.*, 31, 685.

Varghese. (1993). Electroplating and other Surface Treatments: *A Practical Guide*. New Delh :Tata McGraw – Hill, Inc., 85-86.

Vagramyan & Solo'eva, Z. A. (1961). *Technology of Electrodeposition Translated by A. Behr*. Teddington:Robert Draper Ltd, 372.

Veeraraghavan, Haran, B. Prabu, S. & Popov, B. (2003) .*J. Elctrochem. Soc.,* 150,B131.

Vermilyea. (1995). *J. Electrochem.Soc.,* 106, 66.

Wen & Hu, C. C (1992). *J. Electrochem.Soc.*, 139, 2163.

Wery, Catonne, J. C. & Hihn, J. Y. (2006). Barrel zinc electrodeposition from alkaline solution .*J. Appl. Electrochem.,* 30, 165.

Yan, Boden, P. J., Haris, S. J. & Dowes, J. (1994). *Philosophical Magazine A*, 70, 391.

Ye & Xing-Pu. (1994). *J.Electrochem Soc.*, 141, 2698.

Ye ,Celis, J. P., De Bonte, M. & Roas, J. R. (1994). *J. Electrochem. Soc.*,141, 2699.

Yim, Hwang, W. S. & Hwang, S. K. (1995). Crystallographic texture and microstructure of electrogalvanized layer in acid sulfate solution. *J. Electrochem. Soc.*, 142, 2604.

Younman. (2000). *J. Appl. Electrochem.*, 30, 55.

Youssef, Koch. C. C. & Fedkiw, P.S. (2004). Improved corrosion behaviour of nanocrystalline zinc produced by pulse current electrodeposition. *Corros. Sci.*,46, 51.

Zhang. (1996). Corrosion and Electrochemistry of Zinc. New York: Plenum, 7

Zuniga, Ortega, R., Meas, Y. & Trejo, G. (2004). Electrodeposition of zinc from an alkaline non-cyanide bath: influence of a quaternary aliphatic polyamine. *Plat. Surf.Finish.*,91, 46.

LIST OF PUBLICATIONS

Journals

I. Journal Paper

i. A. L. Nor Hairin, Raihan Othman, M. H. Ani and H. Saputra, "Evaluation of Porous Electrode Properties Using Metal-Air Electrochemical System", Adv. Mater. Res., *under review*

ii. A. L. Nor Hairin, Raihan Othman, M. H. Ani and H. Saputra, "High Discharge Rate Electrodeposited Zinc Electrode For Use in Alkaline Microsystems", IIUM Eng. J, 12 (2011) 115-122

II. International Conference

i. A.L. Nor Hairin, Hens Saputra, M. H. Ani and Raihan Othman, "Optimization of Zinc Electrodeposition from Zinc-Air Cell Discharge Performance", 3rd International Conference on Functional Materials and Devices (ICFMD), Kuala Terengganu, Terengganu, Malaysia, 14-17 June, 2010, Centre for Ionics, University of Malaya

LIST OF AWARDS

Bronze Medal

Hens Saputra, A.L. Nor Hairin, A.G.E. Sujipto, R. Muhida, M.H. Ani and Raihan Othman "A Breathing Microbattery: Zn/MCM-41/O_2 System", Malaysia Technology Exhibition 2010 (MTE 2010), February 2010, Kuala Lumpur.

Hens Saputra, A.L. Nor Hairin, A.G.E. Sujipto, R. Muhida, M.H. Ani and Raihan Othman "A Breathing Microbattery: Zn/MCM-41/O_2 System", International Islamic University Malaysia Research Innovation and Exhibition (IRIE 2010), February 2010, Kuala Lumpur.

Silver Medal

A.L. Nor Hairin, Hens Saputra, M.H. Ani and Raihan Othman "A Novel Method to Evaluate Metallic Coating Properties Metal-Air Electrochemical System", International Islamic University Malaysia Research Innovation and Exhibition (IRIE 2011), February 2011, Kuala Lumpur.

APPENDIX A: X-Ray Difractogram of Zinc Electrodeposits

Fig. A1
XRD of zinc electrodeposits from 2M-$ZnCl_2$ bath prepared for 45 minutes

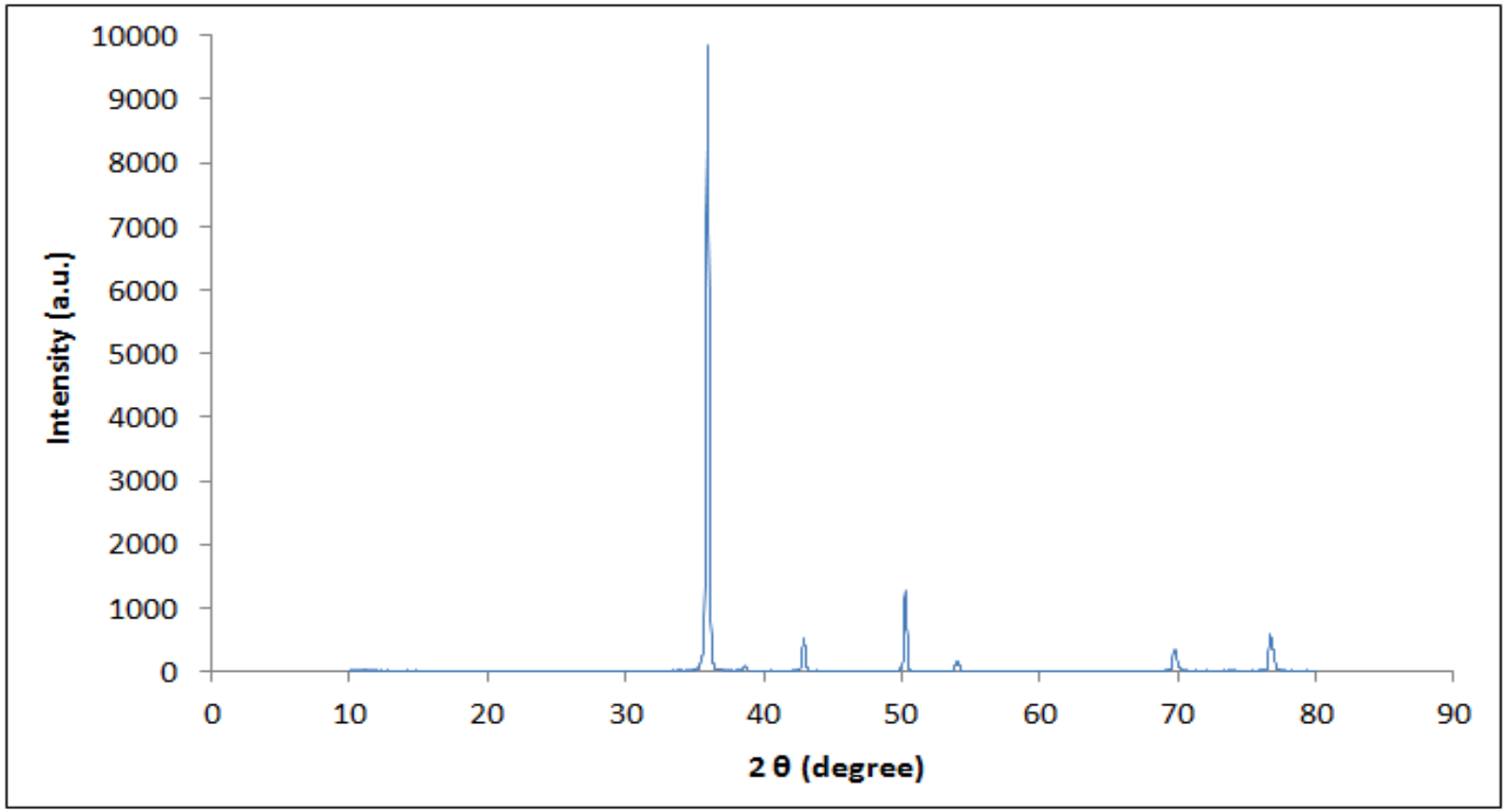

Fig. A2
XRD of zinc electrodeposits from 1M-NH_4Cl bath prepared for 45 minutes

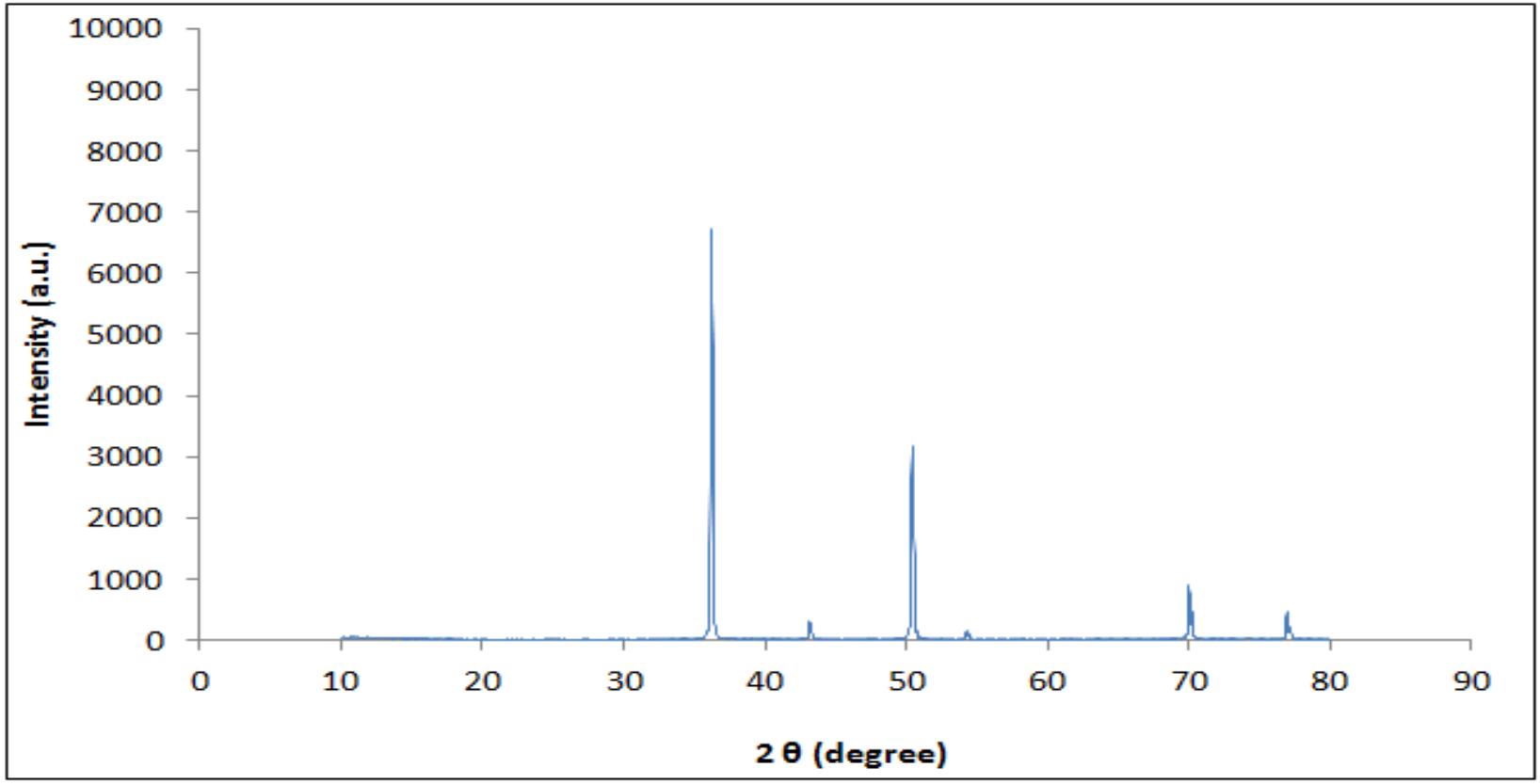

Fig. A3
XRD of zinc electrodeposits from 2M-NH_4Cl bath prepared for 45 minutes

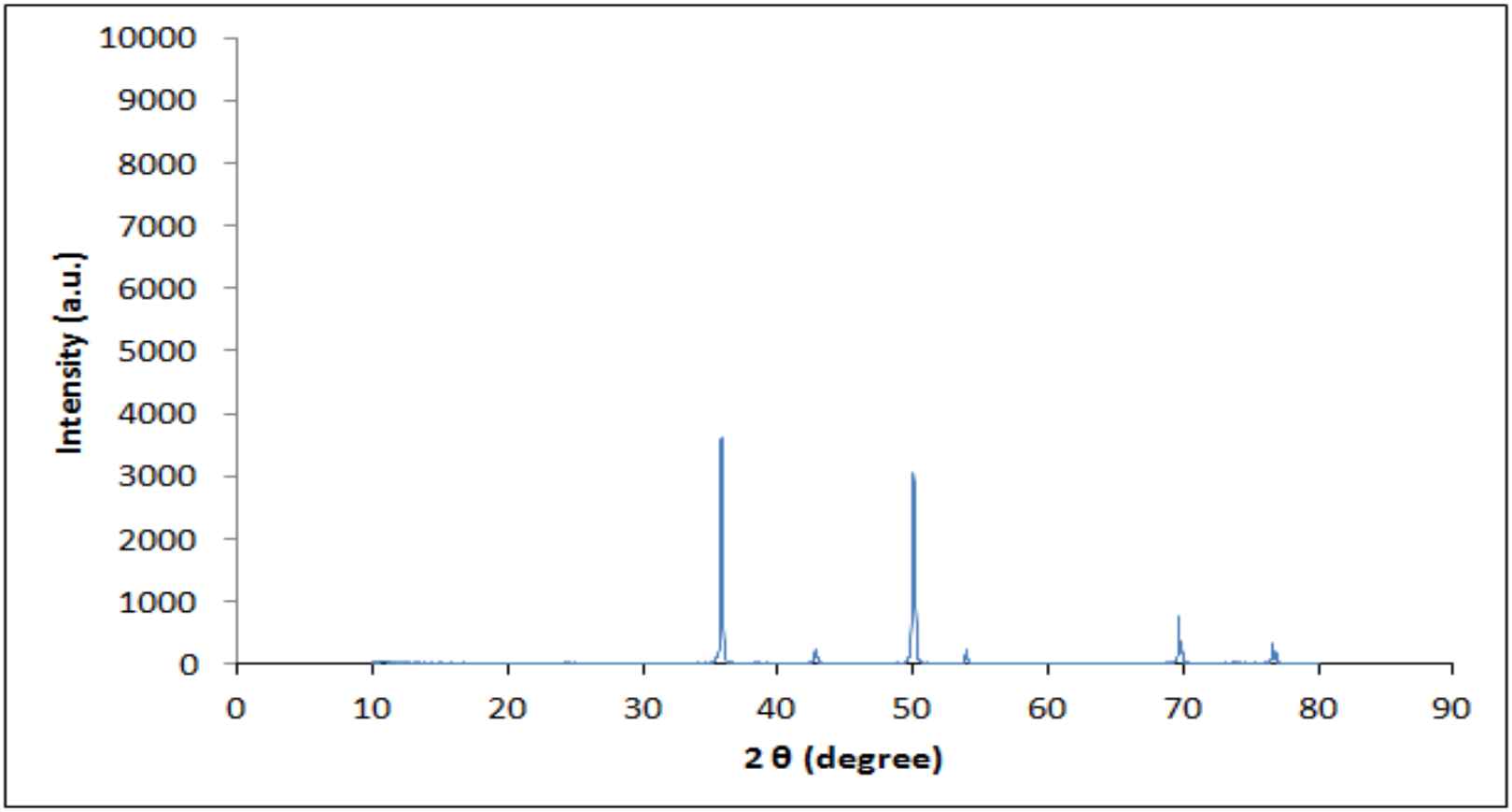

Fig. A4
XRD of zinc electrodeposits from 3M-NH_4Cl bath prepared for 45 minutes

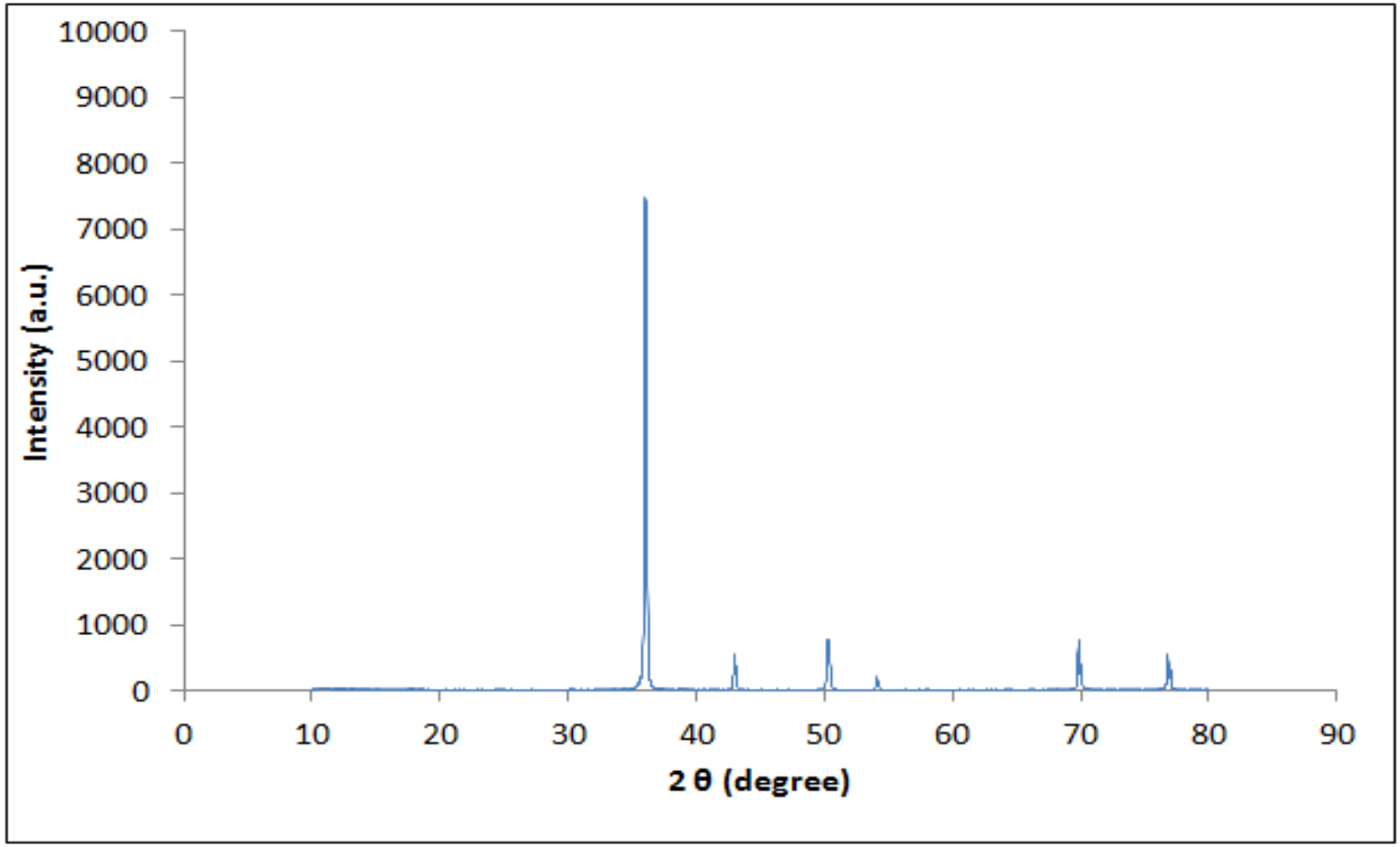

Fig. A5
XRD of zinc electrodeposits from 4M-NH_4Cl bath prepared for 45 minutes

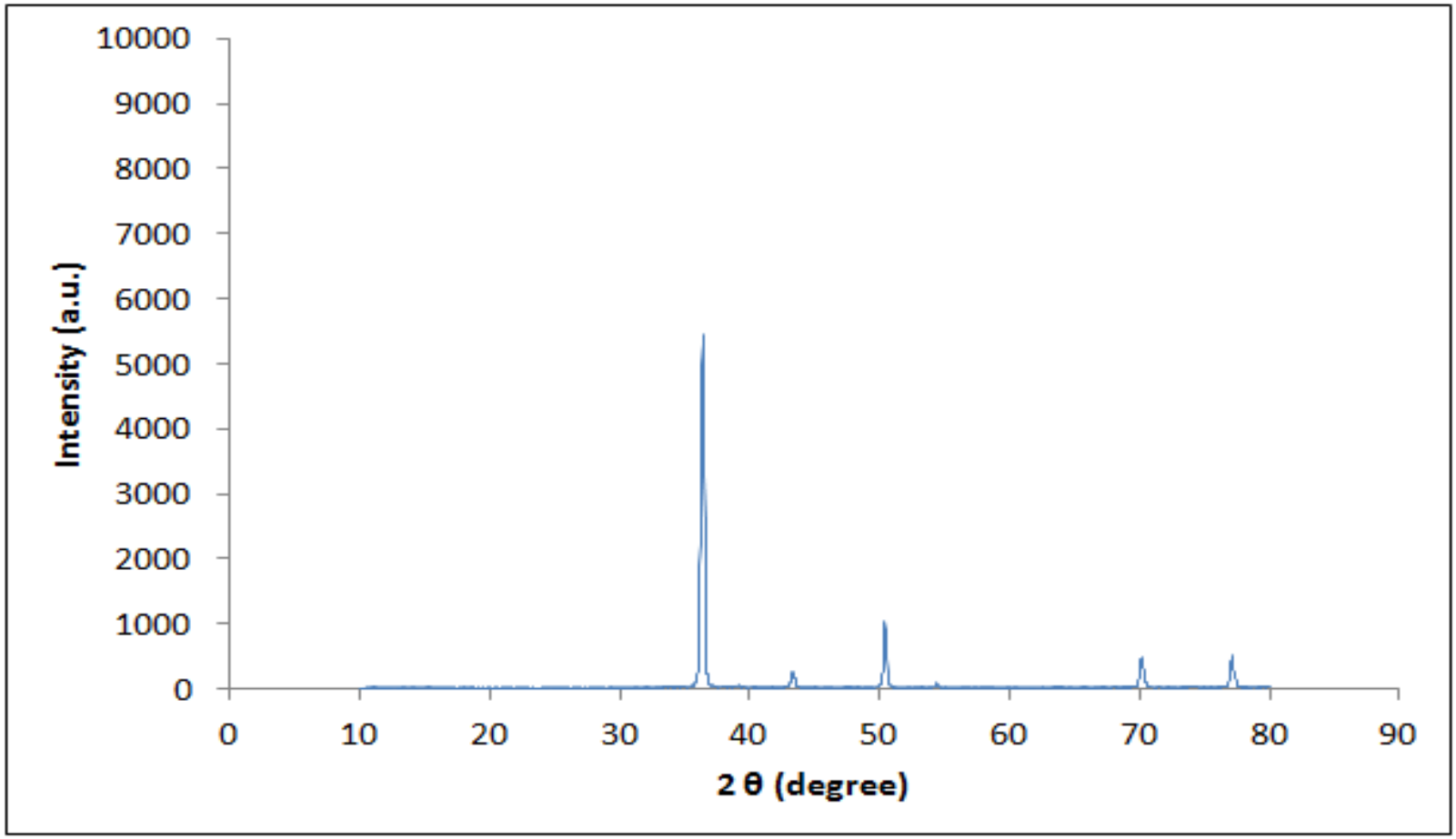

Fig. A6
XRD of zinc electrodeposits from 2M-$ZnCl_2$ bath prepared for 90 minutes

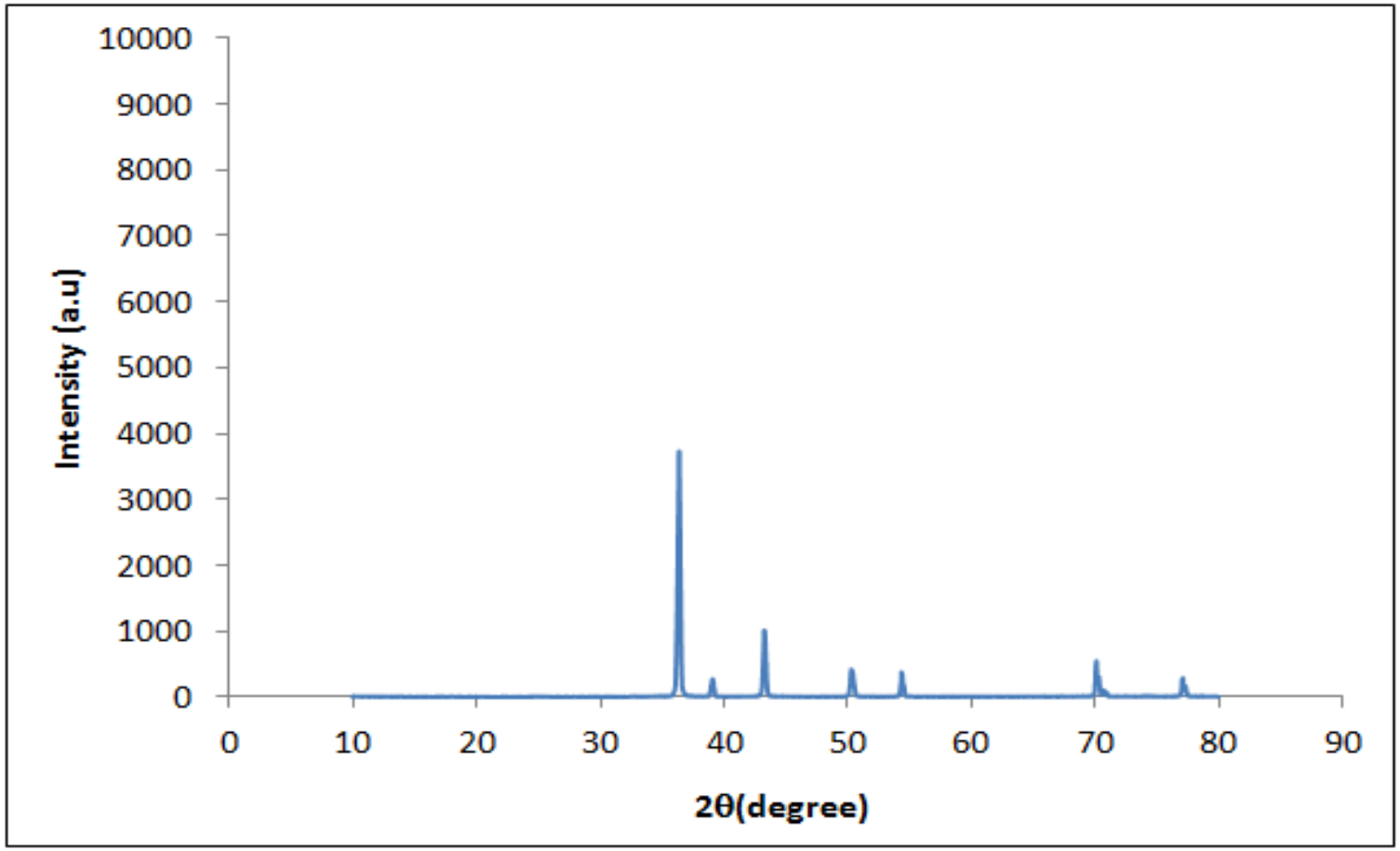

Fig. A7
XRD of zinc electrodeposits from 1M-NH_4Cl bath prepared for 90 minutes

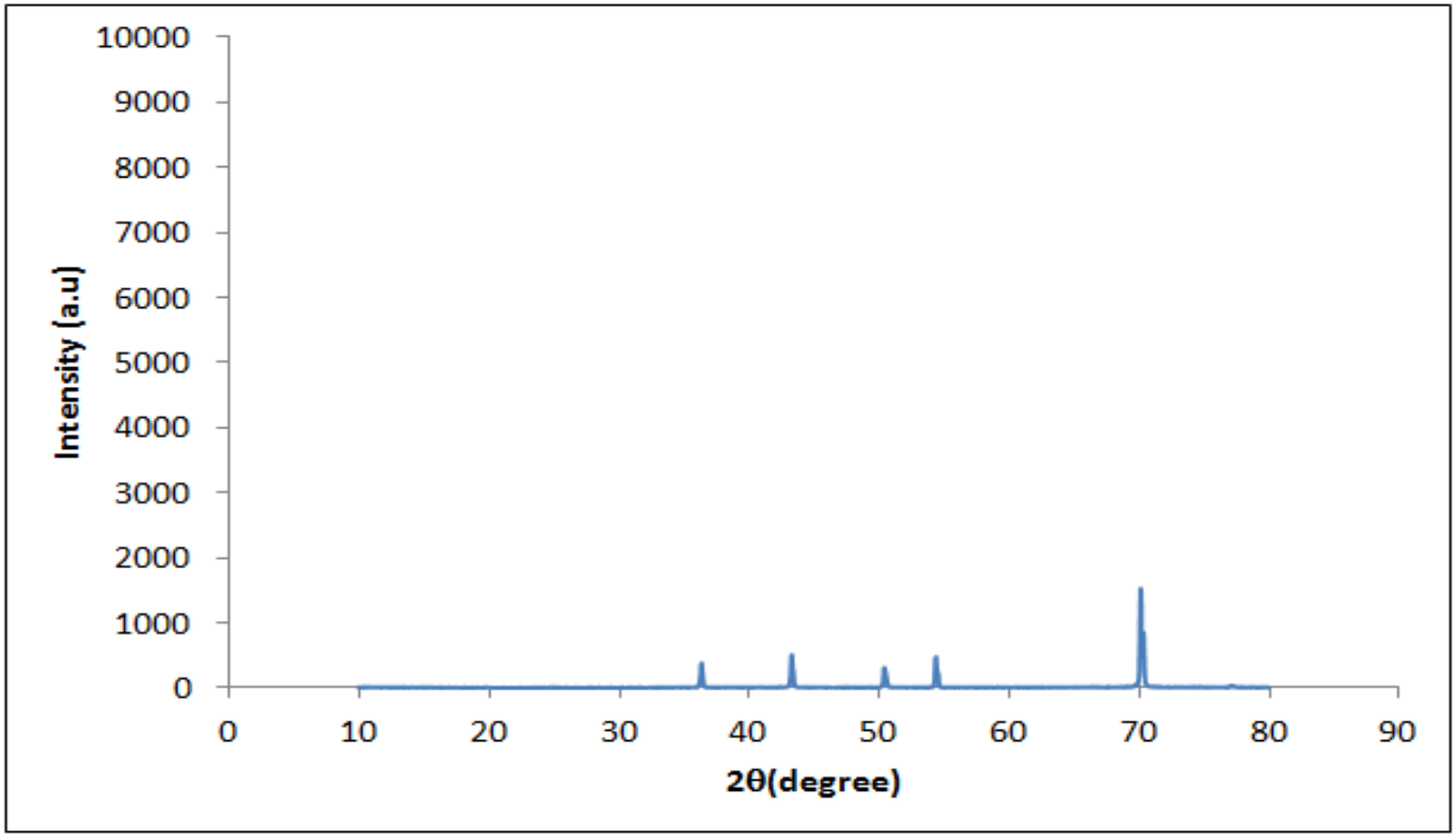

Fig. A8
XRD of zinc electrodeposits from 2M-NH_4Cl bath prepared for 90 minutes

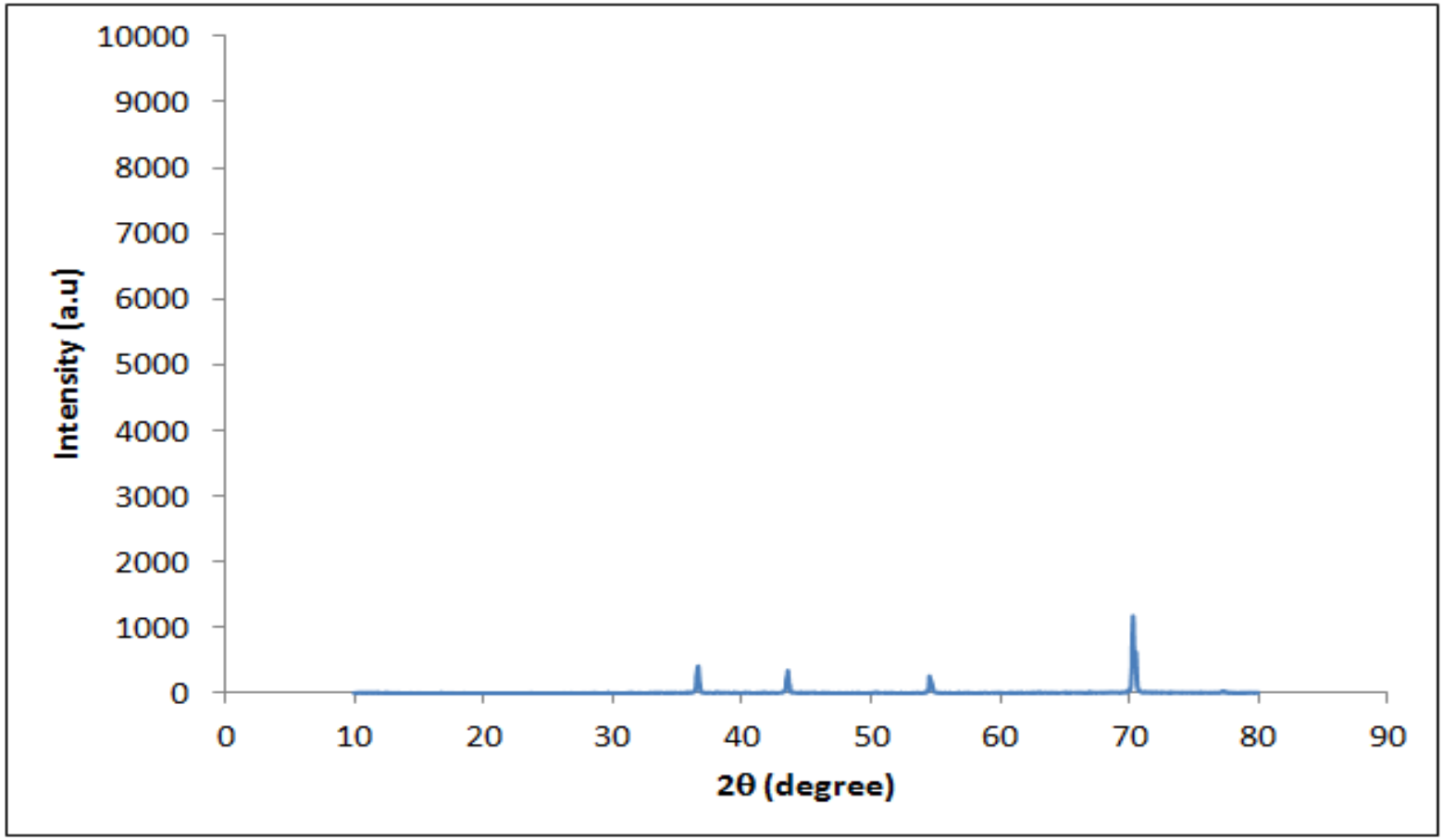

Fig. A9
XRD of zinc electrodeposits from 3M-NH_4Cl bath prepared for 90 minutes

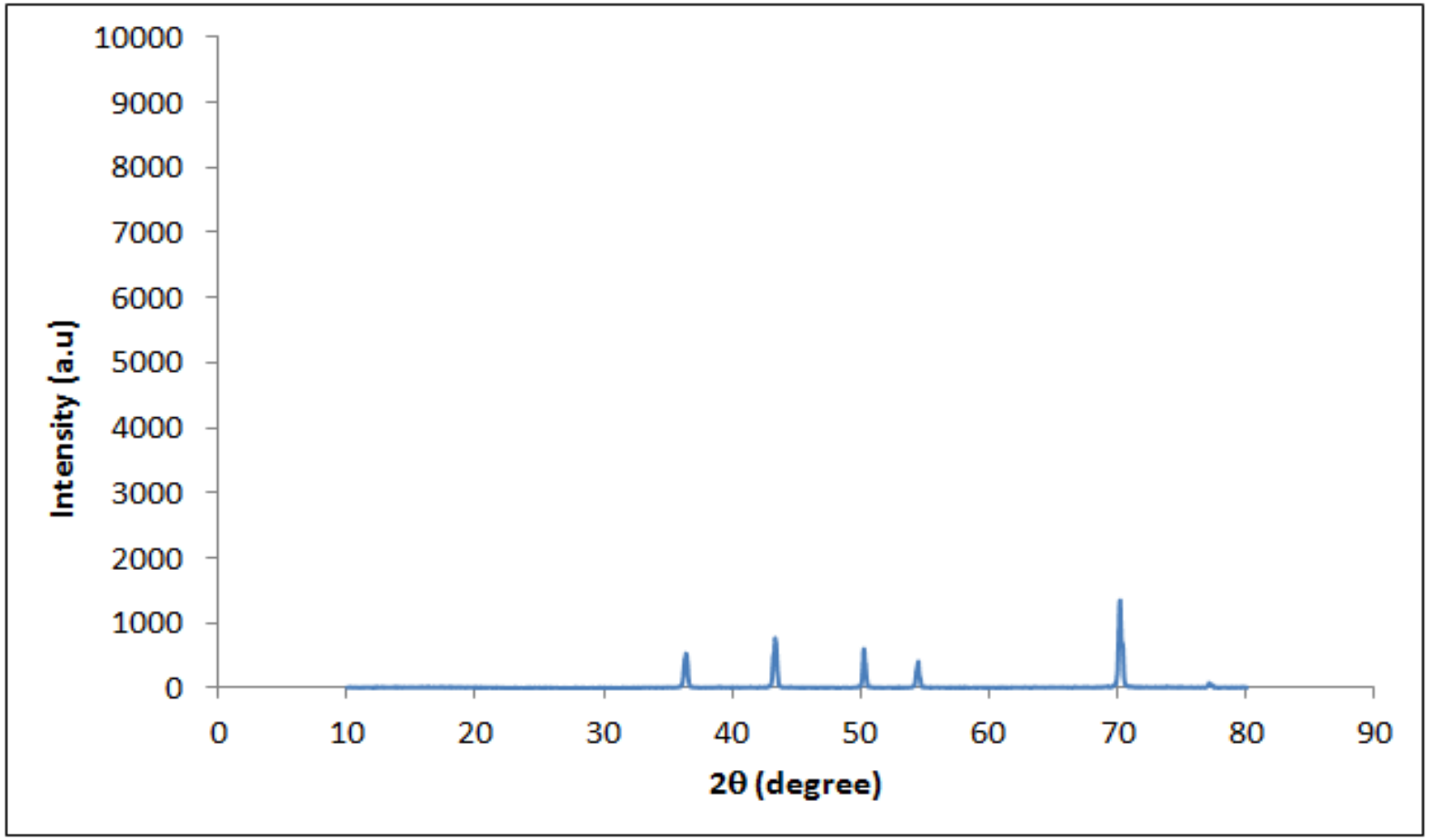

Fig. A10
XRD of zinc electrodeposits from 4M-NH_4Cl bath prepared for 90 minutes

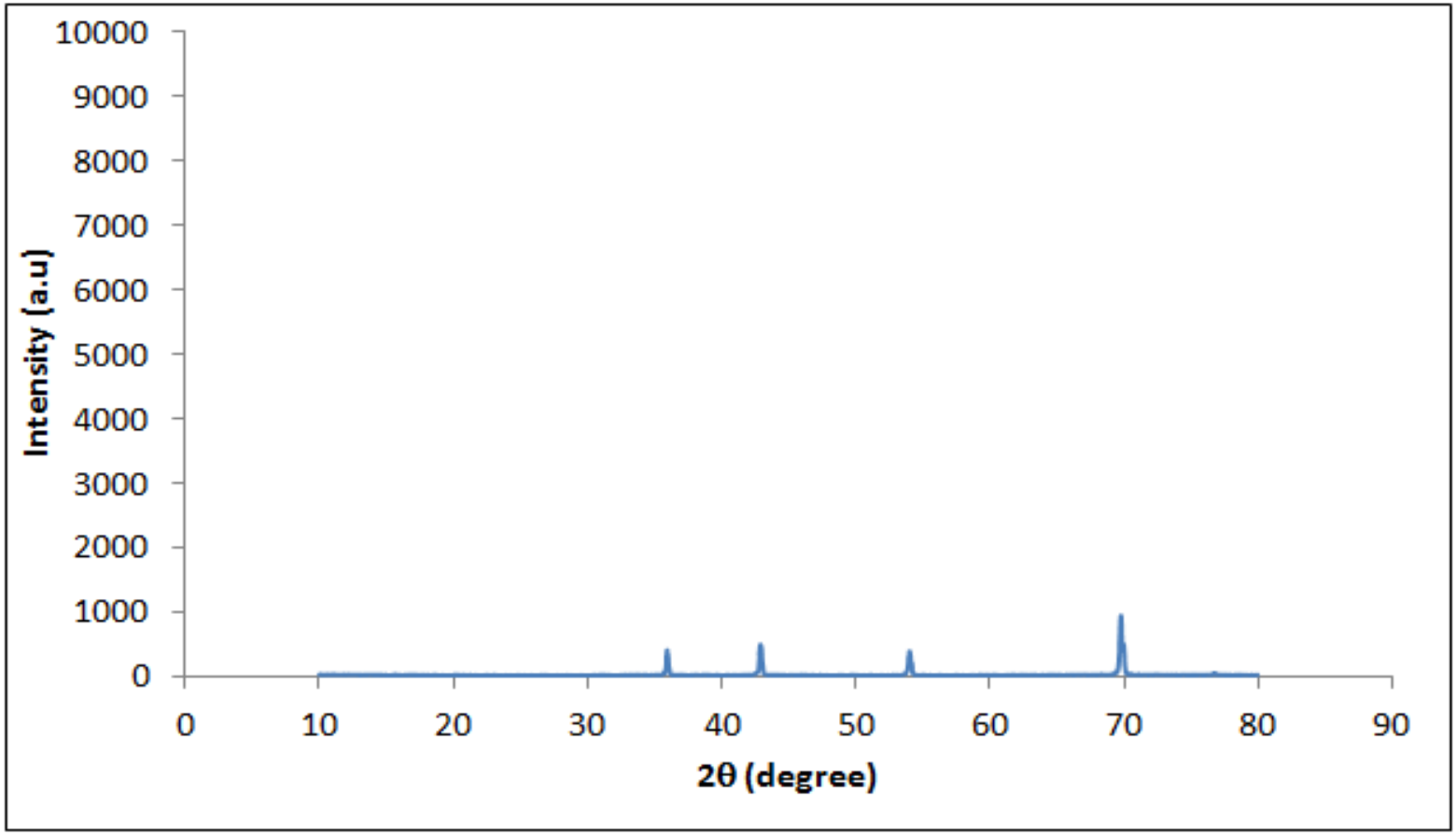

Fig. A11
XRD of zinc electrodeposits from 2M-$ZnCl_2$ bath prepared for 180 minutes

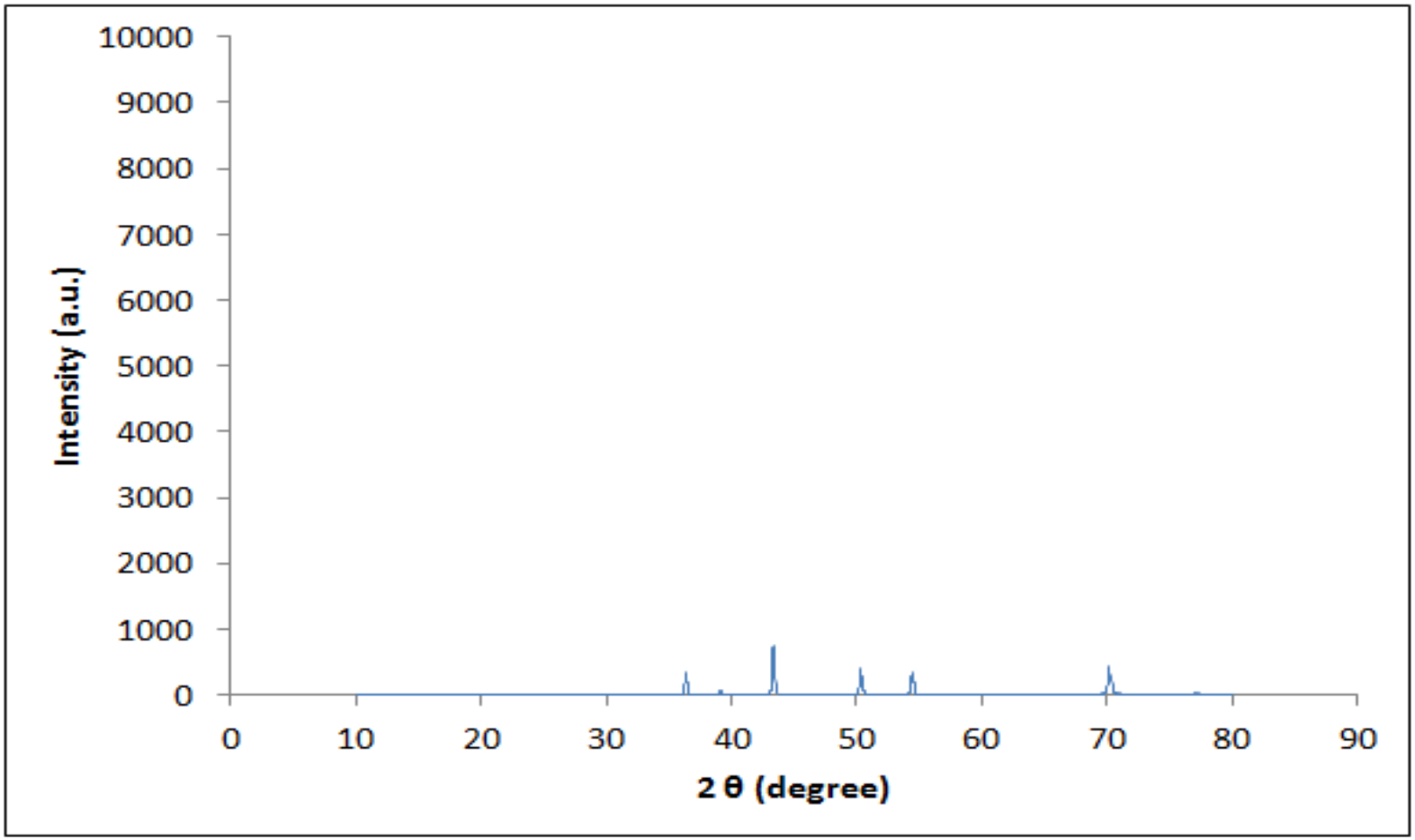

Fig. A12
XRD of zinc electrodeposits from 1M-NH_4Cl bath prepared for 180 minutes

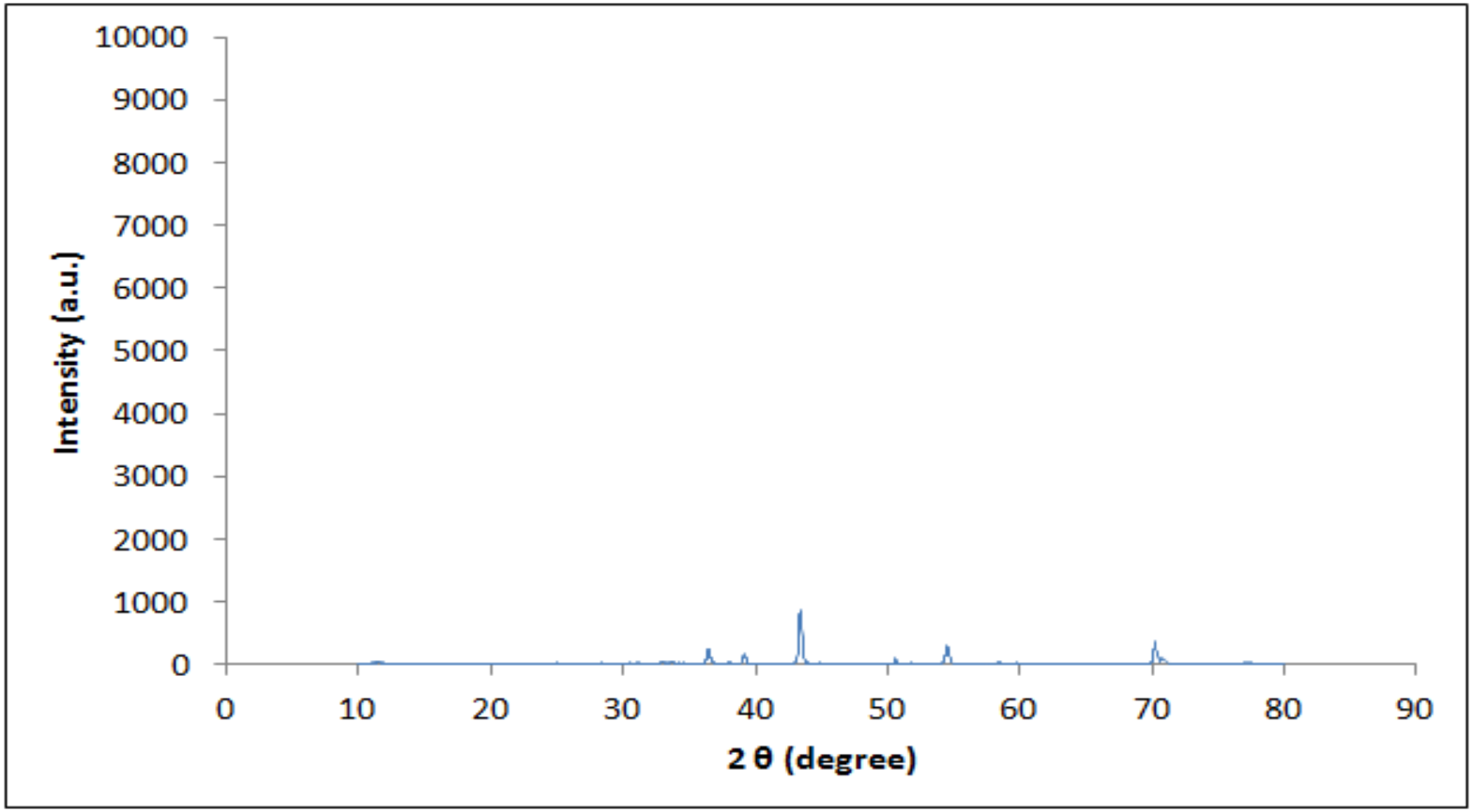

Fig. A13
XRD of zinc electrodeposits from 2M-NH_4Cl bath prepared for 180 minutes

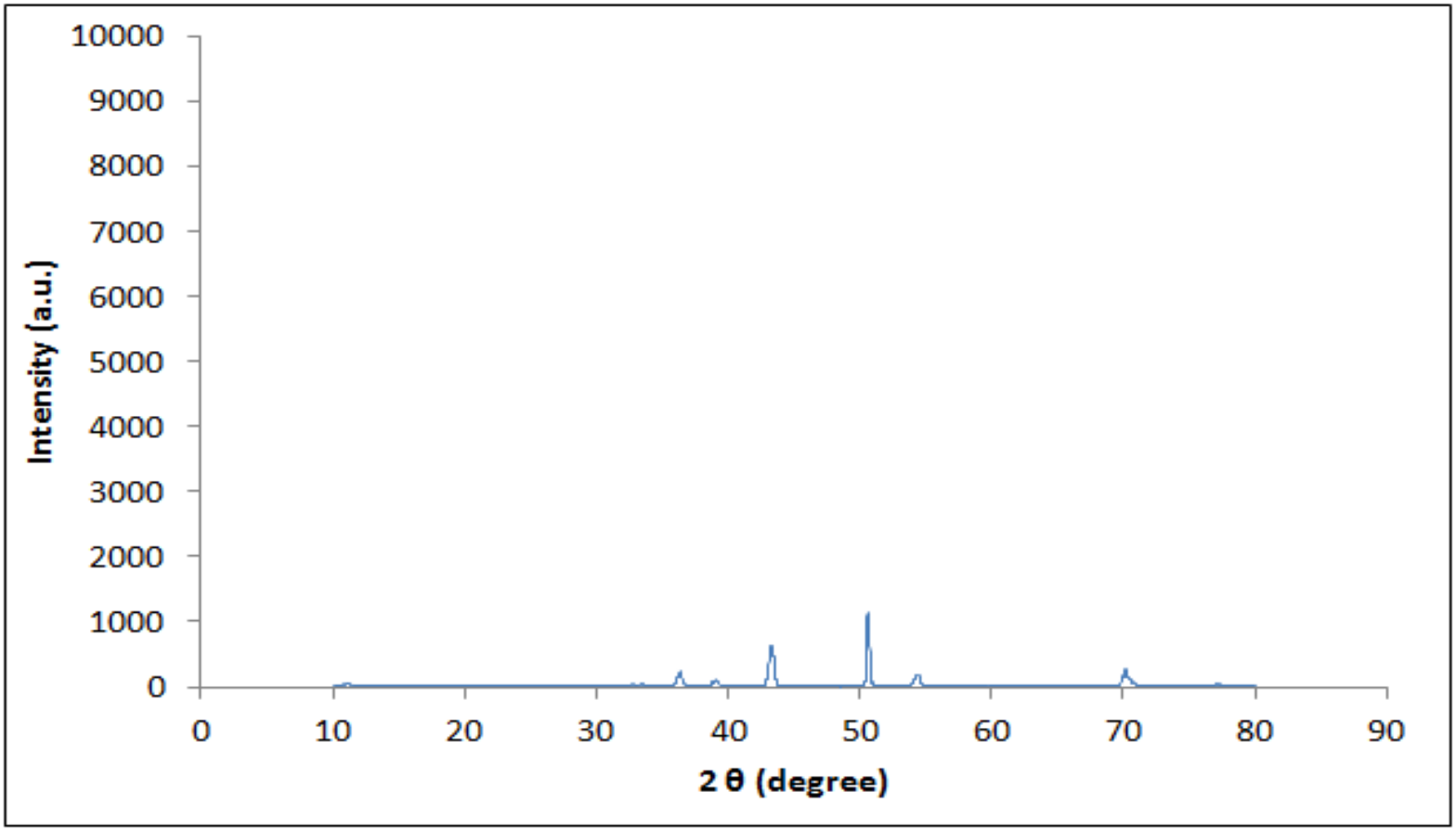

Fig. A14
XRD of zinc electrodeposits from 3M-NH_4Cl bath prepared for 180 minutes

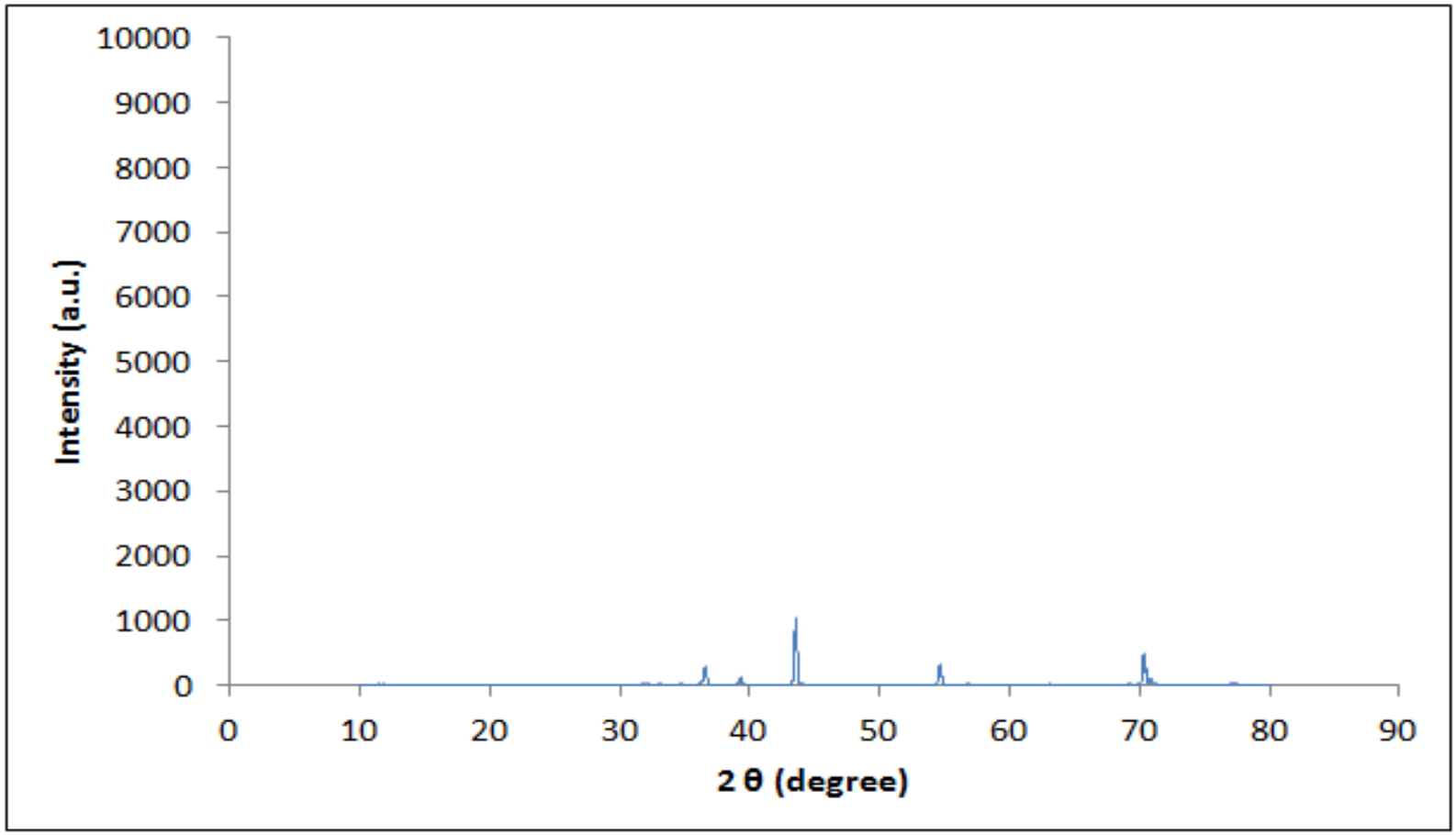

Fig. A15
XRD of zinc electrodeposits from 4M-NH_4Cl bath prepared for 180 minutes